EFFECTS OF ENVIRONMENTAL FACTORS ON HEAT-INDUCED β-LACTOGLOBULIN FIBRIL FORMATION

A THESIS PRESENTED IN PARTIAL FULFILMENT OF THE REQUIREMENTS FOR THE DEGREE OF MASTER IN FOOD TECHNOLOGY

RIDDET INSTITUTE

MASSEY UNIVERSITY, PALMERSTION NORTH, NEW ZEALAND

XIANGLI WANG

2009

ABSTRACT

The heat-induced fibrillar aggregation of β-lactoglobulin was studied under various environmental conditions. The formation of β-lactoglobulin fibrils was monitored by Thioflavin T (ThT) fluorescence and their morphology was studied using transmission electron microscopy (TEM). Amyloid-like fibrils were formed under standard conditions (pH 2.0, 80°C and low ionic strength). The β-lactoglobulin fibrillation kinetics exhibited sigmoidal behaviour, and the two-step autocatalytic reaction model fitted ThT fluorescence data well. The studies of the individual effect of pH, temperature, NaCl, $CaCl_2$ on β-lactoglobulin fibril formation showed that decreasing pH (2.4 - 1.6), increasing temperature (75 - 120°C) and increasing salt concentration (NaCl 0-100 mM; $CaCl_2$ 0-100 mM) accelerated the fibril formation process and altered the morphology of fibrils. The two-step autocatalytic reaction model did not fit the ThT fluorescence data well at higher temperature (>100°C) or at low pH (1.6). The effects of the four factors (pH, temperature, NaCl and $CaCl_2$) on β-lactoglobulin fibril formation were studied by using a central composition design (CCD) experiment. Results showed that the four main and some of the non-linear effects were significant (95%) on fibril formation, including fibrillation time and the fibril yield.

Taking all results together, it can be implied that β-lactoglobulin fibril formation can be promoted by choosing the external incubation conditions. This study is the first step towards the application of protein fibrils as texture-modifying ingredients in food systems.

Keywords: β-lactoglobulin, amyloid fibril, Thioflavin T fluorescence, TEM

ACKNOWLEDGEMENTS

I am taking this opportunity to thank all those who have assisted me in the ways with my master project.

I would first like to thank Dr. Simon Loveday of Riddet Institute for his role as the main supervisor during the completion this project. His supervision, support, and expert knowledge have contributed significantly to the outcome of this work. He has always been the first person I approached when I had questions about the research. He always left whatever he was doing to listen to me and discuss things with me. Furthermore, my gratitude is extended to Dr. Lawrie Creamer and Professor Harjinder Singh, the two supervisors who have provided expert knowledge and assistance in thesis writing. Dr Skelte Anema and Dr Steve Taylor of Fonterra Co-operative Limited provided valuable strategic guidance and mechanistic insight for this work.

I am very grateful for the opportunity to have worked with such renowned academic scientists.

The TEM studies were carried out under the supervision by Mr. Doug Hopcroft at the Manawatu Microscopy & Imaging Centre of Institute of Molecular Biosciences, Massey University. Mr. Hopcroft is gratefully acknowledged by providing the help of teaching me how to use the transmission electron microscopy (TEM) and discussion of the imaging results.

I thank Mrs Michelle Tamehana and Mrs Ann-Marie Jackson for giving me the opportunity to work in their laboratories of Institute of Food, Nutrition and Human Health (IFNHH) at Massey University. I also thank Janiene Gilliland who introduced me to do the some of my experimental work at the laboratory in Riddet Institute, during which period I was fortunate enough to meet a very helpful intern student, Daniela Endt, who help me in preparing samples of the Central Composite Design experiments.

For their valuable contributions at different stages of my research work, I would like to thank:

- Dr Simon Loveday for choosing the two-step autocatalytic reaction model and making the Central Composite Design, writing SigmaPlot code for non-linear regression with the model and help in use of Endnote software.
- Mr Doug Hopcroft for help doing the staining of TEM grids and processing the gel particle specimen.
- Dr Alasdair Noble for help in statistical analyses.
- Dr Libei Bateman for helping in using fluorescence spectrophotometer.

This work was funded by Fonterra Co-operative Limited and Foundation for Research, Science and Technology (FRST) as a part of the project of "COMBI Foods: Novel Dairy Protein-Based Nanostructures". I would like to thank Fonterra for providing the scholarship.

TABLE OF CONTENTS

LIST OF TABLES

LIST OF FIGURES

CHAPTER 1

INTRODUCTION

1.1 Protein fibrils

Many proteins have the ability to self-assemble into long, semi flexible structures, known as amyloid fibrils, under appropriate conditions (Rogers *et al.*, 2006). Amyloid fibrils are characterised by a cross β-conformation where the β-sheets are arranged parallel to the fibril axis with their constituent β-strands perpendicular to the fibril axis. They are long (several micrometres), thin (a few nanometres), and unbranched polymeric forms of protein (Nelson *et al.*, 2005).

This assembly of protein into fibrils has received considerable attention in varied fields, from medical to materials science (Krebs *et al.*, 2007). Recently, the assembly of proteins into fibrils has gained more attention in the field of food technology, mainly because of the potential utility in modifying the physical properties of food products, such as viscosity, flow behaviour, and weight effective gelation. Examples of food proteins that can form amyloid fibrils are β-lactoglobulin (Gosal *et al.*, 2001; Jung *et al.*, 2008; Kavanagh *et al.*, 2000a), lysozyme (Mishra *et al.*, 2007), ovalbumin (Pearce *et al.*, 2007) and BSA (Veerman *et al.*, 2003b).

1.2 β-Lactoglobulin fibrils

The most intensely studied food protein with respect to fibril formation is β-lactoglobulin. This protein is the major component of whey protein (approximately 50 % of the whey proteins). It is a globular protein with a monomer molecular weight of approximately 18.3 kDa (Caessens *et al.*, 1999). β-Lactoglobulin is not only widely used in food industry, it is also a good model system to study and it is important to understand the heat-induced portion aggregation process (Bromley *et al.*, 2004; Durand *et al.*, 2002). β-Lactoglobulin fibrils can be induced upon heating above the denaturation temperature, at low pH and low ionic strength (Bolder *et al.*, 2007b;

Schokker *et al.*, 2000). These fibrils are polydisperse in length (typical lengths are in the 1-10 μm range) and monodisperse in cross-section, with a diameter of about 4 nm (Arnaudov *et al.*, 2003; Rogers *et al.*, 2006). Investigation of these fibrils shows that they may be classified as amyloid fibrils because their X-ray fibre diffraction pattern is indicative of the cross β-motif and they can bind the amyloid-specific dyes, such as Thioflavin T and Congo red and they also show increased β-sheet content relative to their native state (Bolder *et al.*, 2007a; Gosal *et al.*, 2004).

1.3 Fibrillation mechanism and the characterisation techniques

Studying the kinetics of fibril formation can lead to a better understanding of the mechanism of the process. The investigation of the morphology of the aggregates at different stages of the process could lead to a more complete picture of the detailed mechanism of the process. Although there is no general mechanism accepted to date that can explain the formation of amyloid fibrils, various models have been proposed describing the formation of protein fibrils. One of the commonly accepted models is the two-step autocatalytic reaction model. This model suggests a mechanism that consists of nucleation and elongation in which unfolded protein molecules form a nucleus which then grows into the linear aggregates. A distinctive feature of such mechanism is the characteristic sigmoidal time-course curve of fibril formation, which has three phases: the lag phase, growth phase and stationary phase (Sabate *et al.*, 2003). This mechanism explains the formation processes of many protein fibrils, such as Aβ40, hen egg white lysozyme (HEWL) and porcine insulin (Arnaudov & de Vries, 2005; Nielsen *et al.*, 2001; Sabate *et al.*, 2003).

Thioflavin T (ThT) fluorescence and transmission electron microscopy (TEM) are the widely used techniques to study protein fibril formation. The fluorescence of ThT is strongly enhanced by its specific binding to β-sheets, therefore, the fluorescent signal is proportional to the fibril concentration (Krebs *et al.*, 2005a). ThT fluorescence has been used to determine the presence of amyloid fibrils and to examine the kinetics of fibril formation (Bolder *et al.*, 2007a; Hawe *et al.*, 2008). TEM can provide direct observations of fibrils.

1.4 Objectives and outline

For the application of fibrils in food products, an acceleration of the fibril formation would be advantageous. Enhanced formation of protein fibril systems by addition of preformed fibrils (seeding) or continuous agitation have previously been established (Akkermans *et al.*, 2006; Bolder *et al.*, 2007). Environmental factors that influence fibril formation are heating time, pH, ionic strength, temperature, etc. Previous work has shown some effects on β-lactoglobulin fibril formation by changing the environmental factors but a systematic study on how they influence the fibril formation (fibrillation kinetics, fibril morphology, fibril yield) during heating has not yet been performed (Aymard *et al.*, 1996; Sakurai & Goto, 2007; Schokker *et al.*, 2000; Veerman *et al.*, 2002). Therefore, in this study the individual and combined effects of the pH, temperature and ionic strength were investigated.

The goal of this project is to optimise the formation of β-lactoglobulin fibrils using salt concentrations (NaCl and $CaCl_2$), acidity and temperature. The research structure is shown in Figure 1.1, it consists of three objectives.

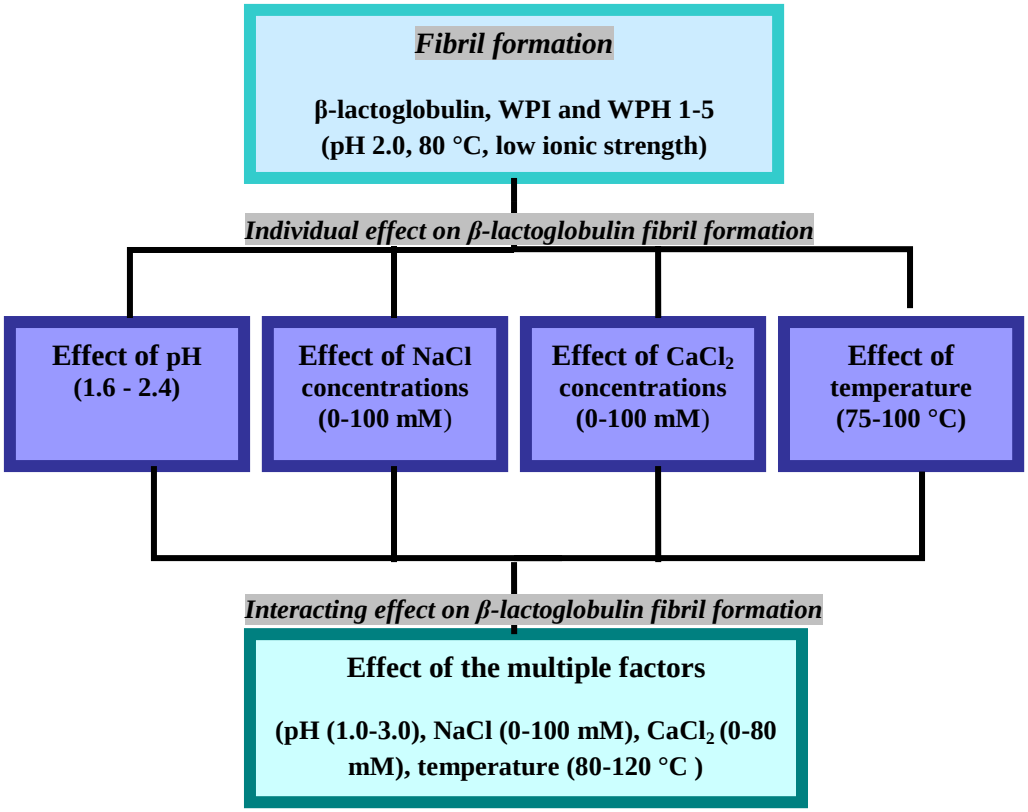

Figure 1.1 The structure of this study

The first objective was to adapt an *in vitro* method of fibril formation from previous studies. In Chapter 4, heat-induced fibril formation from β-lactoglobulin, whey protein isolates (WPI) and hydrolysed whey protein (WPH) 1-5 was studied under control conditions (pH 2.0, 80 °C, and low ionic strength). ThT fluorescence and TEM as the commonly used characterisation techniques were employed to study the kinetics of fibrillation and the morphology of the fibrils formed. In order to gain more insight into the effect of fibril formation, the two-step autocatalytic reaction model was applied and analysed using SigmaPlot version 10.

The second objective was to investigate the individual effects of the environmental factors. In Chapter 5, the effects of pH (1.6-2.4), NaCl concentrations (0 - 100 mM), $CaCl_2$ concentrations (0 - 100 mM) and temperature (75 – 120 °C) were studied based on the methods developed in Chapter 4.

The final objective was to study the interacting effects of the four environmental factors on β-lactoglobulin fibril formation. In Chapter 6, fibril formation was studied under various incubation conditions using a Central Composite Design (CCD) experiment. The investigated level of the four factors (pH [1.0 - 3.0], NaCl concentrations [0 - 100 mM], $CaCl_2$ concentrations [0 - 80 mM] and temperature [80 - 120 °C]) were based on the results from the individual studies of the four factors (Chapter 5). The main effect, interaction effect and non-linear effect of the four factors were analysed using Minitab. Some incubation conditions were selected based on the quantity of fibril yield and the fibrillation time used.

The present study focused on the lag and growth phases, but not the stationary phase, because of consideration of industrial applications. In this study, a first step was made towards the optimization of heat-induced β-lactoglobulin fibril formation. The functionality of the fibrils formed under different conditions should be investigated in the future.

CHAPTER 2

LITERATURE REVIEW

Fibril formation of proteins or peptides has been studied extensively because of the potential important technical implications in biotechnology and food science (Carrotta *et al.*, 2001). Fibrils have been involved in a number of diseases, e.g., Alzheimer's disease, systemic amyloidoses, and type II diabetes mellitus (Ionescu-Zanetti *et al.*, 1999). When properly controlled, protein fibrillation can produce novel material with many potential uses. For example, amyloid-like fibrils can be used as structural or structuring elements in chemistry, medicine, material science and food science (Krebs *et al.*, 2007). Recently, the assembly of proteins into fibrils has obtained considerable attention in the field of food technology, mainly due to the potential utility in modifying the material properties of food products. This review is intended to focus on recent advances in amyloid-like fibrils with particular relevance to β-lactoglobulin.

The first section of this review focuses on β-lactoglobulin and its thermal denaturation. In section 2, the structure of amyloid-fibrils and β-lactoglobulin fibril are described. Section 3 describes the commonly used methods to characterise fibrils. Section 4 discusses aspects of the mechanisms and kinetics of fibril assembly. Section 5 concerns the effect of environmental factors on fibril formation. Finally there is the summary and future prospects section.

2.1 Heat-induced β-lactoglobulin aggregation

2.1.1 β-Lactoglobulin

β-Lactoglobulin is one of the more intensively studied globular proteins as well as the major component of whey. β-Lactoglobulin is 10 % of the total milk protein or about 50 % of the whey protein (Caessens *et al.*, 1999). β-Lactoglobulin is widely used in the food industry and it is important to understand the heat-induced aggregation process either because one wants to avoid it, e.g. in sterilization of milk, or one wants to exploit it for applications (Durand *et al.*, 2002).

In β-lactoglobulin's native monomer form, it contains 162 amino acids with eight antiparallel β-sheets and one α-helix. It has a molar mass of 18.3 kDa and a radius of about 2-3 nm. The molecule contains two disulphide bonds and one free sulphydryl (Cys121) groups and no phosphoserine. One of the disulfide groups is between Cys66 and Cys160 (Cys66-Cys160), the other seems to be a dynamic one that involves Cys106 and is sometimes found with Cys 121 and sometimes with Cys 119 (Sakurai *et al.*, 2001). There are two major genetic variants, A and B, which differ in the positions 64 and 118 where the aspartic acid and valine of Variant A are replaced by glycine and alanine in Variant B (Boye *et al.*, 2004; Damodaran, 1996).

The protein assumes a dimeric structure at neutral pH, but dissociates into monomers at acidic pH. The isoelectric region is pH 5.1-5.6. At neutral pH, β-lactoglobulin exists as a dimer. Below pH 3.0 and above pH 8.0, β-lactoglobulin is monomeric (Sakurai *et al.*, 2001; Simons *et al.*, 2002). At neutral pH, the quaternary structure of β-lactoglobulin is dimeric in equilibrium with the monomeric form; this monomer-dimer equilibrium depends on the protein concentration, ionic strength and temperature (Aymard *et al.*, 1996; Sakurai *et al.*, 2001) .

The structures at the different pH values possess the same basic topology, having nine antiparallel β-strands (A-I) and one short and one long α-helix at the carboxyl terminus (Sakurai *et al.*, 2001) (Figure 2.1). In particular, each monomer has an internal core containing predominantly hydrophobic residues, while the hydrophilic amino acids are mostly located on the protein surface (Sakurai *et al.*, 2001; Simons *et al.*, 2002).

.

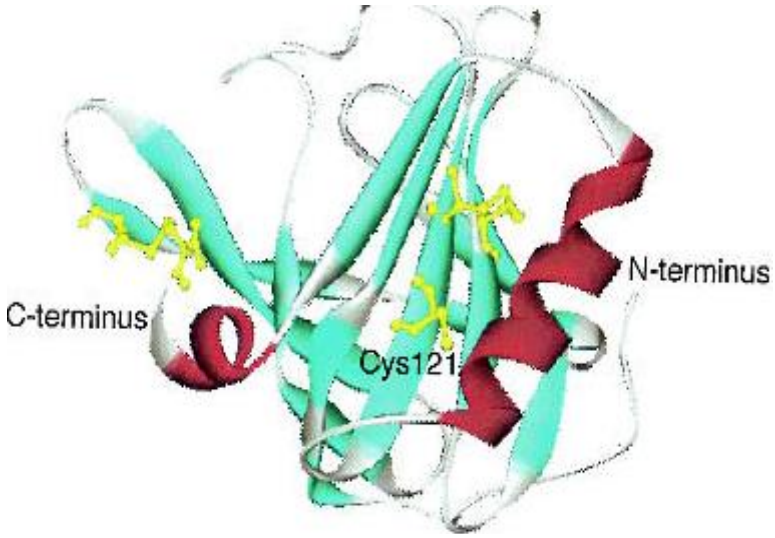

Figure 2.1 The schematic representation of the native structure of bovine β-lactoglobulin. (Drawn using WebLab Viewer Lite, Molecular Simulations Inc. (San Diego, CA)). The β-strands and α-helices are coloured in cyan and red, respectively. Reproduced from Hamada and Dobson's paper (2002).

2.1.2 β-Lactoglobulin thermal denaturation and gelation

Aggregation of heat-denaturated β-lactoglobulin can be a useful property to modify the texture of foods. Heat-induced aggregation and gelation of β-lactoglobulin have received great research attention (Euston *et al.*, 2007; Nicolai & Durand, 2007).

Upon heating, β-lactoglobulin undergoes conformational changes (Simons *et al.*, 2002). At neutral pH, when the temperature is increased above 70°C, β-lactoglobulin partially denatures and aggregates, leading to the formation of soluble aggregates if the protein concentration is below the critical gelation concentration ($C < C_{gel}$), but if $C > C_{gel}$, a continuous network will form (Veerman *et al.*, 2003a). At temperatures higher than 80°C, noncovalent interactions become more important and the aggregation process is dominated by both interchange of disulphide bonds and hydrophobic interactions (Galani & Apenten, 1997; Havea *et al.*, 2004). These structural changes become irreversible at temperatures beyond 80ºC. As the denaturation process progresses, the intra-chain disulphide bridges begin to break and the free sulphydryl groups on different molecules can react with each other to form aggregates (Jung *et al.*, 2008).`

The gelling property of β-lactoglobulin arises from its ability to denature and aggregate (Euston *et al.*, 2007). If the protein concentration is sufficiently high, the aggregation of denatured β-lactoglobulin leads to gel formation. β-Lactoglobulin can form gels in solution under various conditions, such as at high temperatures and high hydrostatic pressure (Dumay *et al.*, 1998; Langton & Hermansson, 1992; Takata *et al.*, 2000). At conditions of low salt and high protein charge density, the gels are transparent and microscopy shows that they consist of thin branched strands of aggregated proteins and the thickness of the strands is similar to the size of the individual proteins (Nicolai & Durand, 2007). When the net charge density is close to neutral or at high salt concentrations, turbid coarse gels are formed (Durand *et al.*, 2002).

2.2 Protein amyloid-like fibrils

Amyloid-like fibril is an extreme case of protein assembly. Amyloid-like fibrils are ordered aggregates of a normally soluble peptide or protein. More than 20 different peptides/ proteins have been identified have the ability to form amyloid fibrils *in vivo*. Beyond the proteins involved in diseases (Alzheimer's disease (AD) etc.), many other proteins can form fibrils under proper conditions in which the protein partially denatured conformations are populated (Krebs *et al.*, 2007). This applies to many food proteins such as β-lactoglobulin, soy-protein, bovine serum albumin (BSA), ovalbumin and pea protein (Akkermans *et al.*, 2007; Schokker *et al.*, 2000; Veerman *et al.*, 2003b).

2.2.1. Structural features of amyloid-like fibrils

In recent years, more detailed structural information on amyloid fibrils has been obtained. The structural data will contribute to an improved understanding of the mechanisms of amyloid formation.

A variety of models have been proposed for the structure of amyloid fibrils (Makin & Serpell, 2005), but there is no absolutely universal molecular structure for amyloid fibrils apart from the common structural motif, a characteristic cross-β-sheet that

forms the core of the fibrils, see Figure 2.2 (b) (the β-sheet structure has the strands perpendicular to the long axis of the fibril and hydrogen bonded along the axis of the fibril) (Malisauskas *et al.*, 2003; Tycko, 2004). The fibrils are usually ~10 nm in thickness and >100 nm in length. A amyloid-like fibril is generally a rod, a stiff /semiflexible fibril with no branche, see Figure 2.2 (a).

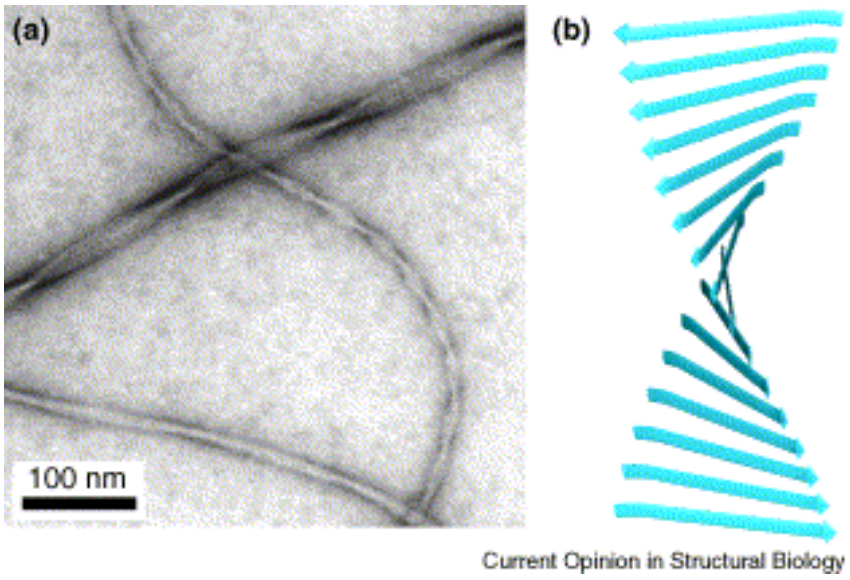

Figure 2.2 Low-resolution structural features of amyloid fibrils. **(a)** Negatively stained EM image of fibrils formed *in vitro* by $A\beta_{1-40}$, illustrating the diversity of morphologies commonly exhibited by amyloid fibrils formed by a single peptide or protein. **(b)** Schematic representation of a twisted cross-β structure, the defining structural motif within amyloid fibrils. The long axis of the fibril runs vertically. Adapt from Tycko (2004).

It was found that there are differences in detail between the various morphologies for specific amyloid fibrils using a range of techniques (Merz *et al.*, 1983). The fibres are different in terms of length of the fibres, stiffness, and in terms of the conditions necessary to make them (pH, salt concentration, temperature). The impact of the environmental factors (pH, temperature and salts) on fibril structure is introduced in Section 2.5.

2.2.2 β-Lactoglobulin fibrils

Whey protein isolate (WPI) is often used as ingredients in foods because of its unique functional properties; it has been extensively studied by the food scientists. β-Lactoglobulin was found to be the only protein that is incorporated into these WPI

fibrils (Bolder *et al.*, 2006). As its forms of fibrils are actually typical of many other proteins under comparable conditions, so it is commonly used as specimen to seek unifying mechanisms for its behaviour (Durand *et al.*, 2002).

Fibrils of β-lactoglobulin can be obtained by heating the protein above denaturation tempearature (75°C) for several hours under acidic conditions (around pH 2) and low ionic strength, or by adding a denaturing agent, like urea (Hamada & Dobson, 2002). The fibrils can have a length up to 10 μm while their thickness is around 4 nm (Akkermans *et al.*, 2007).

A β-lactoglobulin fibril is a polymeric assembly of protein molecules, based on the cross- β-structural pattern, in which intermolecular β-sheets extend over the length of the fibril such that each β-strand within the β-sheets runs perpendicular to the fibril axis (Bromley *et al.*, 2004). To date, it is not known what effect the heat treatment under acidic conditions has on the molecular structure of β-lactoglobulin (Akkermans *et al.*, 2007).

2.2.3 Application of protein fibrils in food

The highly ordered protein fibrils have received considerable interest in the use for nanotechnology and other applications in material science.

Protein fibril is an extreme case of protein assembles. Protein fibrils are long and thin, which makes it possible for them to form meso-phases (The various liquid crystalline phases) such as a nematic phases (one of the most common liquid crystalline phases, where the molecules have no positional order, but they have long-range orientational order). Such properties give opportunities for development of protein based new functional materials (van der Linden & Venema, 2007).

Properties that can be affected using protein fibrils as ingredients are the viscosity, flow behaviour and gelation. In food product development, protein fibrils can be used to improve the textural properties of high protein foods or used as an ingredient in meat replacement products.

2.3 Characterisation of fibrillation

Quantitative analysis of the kinetics of fibril formation requires both well-characterised protein preparations and appropriate monitoring techniques. Several techniques have been employed in the study of protein fibrillation, including dye staining, nuclear magnetic resonance (NMR) spectroscopy, liquid environment atomic force microscopy (AFM), transmission electron microscopy (TEM) imaging, X-ray fiber diffraction, circular dichroism (CD) and Fourier transform infrared (FTIR) spectroscopy (Ionescu-Zanetti *et al.*, 1999; Nielsen *et al.*, 2001).

Two aspects of amyloid fibril formation can be characterised *in vitro;* the structure (dimensions, morphology) of the fibril and the fibril formation process (mechanism and kinetics) (Nilsson, 2004).

2.3.1 Dye binding

The fluorescent molecules Thioflavin T, Congo Red and Nile Red are the most frequently used dyes to detect the presence of amyloid fibrils (Hawe *et al.*, 2008).

- **Thioflavin T**

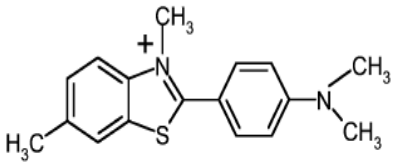

Figure 2.3 Structure of Thioflavin T

Thioflavin T (ThT) is a benzothiazole dye that shows enhanced fluorescence upon binding to amyloid fibrils and is commonly used to diagnose amyloid fibrils; the structure of ThT is shown in Figure 2.3. In aqueous solutions, when ThT used to monitor fibrils by fluorescence assay the commonly adopted concentration is between 10-60 μM and the excitation maximum is situated at 442 nm and emission is located around 486 nm (Volkova *et al.*, 2007). At such concentrations, thioflavin T exist as micelles. The outside of the ThT micelles take positive charges which lead to the

selectivity due to specific electrostatic interactions to amyloid fibrils (Khurana *et al.*, 2005). The binding of ThT to amyloid fibrils will be reduced by several-fold upon decreasing the pH to below 3 (Khurana *et al.*, 2005). Hence, ThT fluorescence assay should be optimized with respect to pH (generally pH 7.0 – 8.0) for each fibril system (Eisert *et al.*, 2006).

ThT fluoresce as a characterisation technique of β-lactoglobulin fibrillation was used in many studies (Akkermans *et al.*, 2008; Bolder *et al.*, 2007a). According to their reports, the enhanced fluorescence emission of the ThT on binding to fibrillar species provides a very convenient probe for studying the kinetics of amyloid fibril formation.

- **Congo red**

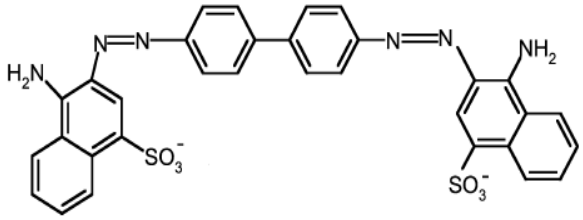

Figure 2.4 Structure of Congo red

The structure of Cogo red is shown in Figure 2.4. The 2 sulfonic acid groups of Congo red specifically bind to 2 positively charged amino acid residues on 2 separate protein molecules that are properly oriented in the β-pleated sheet conformation in the protofibril laminate structure. Under polarized light, amyloid samples exhibit green birefringence when stained with Congo red. The fact that Congo red binds to native, partially folded conformations and amyloid fibrils of several proteins shows that it must be used with caution as a diagnostic test for the presence of amyloid fibrils in vitro (Khurana *et al.*, 2001b) . Concentrations of CR between 10 and 15 μM are suggested for optimum detection of fibril structures (Klunk *et al*., 1999).

Congo Red absorbance spectroscopy was used to detect the fibril-like structure in bovine casein micelles, using absorbance spectra between 450 and 625 nm (Lencki, 2007).

Technical limitations

All of these instrumental techniques suffer some associated technical limitations. ThT and Congo red require a close to neutral pH to provide a good signal; ThT binds poorly at pH<3 and Congo red precipitates at pH < 5 (Mishra *et al.*, 2007). Congo red is not a specific dye and it is a kinetic inhibitor molecule. The quantum yield of ThT fluorescence depends dramatically of amyloid fibril type and there is a number of amyloid fibrils with a very modest and unappreciable ThT fluorescence (Sabate & Saupe, 2007).

2.3.2 Atomic force microscopy and transmission electron microscopy

Atomic force microscopy (AFM), which is a scanning probe microscopy technique, provides images at the surface. To date, the method has mainly been used to image fibrils from solutions dried onto planar solid substrates, such as mica. AFM technique has been widely used in the research of protein fibrillation (Arnaudov *et al.*, 2003; Gosal *et al.*, 2004).

Transmission electron microscopy (TEM) uses electrons as "light source" to provide images of dried films on perforated grids. Staining is typically performed with a 2% solution of uranyl acetate in water to enhance contrast for quality TEM data. The composition of the protein sample solution must not damage the EM grids and excessive salt should be avoided since salt crystals can obscure the identification of fibrils. Many objects on an EM grid are artefacts that can be mistaken for protein aggregates (Nilsson, 2004).

AFM provides accurate measurements of the height of the sample above the mica substrate, but the large size of the scanning tip relative to the sample leads to an over estimation of the sample width. Despite the inaccuracy in widths, AFM has several advantages over TEM in imaging samples. AFM is a non-invasive technique by which the fibrils are observed directly. Therefore, the images represent true morphology, in contrast to the negative staining used in TEM studies, which may affect the morphology of the fibrils (Ionescu-Zanetti *et al.*, 1999). Both AFM and TEM are

commonly used in β-lactoglobulin fibril formation (Arnaudov *et al.*, 2003; Gosal *et al.*, 2004; Veerman *et al.*, 2003a).

2.3.3 Other commonly used techniques

The commonly used techniques to monitor the formation of amyloid-like structure of protein are summarised in Table 2.1

Table 2.1 The other commonly used characterisation techniques of fibril formation

Method	**Reference**	**Protein**
X-ray diffraction	(Gosal *et al.*, 2004)	β-lactoglobulin
	(Pearce *et al.*, 2007)	bovine serum albumin
	(Arnaudov *et al.*, 2006)	β-lactoglobulin
Dynamic and static light scattering	(Arnaudov & de Vries, 2006)	β-lactoglobulin
	(Lomakin *et al.*, 1996)	Aβ fibrils
	(Modler *et al.*, 2003)	phosphoglycerate kinase (PGK)
Nuclear magnetic resonance (NMR)	(Tycko, 2004)	$A\beta_{1-40}$
	(Arnaudov *et al.*, 2006)	β-lactoglobulin
	(Arnaudov *et al.*, 2003)	β-lactoglobulin
Circular dichroism spectroscopy (CD)	(Nielsen *et al.*, 2001)	bovine insulin
	(Modler *et al.*, 2003)	phosphoglycerate kinase (PGK)
	(Farrell *et al.*, 2003)	bovine κ-Casein
	(Pearce *et al.*, 2007)	bovine serum albumin
Fourier transform infrared (FTIR)	(Gosal *et al.*, 2001; Gosal *et al.*, 2004; Kavanagh *et al.*, 2000b)	β-lactoglobulin
	(Farrell *et al.*, 2003)	bovine κ-Casein
Small-Angle X-ray Scattering (SAXS)	(Nielsen *et al.*, 2001)	bovine insulin

2.3.8 Strategy for detecting amyloid fibril formation

To determine if a peptide or protein will form amyloid fibrils, a systematic approach can be used which minimizes cost but maximizes sensitivity.

Dye binding is relatively simple and in-expensive technique to identify the presence of β-sheet, which is related to the formation of cross-β fibril. TEM and AFM are the directly ways to identify the presence of fibrils. The other methods, such as light scattering techniques, can be used in-situ during the aggregation process and provide the information of inter-residue distances and backbone dihedral angles for amyloid fibrils (Nicolai & Durand, 2007).

The suggested practical work can be carried out as follow:

1. The sample is incubated under proper conditions which promote fibril formation.
2. The sample is visually examined for an increase in viscosity, gel formation, if a change in viscosity or a gel is observed. The sample is analyzed by the dye binding assay such as Thioflavin T or Congo Red.
3. If a positive result is obtained, the sample should be examined for the presence of fibrils by TEM or AFM. If fibrils are found, CD, FTIR or X-ray fibre diffraction can be used to determine the characteristic β-sheet presence (Nilsson, 2004).

2.4 Mechanisms of fibril formation

Protein fibril formation generally occurs in a narrow pH, ionic strength and protein concentration range. It is often induced by heat denaturation or chemical denaturation (Gosal *et al.*, 2004; Hamada & Dobson, 2002; Veerman *et al.*, 2003b). Understanding the processes and mechanisms that control the aggregation of the formation of fibril, are important in technological applications.

2.4.1 Nucleation - elongation mechanisms

The most widely accepted and characterized mechanism of amyloid formation is the so-called “nucleation - elongation” or “nucleated growth” mechanism. It is recognised

earlier that there are three reactions involved in fibril formation: nucleation (formation of nuclei), growth (elongation nuclei to fibrils) and precipitation (floccules formation) (Waugh *et al.*, 1953). Fibril formation later has been described by a nucleation elongation mechanism. In this mechanism, nucleation is believed as the assembly of several protein monomers (peptides) to form an organized structure, nucleus, as a precursor for fibril formation. The subsequent addition of the monomers (peptides) to the nucleus elongates it into fibrils (Naiki and Nakakuki 1996; Perutz and Windle 2001). As the structure of amyloid fibril is significantly different from those of native state protein, some researchers believed that structural perturbation occurred before nucleation; it involves destabilization or unfolding of the native state protein (Thakur & Rao, 2008). The nucleation-elongation mechanism, gives a sigmoidal shape of fibril formation, as shown in Figure 2.5.

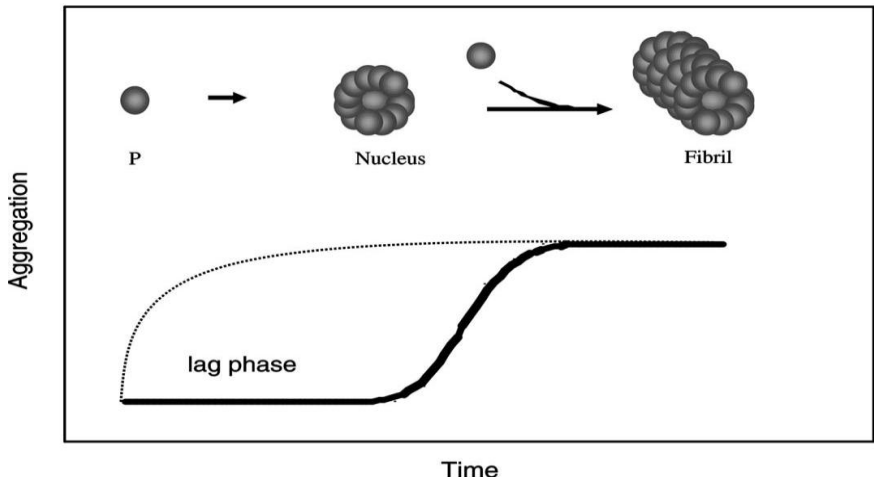

Figure 2.5 Nucleation and elongation scheme: The aggregation of a protein or peptide into amyloid fibrils. The lag phase can be eliminated (dotted line) by the addition of seed. Reproduced from Nilsson (2004).

A typical feature of nucleation-dependent polymerisation is a sigmoidal time-course curve of fibril formation. Such a curve has three phases: lag phase, growth phase and stationary phase as shown in Figure 2.6 (Padrick & Miranker, 2002). The lag phase is defined as the time required for the formation of "nuclei" – the structures which are able to grow into amyloid fibrils. Once the nucleus is formed, fibril formation enters the growth phase, where the nuclei are elongated to form fibrils by the attachment of monomers. Eventually, the growth rate decreases and reaches nearly zero, indicating either a limitation in monomer supply or a thermodynamic equilibrium (Nielsen *et al.*, 2001).

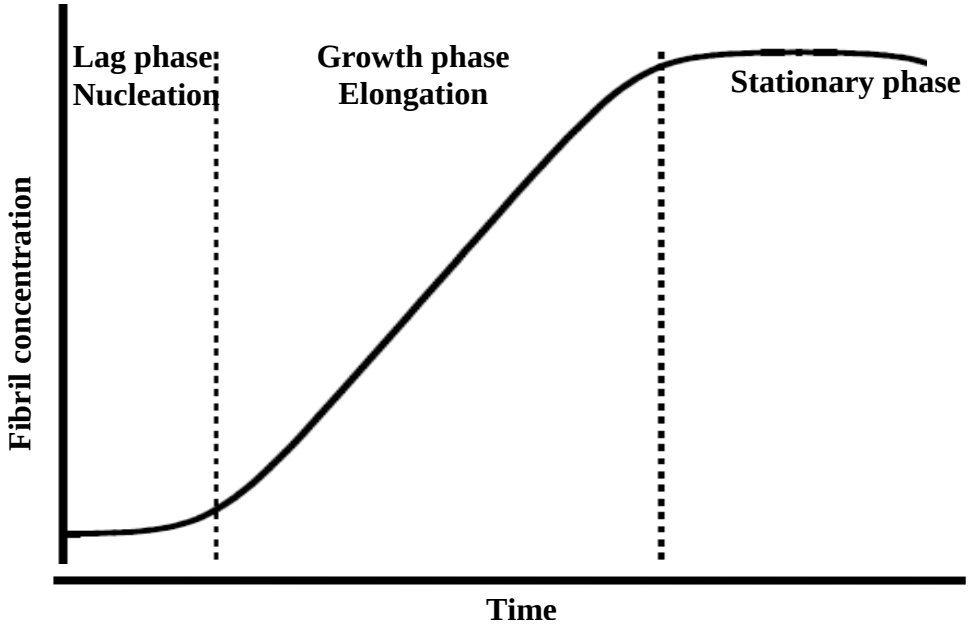

Figure 2.6 Different stages of fibril formation

Nucleation process is the rate-limiting step, it consists of a series of association steps that are thermodynamically unfavourable (Sabate *et al.*, 2003). This rate-limiting phase is reflected as the lag phase in kinetics of amyloid fibril formation. While it was suggested that the elongation reaction is thermodynamically favourable, it reacts fast (Sabate *et al.*, 2003).

Huge effort towards studying the nucleation process and the identification and characterization of the structures forming prior to fibrils has been made recently. It has been shown that globular proteins need at least partial unfolding to be able to aggregate and form amyloid fibrils (Hamada & Dobson, 2002; Thakur & Rao, 2008). In some cases, the presence of structured oligomers (Quintas *et al.*, 2001) or unstructured aggregates (Modler *et al.*, 2003) has been reported.

2.4.2 Two-step autocatalytic reaction model

A mathematical analysis will permit the quantitative monitoring of the kinetics of fibril formation. The two-step autocatalytic reaction model is the current record of the commonly used model of protein fibril formation and it is also the simplest model offered to date (Morris *et al.*, 2008; Sabate *et al.*, 2003).

This model is an assembly mechanism model based on the nucleation-elongation theory. This two-step mechanism consists of two major reactions.

$$A \xrightarrow{k1} B \quad (1)$$

$$A + B \xrightarrow{k2} 2B \quad (2)$$

Here A represents a molecule of monomeric protein and B is the nucleus or fibril. The reaction A → B represents the monomer or peptide assembly to nucleus of fibril, which is slow, continuous nucleation. This is typically followed by fast, autocatalytic surface growth mechanism, A + B →2B, which represents the addition of a monomer or a peptide adds to nucleus to form elongated fibril (Morris *et al.*, 2008; Sabate *et al.*, 2003).

The reaction A → B and A + B → 2B are possibly composites of hundreds or even thousands of actual elementary steps, so the resultant rate of nucleation, k_1 (h^{-1}) and the rate of elongation, k_2, ($RFU^{-1}h^{-1}$) (RFU, the relative fluorescence unit) are the average values of all the elementary steps (Morris *et al.*, 2008). Note that k_1 is inversely related to the lag time, k_2 is positively related to the maximum growth rate.

After the necessary simplification and assumptions (Morris *et al.*, 2008), the mathematical kinetic equation can be expressed as:

$$[B]_t = [A]_0 - \frac{\frac{k_1}{k_2} + [A]_0}{1 + \frac{k_1}{k_2[A]_0}\exp[t(k_1 + k_2[A]_0)]} \quad (3)$$

$[B]_t$: the concentration of fibrils formed at time t; $[A]_0$: the initial concentration of protein monomer.

It needs to note that the two-step autocatalytic reaction model has some limitations. The main limitation is that the model is an oversimplified phenomenological model of the true, multistep process. It provides average k_1 and k_2 values that may hide important changes in k_1 and k_2 with growing aggregate size. Moreover, B represents all the growing aggregate which will hide the differences in the growing aggregates and protofibrils as a function of their size (Morris *et al.*, 2008).

2.4.3 Fibril formation pathway

The partially folded states of proteins are favoured to form amyloid fibrils (Hamada & Dobson, 2002). In a partially folded state, several pathways are open to the protein, including aggregation or refolding. Moreover, on-pathway intermediates and off-pathway species aggregations occurred during the process of fibril formation. The simultaneous occurrence of random aggregation and amyloid fibril formation has been observed in some studies (Carrotta et al., 2001; Khurana et al., 2001a). The presence of these two pathways results the formation of both amyloid fibrils and spherulites. Those spherulites are characterised as the regular arrangement of polymer chains within them and resulting in the appearance of Maltese cross extinction pattern when studied by polarized light microscope. (Krebs et al., 2005b).

Recent studies have shown that the fibril formation mechanism of β-lactoglobulin, involoves on multiple and competing paths. Worm like and long straight fibrils are formed on two distinct pathways that compete for assembly competent species early in fibril formation (Gosal *et al.*, 2005).

2.4.4 β-Lactoglobulin fibril formation

Fibril formation of β-lactoglobulin is suggested to follow a nucleation-elongation mechanism, as a sigmoidal curve was observed when monitored with ThT florescence assay (Hamada & Dobson, 2002).

There are different opinions on the composition of β-lactoglobulin fibrils. Rogers *et al.* (2006) believed that β-lactoglobulin fibrils are composed of a complete protein, fibril is an ordered joining of monomers in the fibril. However, it was recently reported that not the intact protein of β-lactoglobulin is incorporated in the fibrils, but peptides derived from it by hydrolysis (Akkermans *et al.*, 2008).

β-Lactoglobulin fibril formation was influenced by protein concentration. β-Lactoglobulin fibrillation occurs above a critical concentration. Arnaudov *et al.* (2003) suggested the critical aggregation concentration of β-lactoglobulin was around 2.5 % w/w (pH 2.0 80°C), referring to the β-lactoglobulin concentration where the

conversion was too low to determine with NMR spectroscopy. However, fibril formation does occur at protein concentrations below this. Fibrils were observed from AFM images of 2% and 1% w/w of β-lactoglobulin after heating (80 °C , pH 2.0 and low ionic strength) (Arnaudov *et al.*, 2003). Fibril formation at 0.5 % w/w were studied using transient electric birefringence by Rogers (2006). The β-lactoglobulin conversion extent increased with protein concentration (43% for 0.5% (w/w) and 70% for 4% (w/w)) after prolonged heating (Veerman *et al.* 2002).

.

The rate of β-lactoglobulin fibrillation is strongly influenced by seeding and shearing. Solutions containing preformed fibrils can reduce the lag time and promotes fibril growth (Bolder *et al.*, 2007). The efficiency of seeding appears to be correlated to the similarity in sequence between the added protein and the seeded protein as suggested by experiments where fibrils of a number of proteins were added to a solution of hen lysozyme (Krebs *et al.*, 2004). Enhanced formation of β-lactoglobulin by continuous stirring during heating has also been demonstrated (Akkermans *et al.*, 2006; Bolder *et al.*, 2007).

2.5 Effect of environmental factors on β-lactoglobulin fibril formation

Several environmental factors (ionic strength, solution pH, temperature and protein concentration) have strong impact on β-lactoglobulin fibril formation (Pearce *et al.*, 2007). The impacts are shown on the fibrillation rate, yield of fibrils and the morphology of fibrils. Until now, except NaCl no other salts have been used to study the effect of ionic strength on β-lactoglobulin fibril formation.

2.5.1 Ionic strength

NaCl is an effective accelerator of β-lactoglobulin fibril formation, at constant temperature and pH. Generally, aggregation is faster at higher ionic strengths and the fibril became curvier and shorter (average) with increasing ionic strength (NaCl 0.01-0.10 M) (Arnaudov & de Vries, 2006; Aymard *et al.*, 1996; Durand *et al.*, 2002; Veerman *et al.*, 2002).

Heat-induced β-lactoglobulin fibrils at pH 2 and different ionic strengths have been probed by TEM, SANS and X-ray scattering; rod-like fibrils were observed at low ionic strength (0.013 - 0.03 mM), whereas a fractal structure was suggested at higher ionic strength (0.1 - 0.2 M) (Aymard *et al.*, 1999; Kavanagh *et al.*, 2000b). The dependence of the morphology on ionic strength was later probed by AFM and light scattering (Arnaudov & de Vries, 2006). At ionic strength of 0.013 M, the fibrils were long and straight, whereas the fibrils became short and curly at 0.1M; these two kinds of fibrils were both observed at ionic strength of 0.05 and 0.07M. The thicknesses of the fibrils obtained at different ionic strengths were all about 3.5 nm.

It was believed that with increasing ionic strength, the repulsive interactions between β-lactoglobulin molecules reduced strongly (Aymard *et al.*, 1996; Veerman *et al.*, 2002). It was also found the monomer-dimer equilibrium shifted towards the monomeric form when the ionic strength decreased (Aymard *et al.*, 1996).

2.5.2 pH

At low ionic strength and pH away from the isoelectric point, β-lactoglobulin forms fibrillar aggregates with heating, while at pH values close to the isoelectric point and at high ionic strength, random aggregates are formed. In Figure 2.7 a schematic representation is given of the various structures that can be formed by heating this protein.

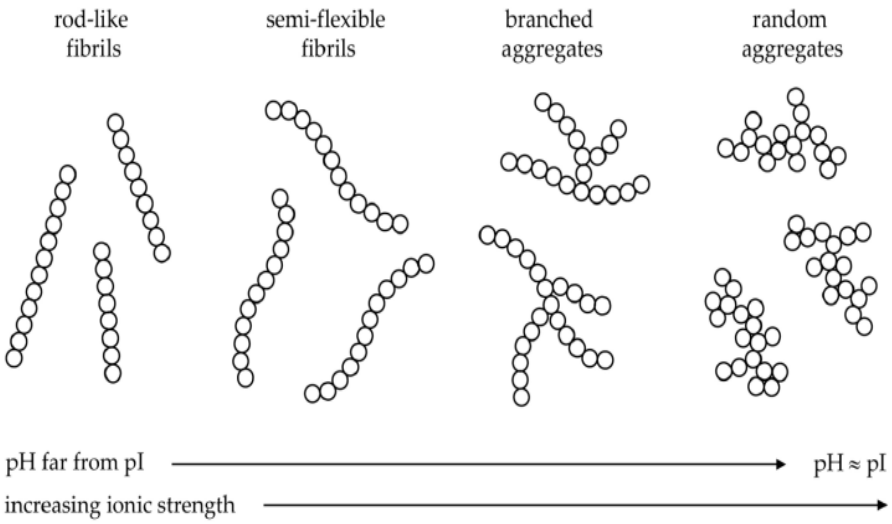

Figure 2.7 Schematic representations of the structures that can be formed by heat-denatured protein as a function of pH and ionic strength. Reproduced from Doi (1993).

Heat-induced β-lactoglobulin (1 wt %) aggregates prepared at different pH (2.0 to 5.8 to 7.0) were studied by Jung *et al*. (2008) using a wide range of techniques, such as SANS, X-ray scattering and TEM. At pH 2.0, thin, rod-like aggregates with the lengths of 1-10 um were observed. By increasing the pH to 5.8, very compact and sphere-like aggregates, with a size about 150 nm, were formed. At pH 7.0, short (<100nm), worm-like aggregates were observed.

It is commonly observed that β-lactoglobulin fibrillation is populated at acidic pH values (Ionescu-Zanetti *et al.*, 1999). Previous studies have examined the fibrils of 3% w/w β-lactoglobulin formed at pH 2.0, 2.5 and 3.0 using TEM, X-ray diffraction and FTIR (Kavanagh *et al.*, 2000b). Their results showed that the length and flexibility of linear aggregate is very sensitive to variations in pH.

The role of low pH in β-lactoglobulin fibril formation has been investigated. β-Lactoglobulin is highly positive charged at low pH (Aymard *et al.*, 1996) and low pH destabilized the protein and accelerated the kinetics of aggregation (Khurana *et al.*, 2001a). At low pH, monomer - dimer equilibrium is shifted in favour of the monomer and the denaturation temperature is higher than at neutral pH (Aymard *et al.*, 1996).

2.5.3 Temperature

High temperature will decrease the stability of the native state and increase the unfolding rate, which will favour the fibrillation process (Sabate *et al.*, 2005). Aymard *et al.* (1996) found the dissociation of dimer increased with increasing temperature (5 - 76°C) and the protein-protein aggregation was fast (Aymard *et al.*, 1996). Not many results have been reported on the impact of temperature on β-lactoglobulin fibril formation; new findings can be anticipated.

2.6 Summary and future prospects

β-Lactoglobulin can form amyloid fibrils under controlled condition, the widely believed fibrillation mechanism is the nucleation-elongation mechanism. Environmental factors (temperature, pH, ionic strength) have strong impacts on β-lactoglobulin fibril formation. They not only influence the kinetics of growth, the morphology of the fibrils but also influence the yield of fibrils.

Knowledge about protein fibril formation can be used to inhibit the disease-related fibrillation of many peptides in *vivo* (Aβ40 and Aβ 42), or to enhance the fibril formation of food proteins as a texture enhancing ingredients. Many questions still remain in this area, such as the detailed fibrillation mechanism, the structure of protein fibril on a molecular level (Nicolai & Durand, 2007). Although some studies about the effects of environmental factors on protein fibril formation have been carried out, most of the studies have focused on the individual effects not the multifactor effects. Meanwhile, much effort is still being spent to improve and optimize the use of protein fibrils in food industry. Protein fibrils with desired properties such as controlled fibril morphology, enhanced stability, and responsive gelation are being studied. This is still a new field; many exciting new findings can be expected.

CHAPTER 3

MATERIALS AND METHODS

The heat-induced fibril formation of β-lactoglobulin was investigated using Thioflavin T fluorescence measurements and transmission electron microscopy.

3.1 Materials and equipment

3.1.1 Materials

β-Lactoglobulin was purchased from SIGMA (90% pure, product no. L0130-5G, lot. no. 078K7430 and 095K7006) containing a mixture of the genetic variants A and B. Deionised water was used throughout. The chemicals used in this study (NaCl, $CaCl_2.2H_2O$, NaH_2PO_4 and Na_2HPO_4) were AnalaR® grade from BDH (Poole, England) and were used as received. The Thioflavin T powder was purchased from Chroma Corp. (McHenry, IL), and stored in the fridge. HCl solution of pH 2.0 was prepared by adding 6M HCl solution to deionised water. Whey protein isolates (WPI) and hydrolysed whey protein (WPH) 1-5 were obtained from Tatua Co-operative Dairy Company Limited and Fonterra Co-operative Group Limited, and used as received. The detailed information of WPI and WPH1-5 are shown in Table 3.1

Table 3.1. WPI and WPH used in this experiment

Protein sample	**Source**
WPI	Control sample Alacen 895 ^{TM}, cypher GQ23, specification 8987 Fonterra
WPH1	HWP202^{TM} Tatua
WPH2	HWP205^{TM} Tatua
WPH3	HWP406^{TM} Tatua
WPH4	NZMP WPH 911^{TM} Fonterra
WPH5	NZMP WPH 916^{TM} Fonterra

3.1.2 Equipment

The equipment and statistical software used in this study are shown in Table 3.2.

Table 3.2 The equipment and software used in this study

Equipment and statistical software		**Application in study**
Centrifuge	Centrifuge 5702, swinging bucket rotor, Global Science	Desalting procedure 3000×g
	Himac CR22G II HITACHI	Super centrifuge, 22600×g
Centrifugal filter Unit	Amicon® Ultra-15, 10KDa, Millipore	Desalting procedure
	Amicon® Ultra- 4, 100KDa, Millipore	TEM sample preparation
Syringe filter	FP0.22 μm syringe filters, Millipore, MillEX® GS Billerica, MA	Protein solution preparation
Syringe	50μl glass syringe fixed needle, HAMILTON® 805N	ThT fluorescence assay
	20mL /cc syringe, TERUMO® Syringe, Philippines	Protein solution preparation
UV spectrophotometer	Ultrospec 2000, Biotech	Protein concentration
Heat block	Dri-Block®, DB-3D and OB-3D TECHNE; Dri-Bath®, DB16525 THERMOLYNE	The temperature and Multi-factors (CCC) experiment
Water bath	W38 Grant, Grant Instruments ltd. England	Fibril formation and the effect of pH, ionic strength
Test tubes	12mL KIMAX® Culture Tubes, with Screw Cap. USA	Contain protein solution in all experiments
Conductivity meter	Personal SC meter, Model SC82 YOKOGAWA	The effect of ionic strength

TEM	Philips CM 10, Eindhoven. The Netherlands	TEM study for all experiments
TEM Grid	Carbon coated FormVar, Agar Scientific Ltd. Stansted, U.K.	TEM study for all experiments
Fluorescence spectrophotometers	FP-6200 FASCO	Multi-factors (CCC) experiment
	RF-1501 SHIMADZU before changing lamp	Individual effect of pH, NaCl experiments
	RF-1501 SHIMADZU after changing lamp	Fibril formation experiments Individual effect of temperature, $CaCl_2$ experiments
Cuvette	Standard fluorescence rectangular quartz cell, 10mm path length, Japan	ThT fluorescence assays for all experiments
pH meter	3510 pH meter JENWAY, Bibby Scientific Ltd, England	All experiments
SigmaPlot 10.0	Systat software, Chicago, IL	Fibril formation, the effect of pH, temperature
Minitab 15.0.	Minitab Inc., State College, PA.	Multi-factors (CCC) experiments

3.1.3 Preparation of β-lactoglobulin solution

The β-lactoglobulin solution preparation procedure as shown in the flow chart (Figure 3.1) was used for all the protein samples in this study.

The β-lactoglobulin powder was firstly dissolved in HCl solution of pH 2.0 then the solution was adjusted to pH 2.0 ± 0.05 using 6 M HCl and left to stir overnight at 4 ºC (magnetic stirring bar, 300 rpm). To remove traces of undissolved protein, the solution was centrifuged at 22,600 g for 30 min and subsequently filtered through a 0.22 μm

syringe filters protein filter. To remove residual salts, the solution was filtered (10 kDa centrifugal filter) against an HCl solution of pH 2.0 for three times (each time for 15 minutes) until the pH and ionic strength of the protein solution were equal to the HCl pH 2.0 buffer (by testing the conductivity of the sample described in Section 3.2.3). Figure 3.1 describes the detailed preparation procedure.

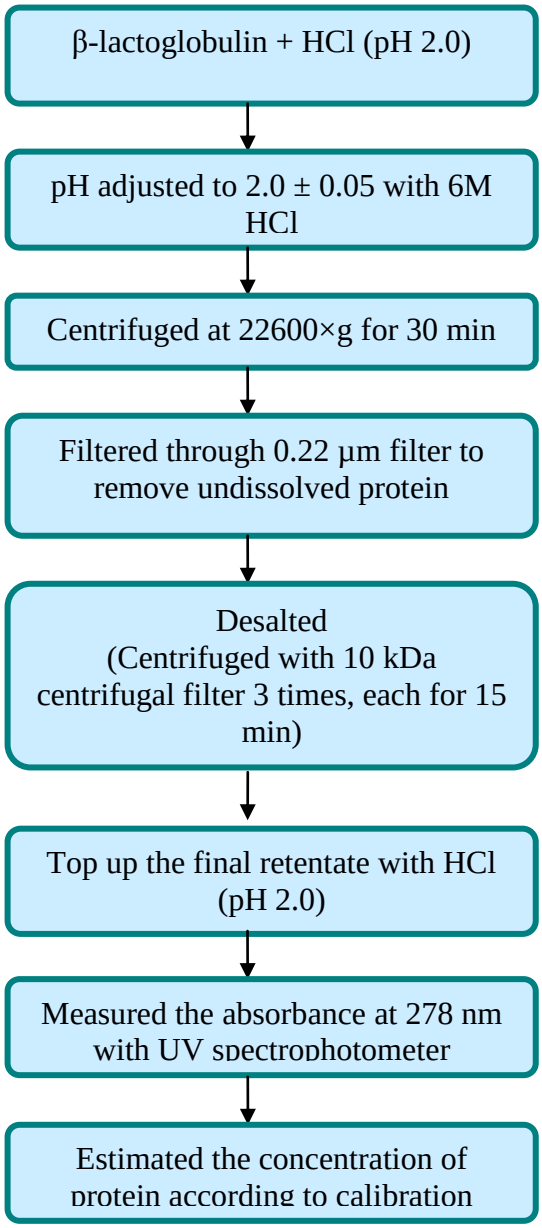

Figure 3.1 Preparation of protein solution

The concentration of the β-lactoglobulin stock solution was determined with a UV spectrophotometer at a wavelength of 278 nm, using a calibration curve of known β-lactoglobulin concentrations (assuming 90% purity of the β-lactoglobulin powder). This is a rapid method of determining the concentration of protein in solution (Bollag *et al.*, 1996). The calibration curves of the two bottles of β-lactoglobulin are shown in Figure 3.2; the raw data are shown in Appendix 3.1.

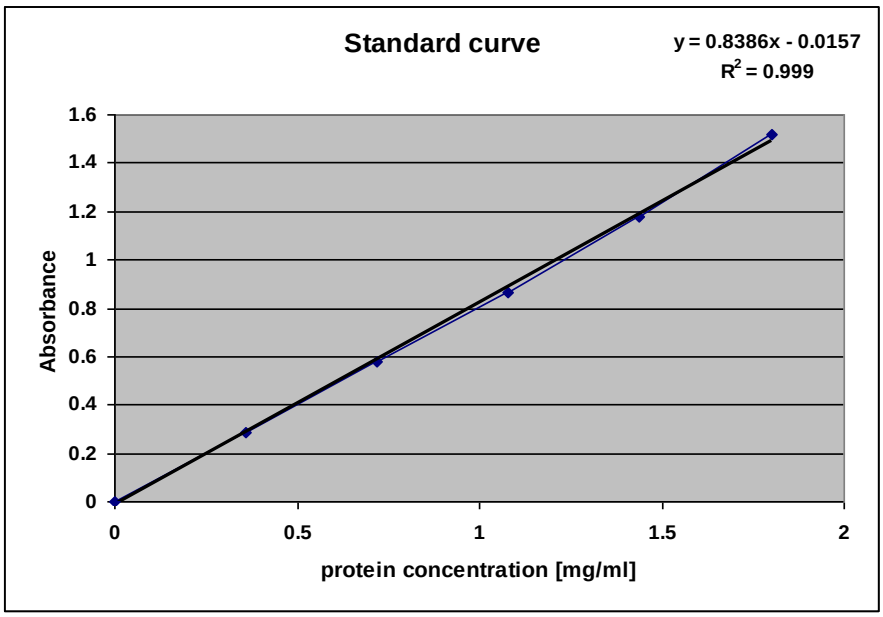

Figure 3.2.a. Calibration curve for protein concentration of β-lactoglobulin bottle 078K7430

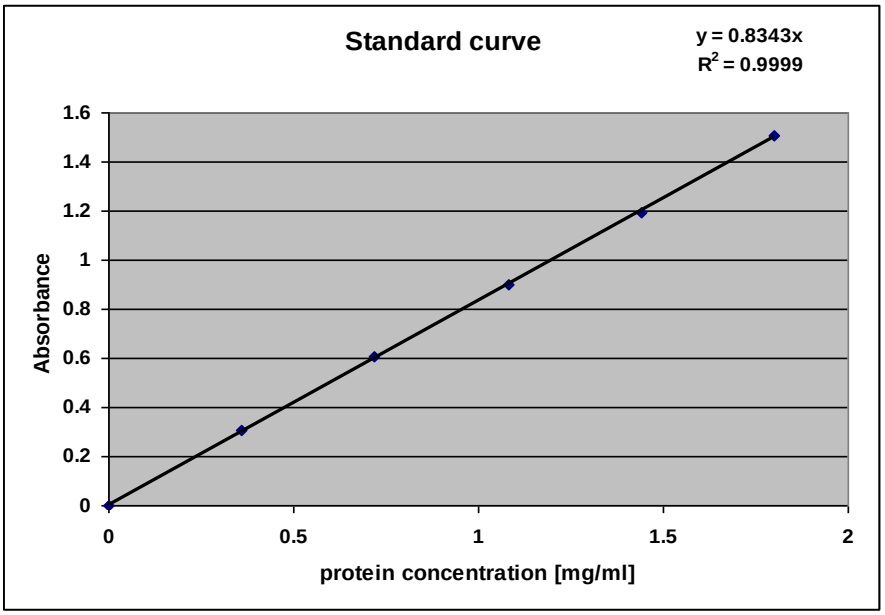

Figure 3.2.b. Calibration curve for protein concentration of β-lactoglobulin bottle 095K7006

The concentration of β-lactoglobulin solution of all samples in this study except Fibril Formation experiments (Chapter 4) was 1 % w/v (protein) and prepared just before use. β-Lactoglobulin concentration at 3.0, 1.0, 0.5 and 0.1% w/v were studied using ThT fluorescence. The results suggested when concentration higher than 1.0 % w/v, large quantities of gel particles were formed while when the concentration was less than 0.5% w/v, no clear enhancement of ThT fluorescence was found. Therefore, concentration of 1.0 % w/v was chosen.

The pH was adjusted by adding mall quantities of 6 M HCl (Section 5.1, The effect of pH on β-lactoglobulin fibril formation). The ionic strength of the solutions was adjusted by adding 1 M NaCl or $CaCl_2$ standard solution (Section 5.2, The effect of ionic strength on β-lactoglobulin fibril formation). The sample preparation of different experiments has been described in detail in the Experimental part of each chapter. Care was taken to minimize dust and contamination for all the experiments. Glassware was cleaned with the detergent (The Pyrogenic Negative Cleaner, Johnson Diversey New Zealand), rinsed repeatedly with deionised water, and dried in a clean environment.

3.2 Methods

3.2.1 Thioflavin T fluorescence assay

Thioflavin T (ThT) fluorescence was used to investigate the total length concentration of fibrils. The preparation of ThT stock solution and working solution are shown in Figure 3.3.

The ThT stock solution was made by dissolving 9.57 mg ThT powder into 10 mL phosphate buffer (10 mM phosphate, 150 mM NaCl, pH 7.0), to obtain a concentration of 3.0 mM, then it was filtered through a FP 0.22 μm syringe filter to remove undissolved particles. The stock solution was put in an amber glass bottle covered with tin foil, and stored at 4 °C; each stock ThT solution was used within one week. The ThT working solution was generated by diluting the stock solution 50-fold into the phosphate buffer (10 mM phosphate, 150 mM Nacl, pH 7.0), the final concentration was 60 μM. Aliquots of the heated protein solutions was added to 4 mL ThT working solution with a 50 μL syringe, then mixed and held at room temperature for 1 minute. In this paper, 48 μL, 24 μL and 12 μL were used for the ThT fluorescence assay of "Effect of protein working solution volume" (Chapter 4), 48 μL was used for the other experiments. The fluorescence of the samples was measured using a fluorescence spectrophotometer. The samples were excited at a wavelength of 440 nm (slit width 10 nm) and subsequent emission was detected between 460-550 nm (slit width 10 nm) at a medium speed. The peak value was determined at 482 nm. The ThT fluorescence intensity (FI) was measured as a function of the heating time of the samples (Bolder *et al.*, 2007a).

Samples were assayed in triplicate. The relative fluorescence intensity of pure ThT working solution, FI0, was subtracted from the fluorescence intensities of the samples to correct the samples for the background intensity. ThT working solution with unheated protein sample, FIp0, was included as a control. The lowest individual replicate of FIp0 was subtracted from FI and resulting FI** (=FI - FIp0) was plotted as a function of the heating time.

Note: The fluorescence intensity of ThT solution might be effected by changing fluorimeter lamp, higher readings are expected by using a new lamp.

3.2.2 Transmission electron microscopy

EM grid preparation and staining

The 200 mesh EM grid was placed carbon side down on a drop of diluted heated protein solution drop for 5 minutes. The excess was removed using a piece of filter paper. To enhance the contrast, the grid was placed onto a droplet of 2 % uranyl acetate (pH 3.8) carbon side down for 5 minute; any excess was removed as before. The grid was covered with a Petri dish and kept at room temperature of 21°C. The sample was then loaded into a sample holder ready for examination by the TEM.

TEM sample preparation

The currently used TEM imaging method was developed based on the previous work in the literature (Bolder *et al.*, 2007b; Veerman *et al.*, 2004). Buffer salts are known to interfere with the negative staining process (Kavanagh *et al.*, 2000b), and the dissolved β-lactoglobulin in the heated protein sample can increase the darkness of the background of the TEM images, so the heated protein sample cannot be used for TEM imaging directly. Two sample preparation methods were tried, one is dilution of the sample to 0.05 % w/v, and the other was to centrifuge the sample with 100 k Da centrifuge filter to remove the dissolved protein and traces of salt. After comparing the TEM results, the filtered protein samples were preferred. A detailed comparison of results is shown in Appendix 3.2.

The centrifugation and filtration procedures for TEM ample preparation is shown in Figure 3.3.

TEM imaging

Images from randomly selected areas of the grid were captured at 19,000-64,000× magnification on a Philips CM 10 transmission electron microscope operating at 80 kV. The TEM images shown in this paper were processed by Adobe Photoshop (8.0) to adjust contrast and size.

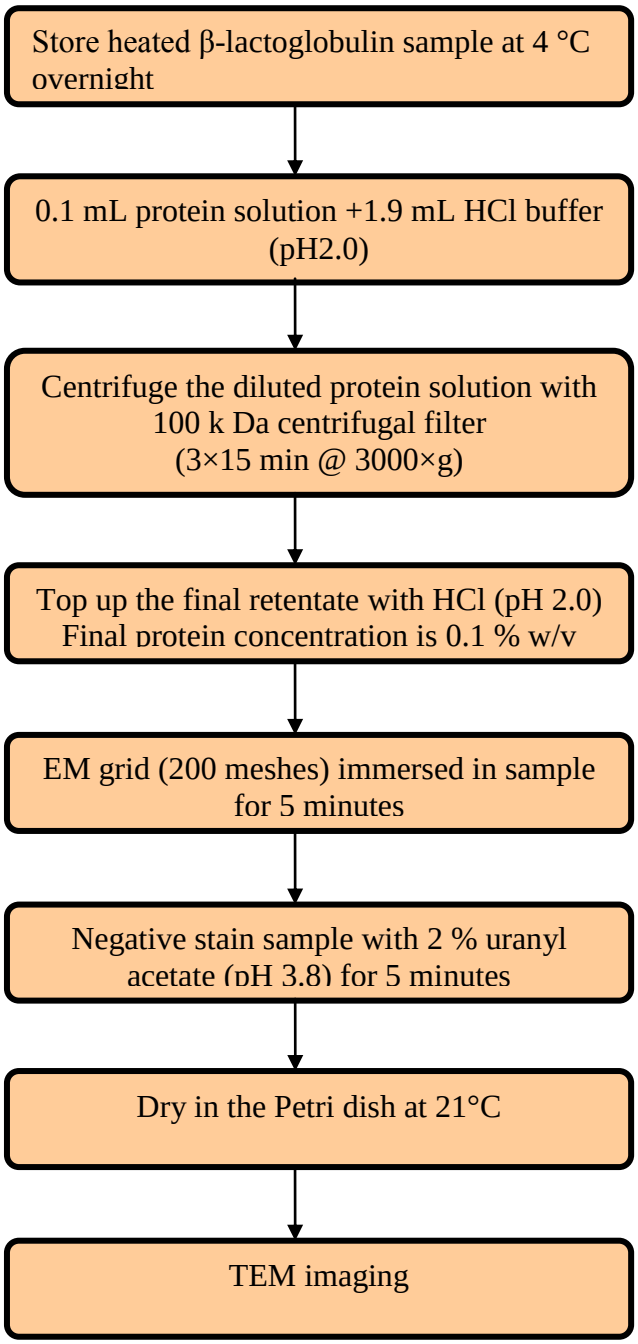

Figure 3.3 Preparation of TEM sample

3.2.3 Conductivity test

The conductivity test was set to investigate the effectiveness of centrifugal filtration steps for removing the salts in protein solution. The 2.5 % w/v protein solution was filtered three times using the 10 kDa centrifugal filter (the same procedure as

described in Section 3.1.3 for preparing protein solution). The conductivity of Milli-Q water, HCl buffer (pH 2.0) and the filtrates was measured with the conductivity meter. The results are shown in Table 3.3.

Table 3. 3 The results of conductivity test

Sample	**Milli-Q water**	**HCl buffer pH 2.0**	**Filtrate 1**	**Filtrate 2**	**Filtrate 3**
Conductivity [µs/cm]	11.29	18.84	46.7	25.1	18.51

The results shown in Table 3.3 suggest that it is necessary to do the centrifugal and filtration process three times to remove the trace of electrolytes in the protein sample solution. Since only after the third centrifugal and filtration step, the conductivity of the protein solution was almost equal to the conductivity of the HCl pH 2.0 buffer.

3.2.4 Statistical analyses

Central Composite Design by using Minitab version 15

A Central Composite Design experiment was used to analyse the effect of the four factors (pH, NaCl, $CaCl_2$ and temperature) on these response variables: ThT fluorescence peak value (FI^{**}_{peak}, the FI** at the end of growth phase) and peak time (the time used to reach FI^{**}_{peak}, peak time = lag time + growth time), obtained from the multi-factors experiment (Chapter 6). Central Composite Design (CCD) is a popular design for modelling and analysis in applications where a response of interest is influenced by several variables. In this study, the Central Composite Circumscribed (CCC) design was adopted which is the original form of the central composite design. Results were analysed using Minitab function "Analyse Response Surface design" and "Analyse Factorial design".

Two –step autocatalytic reaction model fitting by using SigmaPlot version 10.0

The two-step autocatalytic reaction equation (Eq.3, described in Section 2.4) was used to fit the experimental data of ThT fluorescence assay obtained from all experiments except the ionic strength and the multi-factors experiments (Section 5.2 and Chapter 6). The modified fluorescence intensity, FI**, was the response variable, heating time was the independent variable.

The variables and all kinds of parameters that used in SigmaPlot 10.0 are shown in Appendix 3.3.

CHAPTER 4

HEAT-INDUCED FIBRIL FORMATION IN WHEY PROTEIN SOLUTIONS

4.1 Heat-induced β-lactoglobulin fibril formation

4.1.1 Introduction

The most common treatment of β-lactoglobulin solution to induce the formation of fibrils is by prolonged heating above denaturation temperature at low pH and low ionic strength (Akkermans *et al.*, 2006). Once conditions that promote fibril formation are established, the kinetics of the process can be examined by assaying the solution for fibrils at particular times. The enhanced fluorescence emission of ThT on association with amyloid fibrils provides a very convenient method to monitor the kinetics of amyloid fibril formation, and TEM allows the direct imaging of amyloid fibrils.

In this study, the approach used by Bolder *et al.* (2007a) was followed, in which fibril formation was induced by heating at 80°C, at pH 2.0 and low ionic strength (control conditions) for 0 - 24 hours. The kinetics of fibril formation were studied by ThT fluorescence. The morphology of aggregates formed during fibril formation was monitored by TEM. The simple two-step autocatalytic reaction model for nucleation- elongation mechanisms was used to describe the ThT fluorescence data.

The aim of this part of work consists of two parts: First is to study the heat-induced fibril formation method and the ThT fluorescence and TEM techniques to make sure they can be used for β-lactoglobulin fibril formation and characterisation, which will pave the way for the later studies. The second is to investigate the fibrillation kinetics, morphology of aggregates, and two-step autocatalytic reaction model fittings of β-lactoglobulin fibril formation under the control conditions (pH 2.0, 80°C, and low ionic strength). Phase conversation experiment was set out to study the percentage of β-lactoglobulin that converted into fibrils under the control conditions.

4.1.2 Experimental

ThT fluorescence assay: Effect of protein working solution volume

The 2 mL 2.5 % w/v β-lactoglobulin solution prepared as described in Section 3.1.3 was added to each of the two sealed glass tubes (the caps screwed tightly to prevent water evaporation), and heated in a water-bath at 80 ± 1 ºC. The two tubes were removed at 4 and 8 h respectively and cooled with ice-water for 10min, then used for ThT fluorescence assay. Small samples of 48, 24 and 12 µL were taken from the 4h and 8h heated samples (protein working solution) and added to 4mL of the ThT working solution. (48 µL of the heated protein solution was used in all subsequent experiments.)

ThT fluorescence assay: Fibril formation under control conditions

A 2 mL 1% w/v β-lactoglobulin solution (prepared as described in Section 3.1.3) was added to each of the sealed glass tubes and the caps screwed tightly, then heated in a water-bath at 80 ± 1ºC. After specific heating times (0 to 24 hour), each tube was taken out and cooled with ice-water for 10 minutes, then used for ThT fluorescence assay. ThT fluorescence emissions were performed as described in Section 3.2.1.

TEM: Fibril formation under control conditions

β-Lactoglobulin stock solution (1 % w/v protein at pH 2.0 low ionic strength) was heated in a water-bath at 80 ± 1°C for specific times (2h, 3h, 4h, 6h and 18h), then took out and cooled in ice water for 10 minutes. After finishing the ThT measurements, the samples were kept at 4 °C overnight. Next day, the samples were processed and studied using TEM as described in Section 3.2.2.

TEM: Gel particles

β-Lactoglobulin solution (4.4 % w/v protein at pH 2.0 low ionic strength) was heated in a water-bath at 80 ± 1°C for 9h. The gel particles formed in this solution were examined by TEM. The sample preparation method is shown in Appendix 4.1

Phase conversion experiments

The phase conversion experiments were conducted using the centrifugal filtration method used by Bolder (2007b). Three test tubes, containing 2 mL of β-lactoglobulin solution (2 % w/v), were heated at 80± 1 °C in a water bath. After heating for 10 hours, the test tubes were taken out and immediately cooled in ice water for 10min.

To determine the extent of conversion of β-lactoglobulin into aggregates, the 3 samples were diluted 20 fold from 2 % w/v to 0.1 wt% in pH 2.0 HCl buffer (0.1mL protein sample + 1.9 mL HCl 2.0 buffer). Diluted samples (2 mL) were added to 100 kDa centrifugal filters and filtered by centrifuging at 3000 ×g for 15min. The filtrate (Filtrate 1) was weighed and the concentration of non-aggregated protein present in Filtrate 1 was measured with a UV spectrophotometer at a wavelength of 278 nm.

The obtained retentate (Retentate 1) was diluted with pH 2.0 HCl buffer to a total volume of 2 mL. The sample was gently mixed and then centrifuged as above. This step was used to remove non-aggregated material left in Retentate 1. The obtained filtrate (Filtrate 2) was processed as Filtrate 1. The centrifugal filtration step was repeated as described above to obtain Filtrate 3. Filtrate 3 was processed as Filtrate 1 and the final retentate was recovered to a volume of 2 mL with pH 2.0 HCl buffer.

The total quantity of protein in the various fractions was quantified by weighing the fractions and determining the protein concentrations in each fraction with a UV spectrophotometer. The UV absorption coefficient of fibrils and non-assembled peptides is assumed the same as for intact β-Lactoglobulin. An unheated protein sample was included as a control in this experiment and the total protein recovery was in the range of 90–94%. Electron microscopy on the filtrate solutions did not show any fibrils in the filtrates.

$$\text{Fibril \%} = \frac{\text{P(retentate)}}{\text{P(Filtrate1)} + \text{P(Filtrate2)} + \text{P(Filtrate3)} + \text{P(retentate)}} \times 100\%$$

$$\text{Recovery\%} = \frac{\text{P(Filtrate1)} + \text{P(Filtrate2)} + \text{P(Filtrate3)} + \text{P(retentate)}}{\text{P(2ml diluted sample)}} \times 100\%$$

P: the protein contained in each fraction

P (fraction) = (fraction mass × protein concentration of this fraction)

4.1.3 Results and discussion

ThT fluorescence assay: Effect of protein working solution added

The heated protein samples (2.5 % w/v) were added to 4 mL ThT working solution at 12, 24 and 48 µL after heating 4h and 8h. The fluorescence measurements are shown in Figure 4.1.1. It can be seen that FI** (FI - FI_{p0}) increased as the increase of heating time and the amount of protein working solution added. As ThT fluorescence is enhanced upon binding to amyloid fibrils, the result indicated that the quantity of fibrils that appeared in the β-lactoglobulin solutions increased with heating time and the amount of protein working solution (heated protein solution) added.

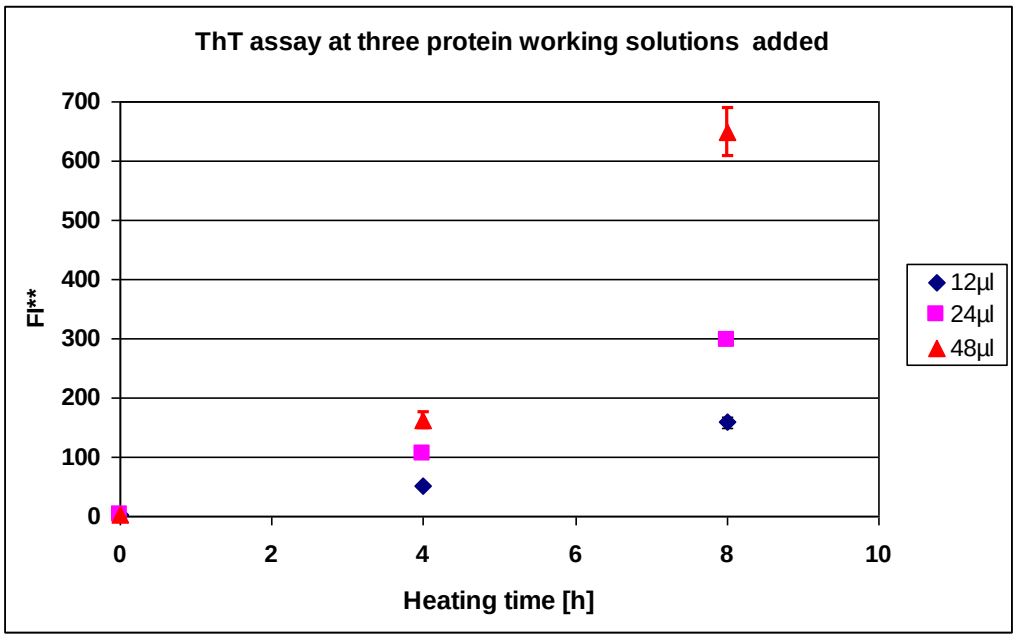

Figure 4.1.1 FI** as a function of heating time for 3 sample sets: 12, 24 and 48 µL working protein solutions (2.5% w/v) added into the 4 mL ThT working solution. Samples were measured in triplicate, the error bars indicate the standard error of the mean (SEM).

The results were re-plotted in Figure 4.1.2 to compare the fluorescence intensity when solutions adjusted to the same dilution factor (48 µL of protein solution to 4mL ThT solution). It shows that the three sets of FI** values are close to each other. The 24 and 12µL samples are almost overlapped. Slight difference was found for the 48 µL sample; this may have been due to the large experimental noise that was caused by the presence of numerous gel particles in the 48 µL sample. Hence, it is possible that the

ThT fluorescence intensity is proportional to the quantity of fibrils appearing in the solution, which is also suggested by other researchers (LeVine III, 1999).

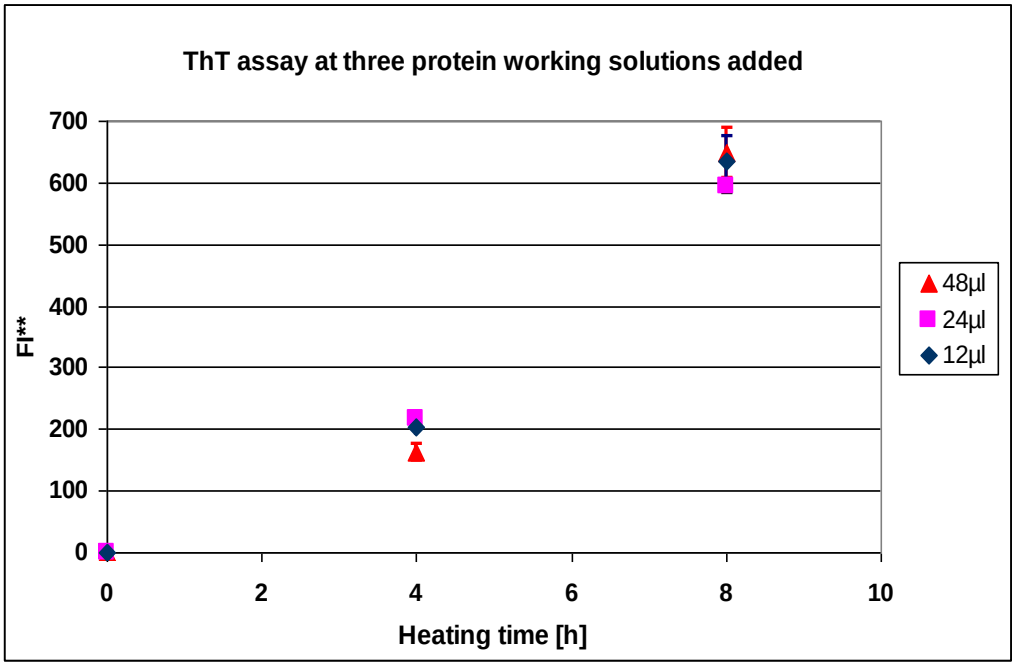

Figure 4.1.2 FI** as a function of heating time for 3 sample sets based on the same dilution factor. Figure 4.1.1 were replotted; adjusted the three trials have the same dilution factor. (FI** of 12 µL ×4; FI** of 24 µL ×2, FI** of 48 µL ×1)

ThT fluorescence assay: Fibril formation under control conditions

In order to study the kinetics of β-lactoglobulin fibril formation under control conditions (80°C, pH 2.0 and low ionic strength), the fibril formation process was monitored with ThT fluorescence. Two individual trials were carried out and the measurements were plotted in Figure 4.1.3.

Figure 4.1.3 illustrates the sigmoidal increase in ThT fluorescence upon β-lactoglobulin fibril formation. Sigmoidal behaviour is commonly observed for protein fibrillation (Hamada & Dobson, 2002; Khurana *et al.*, 2001a). Such curve is described by a lag phase, a subsequent growth phase and a final stationary phase. As can be seen in this figure, the lag phase extends to around 2 hours after which, ThT fluorescence shows a rapid and steady increase up to 12h. After the growth phase, ThT fluorescence increased slowly and finally levelled off at around 16h, which means the completion of the fibril formation process .

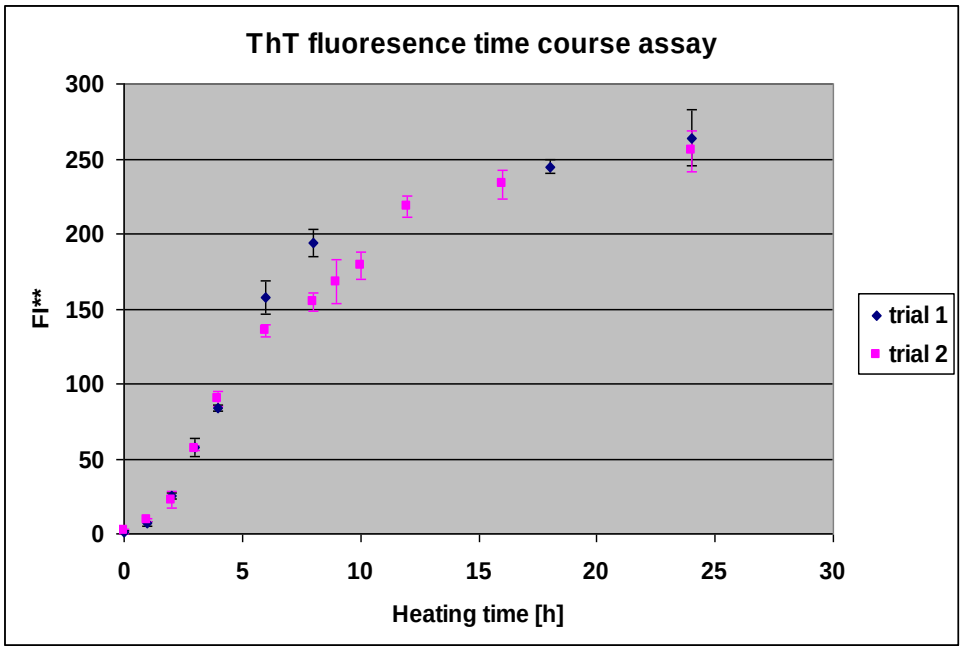

Figure 4.1.3 FI**, as a function of heating time for individual trials. The samples were at the same protein concentration, 1 % w/v, and incubated under the control conditions (80°C, pH 2.0, low ionic strength). Samples were measured in triplicate. The error bars indicate the standard error of mean (SEM).

TEM and sample appearance: Fibril formation under control conditions

To follow the fibril formation process, fibril morphology was then monitored as a function of time using TEM. TEM images were taken after heating the sample for 2, 3 4, 6 and 18 hours (Figure 4.1.4). As expected, almost no linear aggregates can be observed from the 2-h TEM image; most of the aggregates are small round particles (shown with red circles). No gel particles were found in the protein solution when the 2-h sample was visually checked. Many short linear aggregates of various sizes were present on the 3-h images, more and longer linear aggregates were formed after heating for 4 and 6 hours and long fibrils eventually dominated the 18-h image. The photographs taken at each time interval show that the quantity of the transparent gel (shown with blue circles) and the viscosity of the protein solutions (observed by shaking the sample in tube) increased with heating time.

It should be noted that small round aggregates were formed in addition of fibrils. They were present in the 2-h image and the quantity of them did not show a clear increase on the later images. It is not clear whether the small round aggregates observed in the early stage were on-pathway amyloidogenic oligomers or off-pathway aggregates. The

proportion of the shorter linear aggregates decreased with longer heating time. It appears that the long fibrils at the later stage were elongated from the shorter fibrils formed at the early stage.

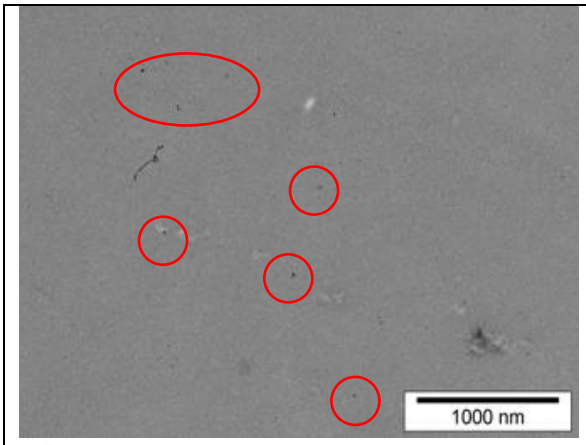 2-h	 Transparent solution without gel
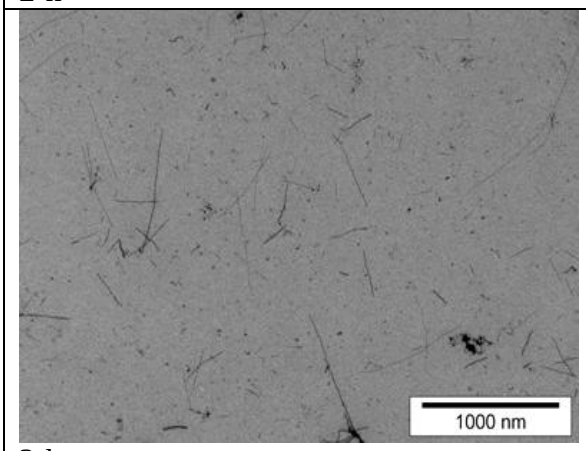 3-h	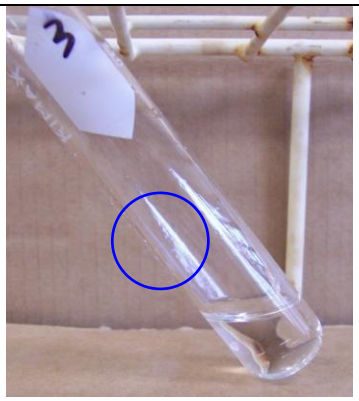 Transparent solution, a few gel particles adhering to the tube wall
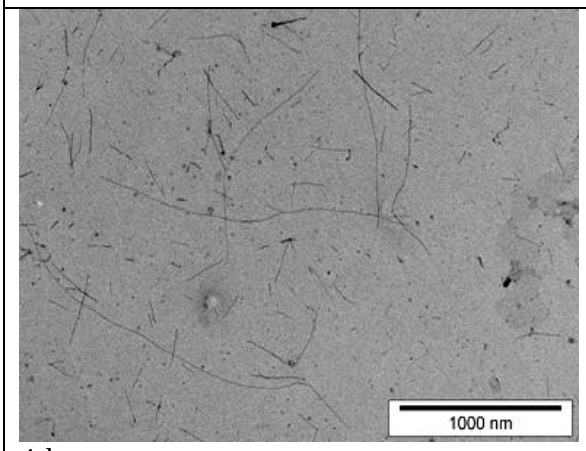 4-h	 Transparent solution with many gel particles adhering to the tube wall

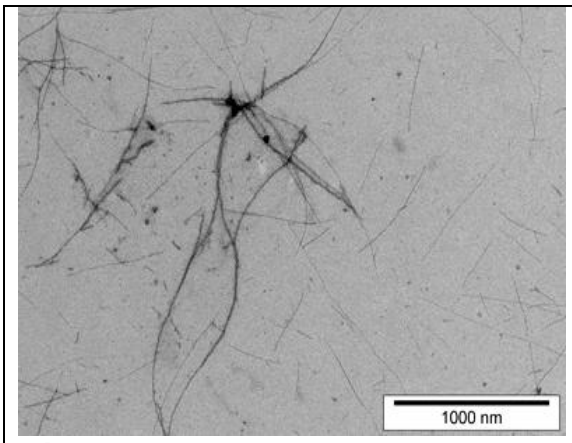

6-h

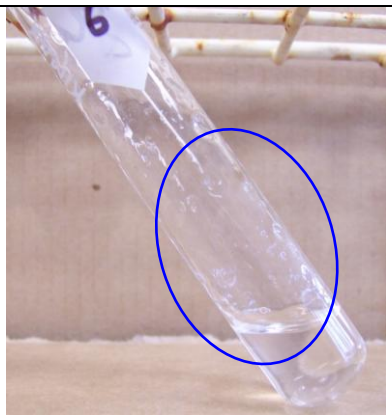

Transparent solution with many clumps of gel particles adhering to the tube wall

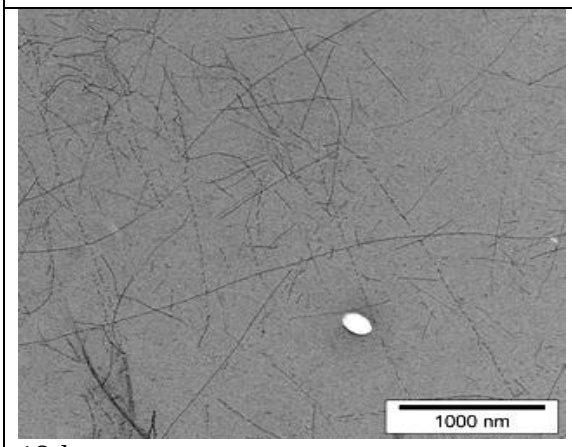

18-h

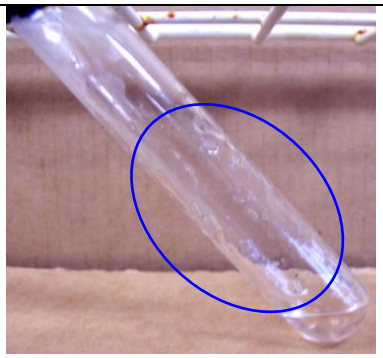

Transparent solution with numerous clumps of gel particles adhering to the wall of the tube

Figure 4.1.4 Negatively stained TEM images of 1% w/v β-lactoglobulin aggregation after heating for different times. Samples were obtained under the control conditions (pH 2.0, 80°C, low ionic strength).

The results from ThT fluorescence assay and TEM imaging of β-lactoglobulin fibril formation under control conditions suggest that no or very few fibrils were formed in the first 2 hours of heating. Fibrils grew quickly between 3 and 12 hours, and then the formation process slowed down. Extended incubation to 24 hours had no clear effect. The slight increase after heating for 16 hours might not have been caused by the increase of fibril but may due to the water loss after prolonged heating. Water loss from screw capped tubes during heating for 27 hours at 80 °C was measured by weighing tubes (Appendix 5.3.1). The average water loss was 0.003 g/hour.

In general, the TEM observations corresponded well with the ThT fluorescence results. TEM images demonstrated the presence of fibrils in systems with high ThT fluorescence and their absence in samples with no increase in ThT fluorescence.

TEM: Gel particles

The gel particles that formed at higher β-lactoglobulin concentration (4.4 % w/v) were studied by TEM, the images are shown in Appendix 4.1. Two types of gel structure were observed, which can be described in terms of finely stranded and particulate gels. Such observations are in agreement with the literature (Kavanagh *et al.*, 2000b; Nicolai & Durand, 2007; Sittikijyothin *et al.*, 2007). The TEM study of gel particles showed that most of the gels formed in solution consisted of amyloid fibrils.

Morphology of aggregates

A closer inspection of the β-lactoglobulin aggregates is shown in Figure 4.1.5. The image was taken after incubation under control conditions for 10 hours. Several different types of aggregates are visible in this image including fibrils and small round aggregates of various sizes. The main coexisting species are:

1. Un-branched, rope-like semi-flexible fibrils (from less than one micrometer to several micrometers in length and a few nanometres in width).

2. Small round aggregates of various sizes.

The small fibrils (yellow arrow marked) were also observed by other researchers who measured the dimensions of the fibrils (100-500nm long and, a few nanometres wide) (Gosal *et al.*, 2001). A very small number of larger fibrils were also seen (blue arrow marked), apparently assembled from two fibrils. It was unclear, whether these fibrils were joined or simply arose from an overlaying of two separate fibrils. It is recommended to measure the height of the fibrils by AFM to distinguish if it was genuine or simply an overlaying of two small fibrils.

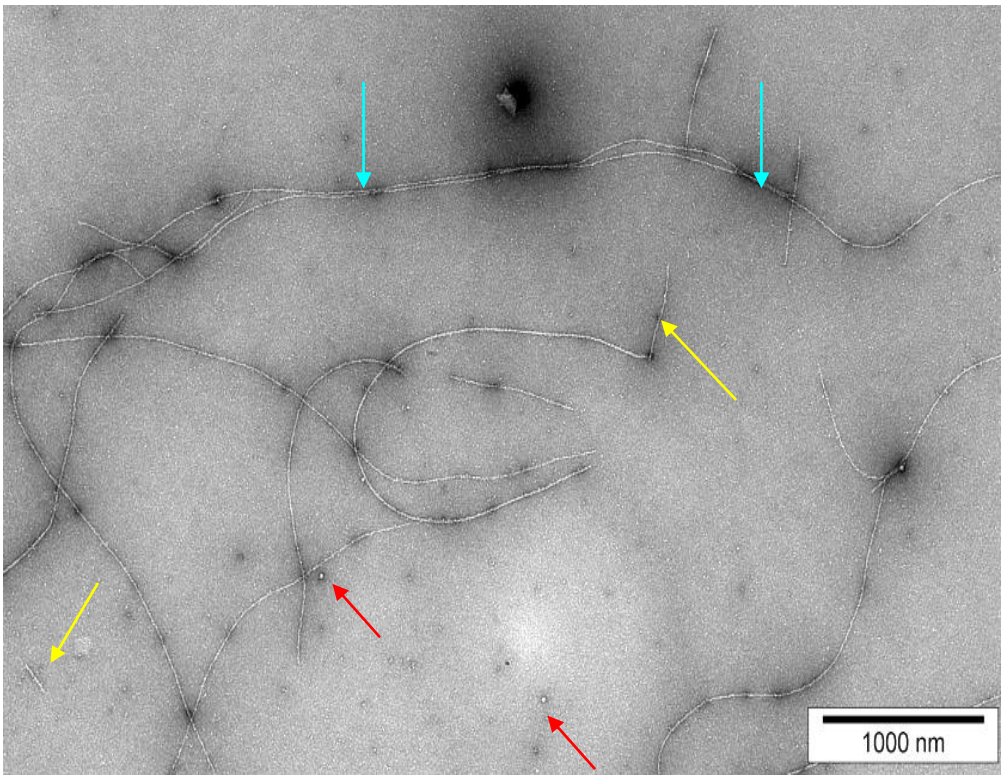

Figure 4.1.5 Negatively stained TEM image of 1 % w/v β-lactoglobulin incubated at 80°C, pH 2.0 for 10h. This image illustrates the diversity of morphologies commonly exhibited by β-lactoglobulin. The image shows the presence of small round aggregates (red arrows), small fibrils (yellow arrows) and big fibrils (blue arrows).

The small round particles appeared earlier than the fibrilar aggregates, and can be seen in the 2h images (Figure 4.1.6). Although there is no direct evidence that the lateral aggregation was from these small species, some of them might be on-pathway amyloidogenic oligomers which can grow to fibrils (blue arrow). However, it should be noted that since the TEM image is an invasive technique, some objects on an EM grid may be artefacts.

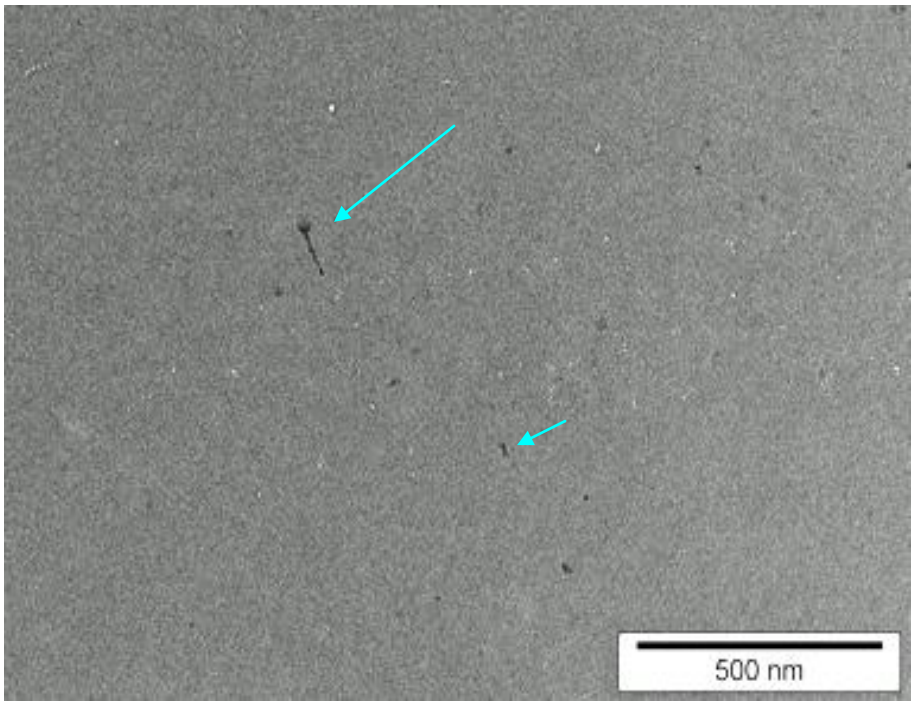

Figure 4.1.6 Negatively stained TEM image of 1 % w/v β-lactoglobulin fibrils formed at 80°C, pH 2.0 for 2h. This image shows fibril 'sprouts' from small round aggregates (blue arrows).

Two-step autocatalytic reaction model fitting

The two-step autocatalytic reaction model (introduced in Section 2.4.2) was adopted to analyse the ThT fluorescence assay data of fibril formation under control conditions. The experimental data (FI** as a function of time) were fitted with Eq. (3) using SigmPlot 10.0.

$$[B]_t = [A]_0 - \frac{\frac{k_1}{k_2} + [A]_0}{1 + \frac{k_1}{k_2[A]_0}\exp\left[t\left(k_1 + k_2[A]_0\right)\right]} \qquad (3)$$

$[B]_t$: the concentration of fibrils formed at time t; $[A]_0$: the initial concentration of protein monomer.

Figure 4.1.7 shows the fitted plots. The model fitting results including the estimated nucleation constant k_1 (h^{-1}) and elongation constant, k_2 ($RFU^{-1}h^{-1}$) were summarised in Table 4.1.1.

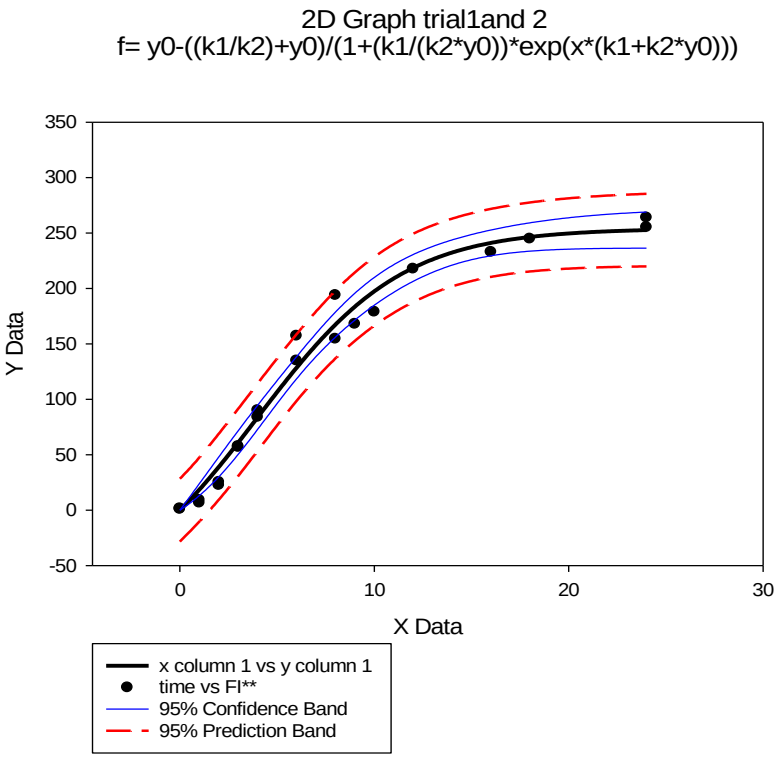

Figure 4.1.7 Two-step autocatalytic reaction model fitting of 1 % w/v β-lactoglobulin under control conditions using SigmaPlot 10.0. The dots represent FI** determined experimentally, and the dark line in the middle is the fitted sigmoidal curve according to Eq. (3).

From Figure 4.1.7, it can be seen that the lag time was short. This observation is agree with Arnaudov's findings that the aggregation of β-lactoglobulin occurred quickly under control conditions (pH 2, 80°C and very low ionic strength) (Arnaudov *et al.*, 2003). When compared to other fibril-forming proteins, such as insulin and hen egg-white lysozyme (HEWL), the lag time of β-lactoglobulin is much shorter, while the growth time is longer (Mishra *et al.*, 2007; Nielsen *et al.*, 2001; Sabate *et al.*, 2003).

Table 4.1.1 Model fitting results of fibril formation under control conditions

Parameter	Value	StdErr	CV (%)	Dependencies	Rsqr
k_1 [h^{-1}]	6.86E-02	1.09E-02	1.59E+01	0.867432	0.9810
k_2 [$RFU^{-1}h^{-1}$]	7.84E-04	2.34E-04	2.99E+01	0.921413	

The fibril formation of β-lactoglobulin afforded a nucleation constant of 6.86E-02 h^{-1}, and an elongation constant of 7.84E-04 $RFU^{-1}h^{-1}$. The Rsqr (0.98) is very high, but the dependency of the two constants is also high, which means that the two parameters are

highly dependent to each other. The detailed statistical analysis report is shown in Appendix 4.2.

Generally, the model fitted the ThT fluorescence intensity (FI**) well, yielding useful kinetic information of the time dependence of fibril formation. Although the model gave very good fits for the ThT kinetic profiles, the expression of Eq. (3) should be considered as an empirical approximation of the underlying kinetic scheme.

Phase conversion

Phase conversion was defined as the percentage of aggregated β-lactoglobulin (>100kDa). The conversion of β-lactoglobulin under control conditions was studied as a function of washing and centrifugation steps, using the centrifugal filtration method. The conversion for 2 % w/v β-lactoglobulin after heating 10h at 80°C is shown in Figure 4.1.8, as determined after subsequent washing and centrifugation steps.

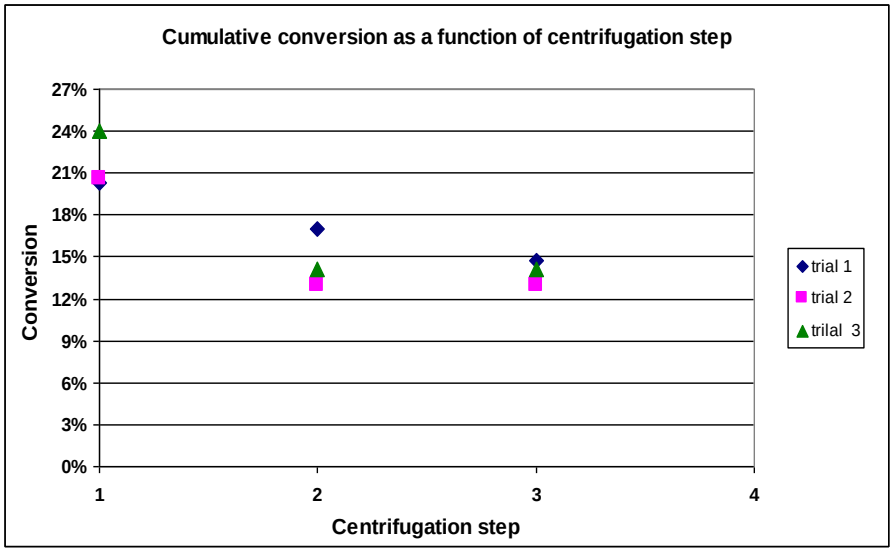

Figure 4.1.8 Aggregated protein as a function of centrifugation steps. 2 % w/v protein samples were incubated at pH 2.0, 80°C for 10 hours.

The plot shows repeated washing and centrifugation steps, the extent of conversion decreased, showing that non-aggregated β-lactoglobulin material (<100k Da) was washed out in the subsequent washing and centrifugation steps. The protein material that was left in the retentate was the larger aggregates (linear or spherical aggregates) which could not pass the 100 kDa centrifuge filter, while the non-aggregated β-lactoglobulin material was collected in the filtrates. This was confirmed by the TEM imaging, no fibrils or large particles were observed from the filtrate sample image.

The final conversion value, 14%, presented here is very close to the conversion value reported by Bolder *et al*. (2007b), which was around 17% of 4% WPI.

The results obtained from this conversion experiment support findings by Akkermans *et al.* (2008) that suggest that it is not the intact protein incorporated in the fibrils, but are the peptides derived from it by hydrolysis.

4.1.4 Conclusions

Together with the results from ThT fluorescence assay and TEM imaging, it was found that fibrillar aggregates can be readily formed by incubating β-lactoglobulin under control conditions (pH 2.0, 80°C, low ionic strength) for 2 - 24h. TEM images revealed the existence of well-defined fibrils. These fibrils were long, thin, semiflexible, and coexisted with small round particles after incubation. Transparent gels appeared in protein solutions after long heating time. TEM observations showed that they consisted of fibrils.

This study also demonstrated how fibril formation can be monitored by ThT fluorescence and TEM imaging. The measurements of ThT fluorescent and the observations of TEM are consistent. All these indicate that ThT dye binding and TEM imaging are good techniques for characterising protein fibril formation under the control conditions.

It was found that the two-step autocatalytic reaction model fitted the ThT fluorescence assay data very well; hence it is suggested that this model can provide useful kinetic information for β-lactoglobulin fibril formation under control conditions.

Phase conversion experiments were used to estimate the extent of β-lactoglobulin that converted to aggregates (> 100 kDa) under experimental conditions. The experimental results were close to those of Bloder *et al.* (2007c) under similar conditions.

4.2 Heat-induced WPI and WPH fibril formation

4.2.1 Introduction

Amyloid fibrils of whey protein isolate (WPI) can be obtained by heating the protein at pH 2 above denaturation temperature for several hours (Bolder *et al.*, 2006; Ikeda & Morris, 2002). Bolder *et al.* (2007b) found that β-lactoglobulin is the only whey protein involved in fibril formation in WPI. By analysing with HPLC and SDS-PAGE, Bolder *et al.* (2007b) believed that mild hydrolysis of the whey protein occurred after prolonged heating at 80 °C at pH 2. So the hydrolysed whey protein (WPH) products may have the ability to form fibrils under the same conditions.

Pure β-lactoglobulin is expensive and not commonly used in food industry, while WPI and WPH are widely used commercial whey protein ingredients. In this study, WPI and WPH1-5 (introduced in Section 3.1.1) samples were studied by ThT fluorescence to investigate their ability in forming amyloid fibrils by using the same experimental method as used for β-lactoglobulin under control conditions.

4.2.2 Experimental

Preparation of protein solution

3% w/v of protein solutions were prepared by adding 0.3 g protein powder into 10mL of pH 2.0 HCl buffer. The pH value of each solution was measured and adjusted to 2.0 ± 0.05 with 6M HCl. After stirring overnight, the solutions were centrifuged at 226000×g for 30 minutes and passed through a 0.22μm syringe filter. The final protein concentration was measured by UV spectrophotometer at 278 nm, the preparation procedure were the same as that prepared for β-lactoglobulin (described in Section 3.1.3).

ThT fluorescence assay for fibril formation under control conditions

2 mL of β-lactoglobulin solution was added to the sealed glass tubes and the caps screwed tightly. The water-bath was preheated to 80 ± 1ºC; the tubes were then placed in the water-bath. The tubes were taken out at designated times (0, 2, 4, 6, 8h) and cooled with ice-water for 10 minutes, then used for ThT fluorescence assay. ThT fluorescence measurements were performed as described in Section 3.2.1

4.2.3 Results and discussion

Solubility of the protein samples

The pH value of all samples was measured directly after dissolving (before adjust to pH 2.0 with 6M HCl). It can be seen from Table 4.2.1 that the pH values of WPH 1-5 were higher than the pH of WPI. The final protein concentrations of the samples were different to each other although they were prepared at the same concentration, 3 % w/v, which means the solubility of each protein sample was different. The results in Table 4.2.1 indicate that the solubility of WPH samples was closely related to their pH value; solubility increased with increasing pH.

Table 4.2.1 pH (before adjustment) and solubility of protein solutions

Protein	**pH before adjustment**	**Final concentration before heat treatment [% w/v]**
WPH3	5.6	2.93
WPH2	5.04	2.27
WPH1	5.01	1.99
WPH5	4.98	1.77
WPH4	4.09	1.29
WPI	4.08	2.73

ThT fluorescence assay under control conditions

The aggregation process of WPI and WPH1-5 was monitored by ThT fluorescence. All samples except WPI showed no increase in ThT fluorescence intensity during heat incubation from 0 to 8h (Figure 4.2.1).

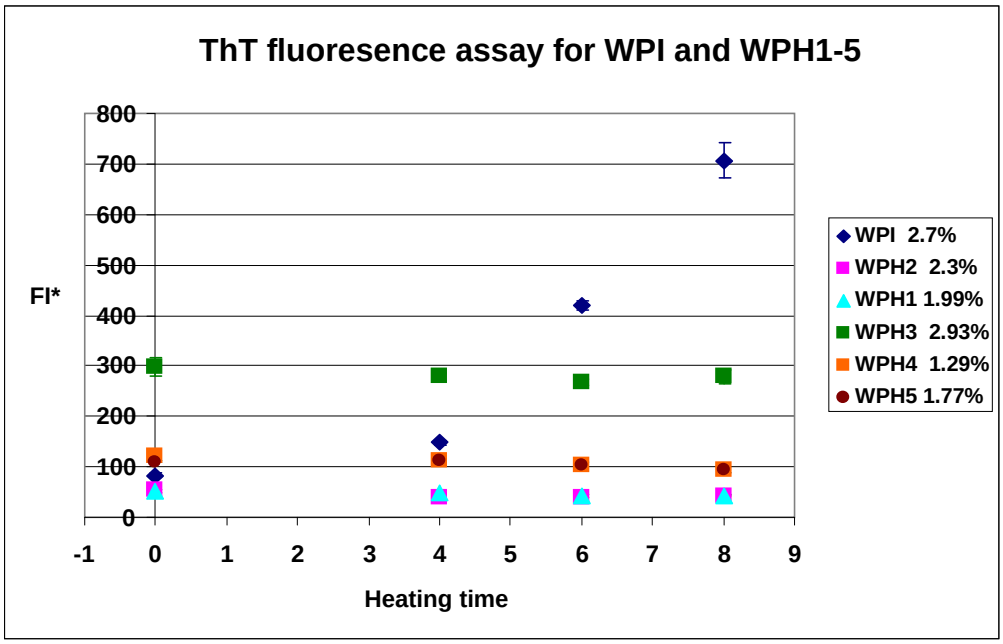

Figure 4.2.1 FI* (= FI- FI_0) as a function of heating time for WPI and WPH (1-5). All the samples were incubated at 80°C pH 2.0. Samples were measured in triplicate. Error bars indicate the standard error of the mean (SEM).

From Figure 4.2.1 it can be seen that the ThT fluorescence intensity (FI*) of WPI increased with heating time, which is similar to the behaviour of β-lactoglobulin in ThT fluorescence assay (Figure 4.1.3). The enhancement on ThT fluorescence of WPI solution indicated the presence of amyloid structures in WPI solution after heating.

The original WPH3 solution shows a high ThT fluorescence value, but no increase was detected after heating, which could be explained by the rich content of β-sheet in original WHP3 sample, and no more amyloid structures were formed during incubation. The ThT fluorescence results demonstrated the presence of fibrils in solution of WPI with high ThT fluorescence and their absence in WPH samples with no increase in ThT fluorescence.

4.2.3 Conclusions

The results indicate that WPI can form fibrils but no hydrolysed commercial samples can produce adequate fibrils. Therefore WPI has the possibility to instead of pure β-lactoglobulin to produce fibrils in the food industry. Further fruitful information using minor hydrolysis to form fibrils is expected.

CHAPTER 5

EFFECTS OF INDIVIDUAL FACTORS ON β-LACTOGLOBULIN FIBRIL FORMATION

5.1 Effect of pH on fibril formation

5.1.1 Introduction

It has been shown that β-lactoglobulin can form amyloid fibrils under a wide variety of conditions (Gosal *et al.*, 2001; Hamada & Dobson, 2002; Veerman *et al.*, 2002). The shape and properties of the aggregates depend on pH and ionic strength (Aymard *et al.*, 1996). At low ionic strength, away from the isoelectric point, the heated β-lactoglobulin solution forms fibrillar aggregates, while at pH values close to the isoelectric point and at high ionic strength, random aggregates are formed (van der Linden & Venema, 2007).

Previous studies have examined the fibrils formed at pH 2.0, 2.5 and 3.0 using TEM, X-ray diffraction and FTIR (Kavanagh *et al.*, 2000b). Their results showed that the length and flexibility of linear aggregate are very sensitive to variations in pH. Although formation of β-lactoglobulin fibrils at an acidic pH has been extensively studied, a detailed study of the effect of pH on fibril formation at lower pH (<2.0) has not been reported.

In this study, β-lactoglobulin solutions (1% w/v) were incubated at pH 1.6, 1.8, 2.0, 2.2 and 2.4 at 80 °C at very low ionic strength. Fibril formation was monitored by Thioflavin T (ThT) fluorescence. The two-step autocatalytic reaction model was fitted to the ThT fluorescence data. The effect of pH on the kinetic parameters (k_1 and k_2) in the pH range of 1.6-2.4 was assessed. TEM was used to examine the morphology of the aggregates formed.

5.1.2 Experimental

ThT fluorescence assay

A 1 % w/v β-lactoglobulin solution (prepared as shown in Section 3.1.3) was divided into 5 bottles and adjusted to the pH values (± 0.05) shown in Table 5.1.1with 6M HCl solution (slight difference in protein concentration may be caused by pH adjustment). 2 mL of each solution at desired pH value was put into the sealed glass tubes (the caps screwed tightly to prevent water evaporation) and heated in a water bath at 80 ± 1 ºC. The tubes were taken out at designated time points shown in Table 5.1.1 and cooled with ice-water for 10 minutes, then used for ThT fluorescence assay. ThT fluorescence measurements were performed as described in Section 3.2.1.

TEM

After finishing the ThT measurements, the 4h and 6h protein samples (without the sample at pH 2.0) were kept at 4 °C overnight. The samples were then processed and examined by TEM as described in Section 3.2.2.

Table 5.1.1 Sample treatments for the pH experiments

Incubation pH	Heating times [h]	TEM times [h]	ThT fluorescence assaytimes [h]
1.6	0, 2, 3, 4, 5, 6, 8	4, 6	all heating times
1.8	0, 2, 3, 4, 5, 6, 8, 24	4, 6	all heating times
2.0	0, 2, 3, 4, 5, 6, 8, 24	No data	all heating times
2.2	0, 2, 3, 4, 5, 6, 8, 24	4, 6	all heating times
2.4	0, 2, 3, 4, 5, 6, 8, 24	4, 6	all heating times

5.1.3 Results

Sample appearance in tube

During heat treatment, transparent aggregate solutions were obtained from all the samples. A few small gel particles (weak gel particles) first appeared in the solutions of pH 1.6, 1.8 and 2.0 after heating for 3 hours, and they were first observed in the solutions of pH 2.2 and 2.4 after heating for 5 hours. The quantity of gel particles increased with heating time (data not shown). These phenomena were also observed by other researchers but at higher protein concentrations (Aymard *et al.*, 1999; Kavanagh *et al.*, 2000a).

ThT fluorescence assay

β-Lactoglobulin fibrils, formed at pH 1.6, 1.8, 2.0, 2.2 and 2.4 were monitored by Thioflavin T fluorescence. The results are plotted in Figure 5.1.1.

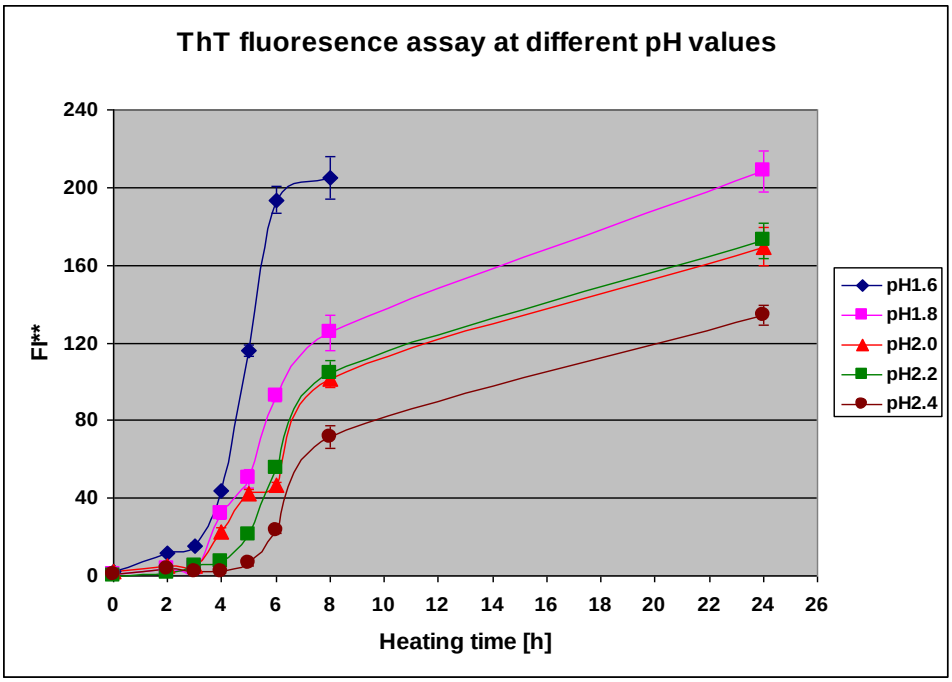

Figure 5.1.1. Effect of pH on fibril formation of β-lactoglobulin(1 % w/v). All the samples were incubated at 80°C. Samples were measured in triplicate, error bars indicate the standard error of mean (SEM).

As can be seen from Figure 5.1.1, the lag time and the growth rate of fibril formation were both affected by pH. The length of the lag time (the FI** was less than 10% of the maximum FI**) was found to be very sensitive to the variation of pH. The lag

time was shortened from 5 hours at pH 2.4 to around 4 hours at pH 2.2 and reduced to approximately 2 hours at pH 1.6. The results suggest that increasing pH leads to a longer lag time.

The growth rate reached a maximum at pH 1.6 and it attained saturation within 6 hours. Comparing to the growth at pH 1.6, the growth for the other four samples did not halt even after heating for 8 hours. It is interesting to note that although at pH 2.4 the lag time is very long (5 hour), when the fibrillation enter the growth phase it increases very rapidly. The quantity of fibrils yielded after heating for 24 hours was also slightly influenced by the incubation pH; yield was higher at lower pH conditions.

Two-step autocatalytic reaction model fitting

The pH-dependence on β-lactoglobulin fibril formation kinetics was estimated by fitting the ThT florescence experimental data with Eq. (3), using SigmaPlot 10.0. The detailed analytical results are shown in Appendix 5.1

$$[B]_t = [A]_0 - \frac{\frac{k_1}{k_2} + [A]_0}{1 + \frac{k_1}{k_2[A]_0}\exp\left[t\left(k_1 + k_2[A]_0\right)\right]} \tag{3}$$

The sigmoidal curve fitted plots of sample at pH 1.6, 1.8, 2.0, 2.2 and 2.4 are shown in Figure 5.1.2**.** All samples, regardless of the variation of pH gave very good fit (Rsqr>0.95), which indicates that varying pH from 1.6 to 2.4 did not appear to influence the undergoing mechanisms (nucleation-elongation) of fibril formation.

Although the ThT fluorescence data fitted the sigmoidal curve well in general, there are some questions concerning the model fitting analysis. The first question is the high values of VIF at pH 1.6 (VIF>10, Appendix 5.1), which means the two estimated reaction constants, k_1 and k_2, were highly dependent on each other. The second question is the less fit of the lag phase for sample at pH 1.6. The third question is the lack of data at the shoulder stage (9-14h), which reduces the reliability of the model fitting.

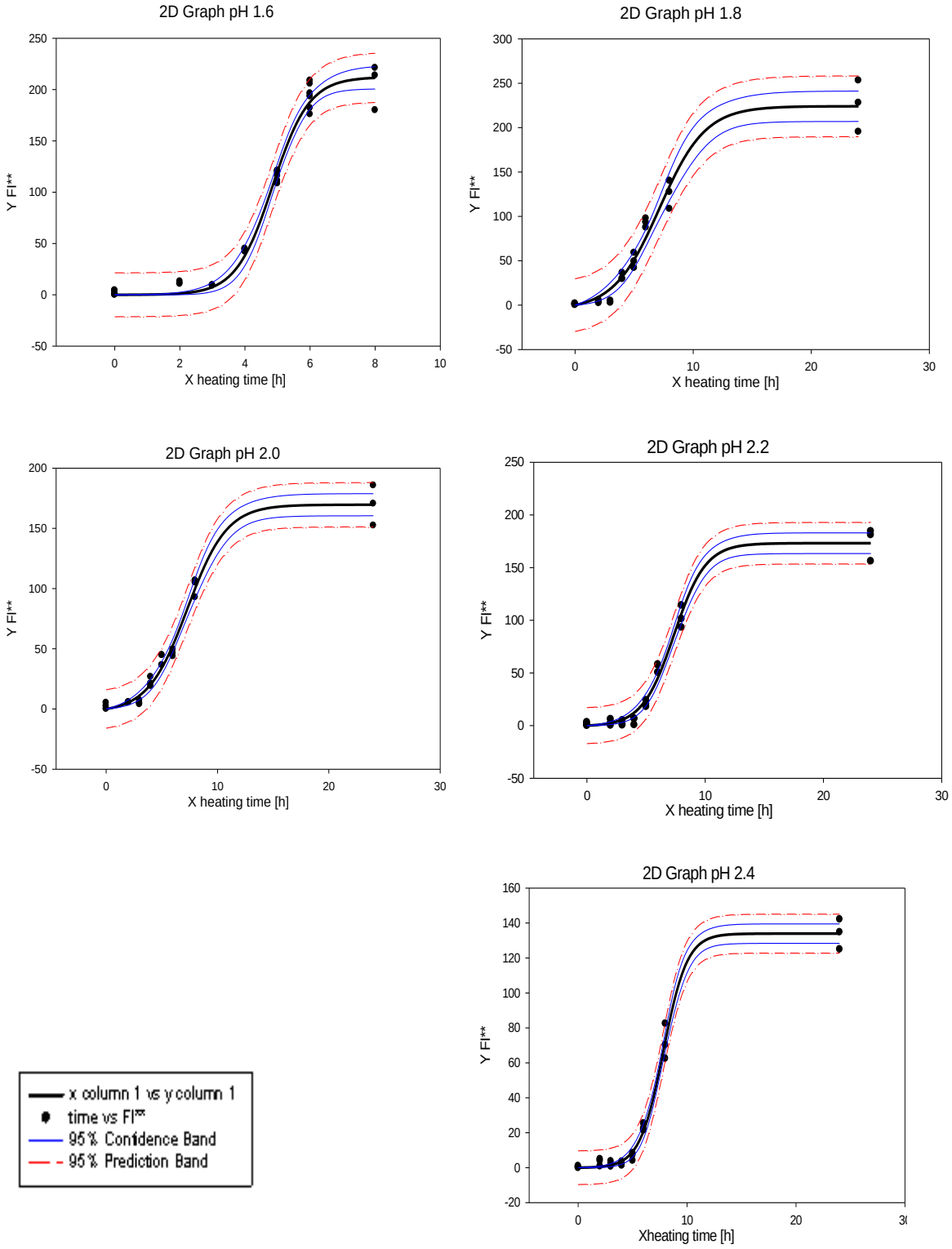

Figure 5.1.2 Two-step autocatalytic reaction model fitting of 1 % w/v β-lactoglobulin at different pHs using SigmaPlot 10.0. The dots represent FI** determined experimentally, and the dark line in the middle is the fitted sigmoidal curve according to Eq. (3).

The estimated nucleation reaction rate, k_1 and elongation reaction-rate, k_2 were plotted as a function of pH (Figure 5.1.3, Figure 5.1.4).

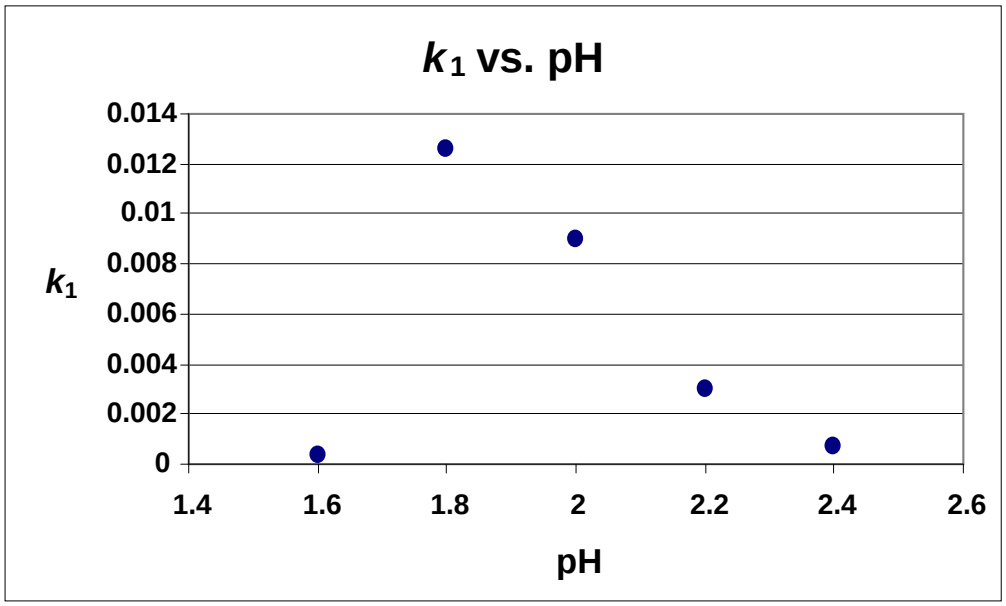

Figure 5.1.3 k_1 value as a function of sample incubation pH

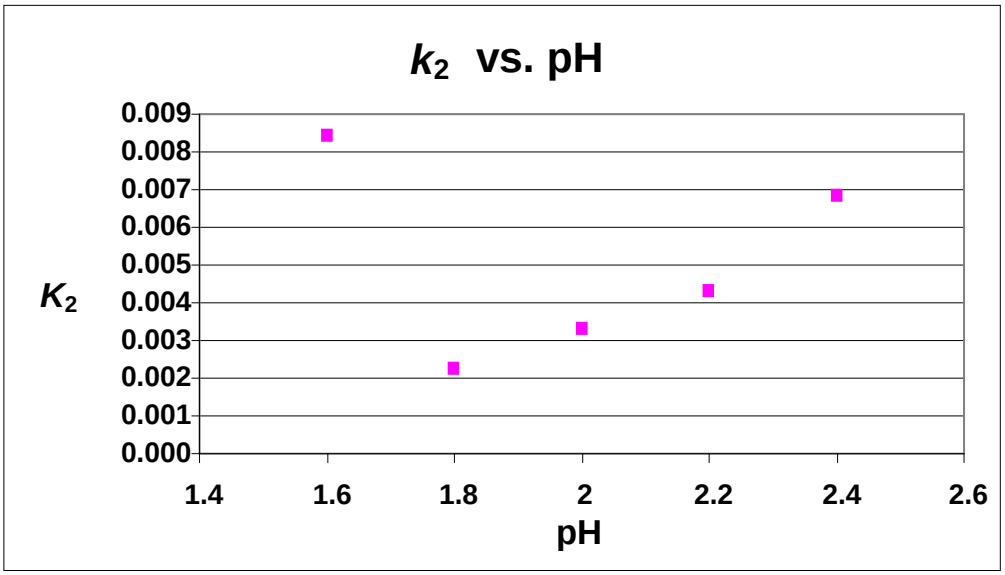

Figure 5.1.4 k_2 value as a function of sample incubation pH

Figure 5.1.3 shows that k_1 (h^{-1}) decreases linearly from pH 1.8 to pH 2.4, while k_2 (RFU^{-1} h^{-1}) increases from pH 1.8 to pH 2.4 (Figure 5.1.4). As k_1 is related to the inverse of the lag phase time and k_2 is positively related to the elongation rate, the nucleation rate decreased while the elongation rate accelerated with increasing pH

from 1.8 to 2.4. Surprisingly, the sample at pH 1.6 was different from all the other samples, with a very slow nucleation rate and a very fast elongation rate.

TEM

After heating for 6 hours, a combination of short and long fibrils could be seen at pH 1.8- 2.2, while the percentage of short fibrils at pH 1.6 was much lower compared to other pH values. Moreover, in comparison to the fibrils formed at pH 2.2 and 1.8, the fibrils formed at pH 1.6 were much longer (in average), and some fibrils were curved (Figure 5.1.5, B red arrows).

Representative TEM images for all samples except pH 2.0 (see Section 4.1), are shown in Figure 5.1.5. The images showed that there was a clear switch in fibril morphology as the pH was lowered from pH 2.4 to pH 1.6. While short, worm-like fibrilar aggregates were formed at pH 2.4 (Figure 5.1.5, G and H), a change in fibril morphology occurred over a narrow pH range. Long semi-flexible fibrils became predominant at pH 2.2 (Figure 5.1.5, E and F). No distinguishable changes in fibril morphology can be observed from pH 2.2 to pH1.6 (Figure 5.1.5, A-F, images for pH 2.0 at 6h is shown in Chapter 4, Figure 4.1.4).

The TEM images also provide some quantitative information of β-lactoglobulin fibril formation:

1. The fibril formation increased with heating time at all pH conditions studied;

2. The quantity of fibril formed at a lower pH was higher than that formed at a higher pH after heating for 24 hours; the fibrils observed from TEM images were significantly less at pH 2.4 in comparison to the fibrils at the other pH values.

The observations from these TEM images are consistent with the results of ThT fluorescence described earlier (Figure 5.1.1.)

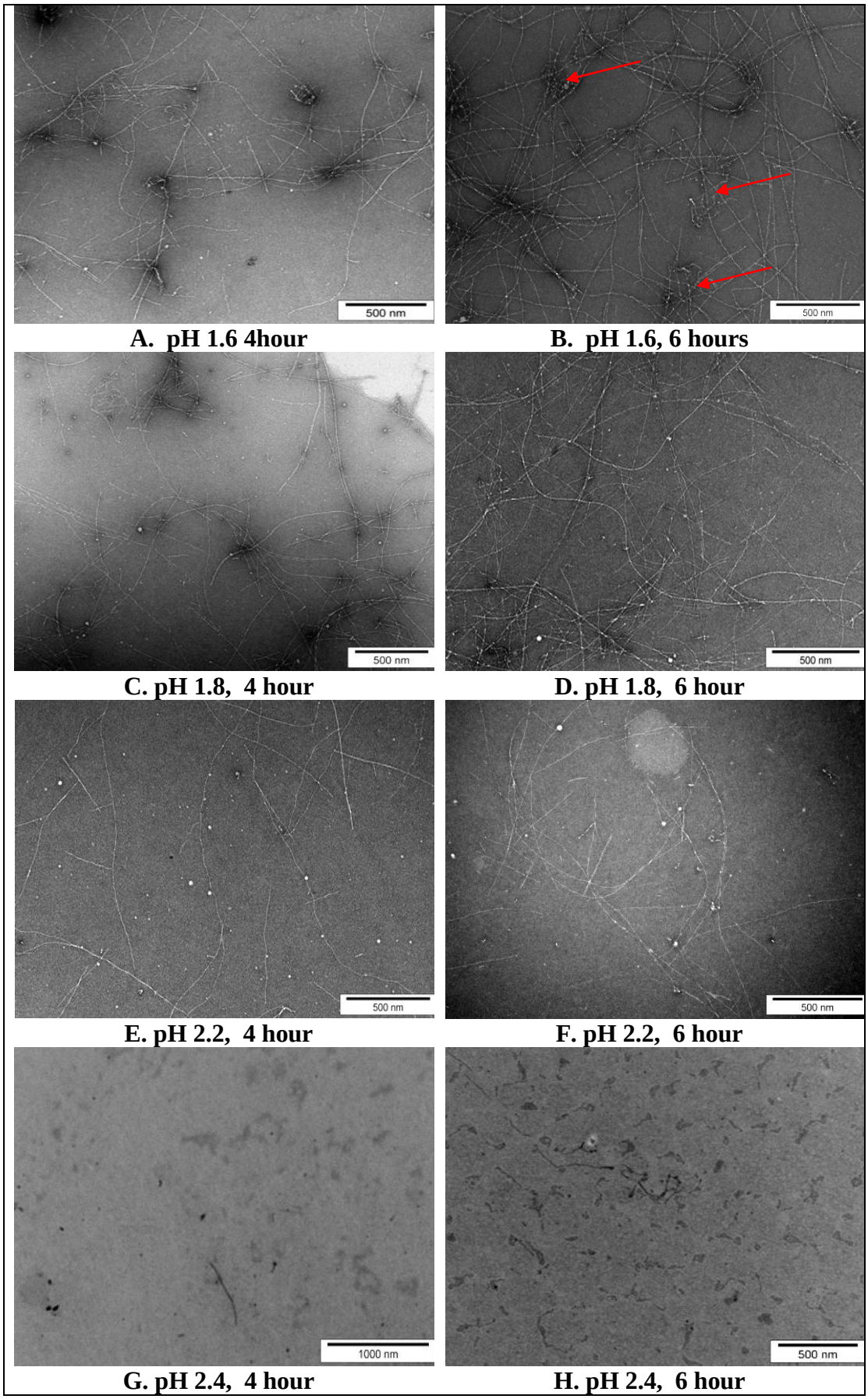

Figure 5.1.5 Negatively stained TEM images of β-lactoglobulin (1 % w/v) heated at 80°C at pH 1.6, 1.8, 2.2 and 2.4 for 4 and 6 h.

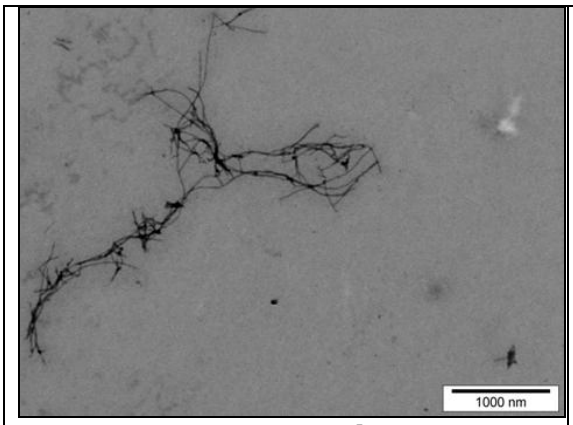

1. pH 2.4, 6h

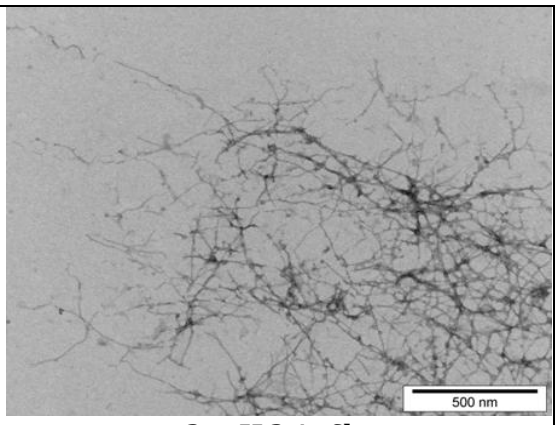

2. pH 2.4, 6h

Figure 5.1.6 Untypical images of the same sample at pH 2.4 heated for 6 hours.

The typical examples of aggregates formed at pH 2.4 are shown in Figure 5.1.5 (panels G and H). It is interesting to note that there were some fibrils formed at pH 2.4 after heating for 6h (Figure 5.1.6). These images show the special case of aggregates which were observed from very limited grids. The long fibrils that connected together were only observed occasionally. Such untypical images reflect that:

1. Long fibrils were also formed at pH 2.4 after heating for 6 hours.
2. The long fibrils formed at pH 2.4 were not many and that they were not the majority of the aggregates.

It remains unclear whether the short worm-like aggregates formed at pH 2.4 represent precursors of the long fibrils or an alternative mode of aggregation

In general, the TEM results are consistent with the observation of Kavanagh et.al (2000b). In their study, the structure of β-lactoglobulin at pH 2.0 – 3.0 was examined by TEM and FTIR. They found that at pH 2.0, without added salt, long rigid fibrils were formed, on increasing the pH to 2.5, and after heating for 6 hours, fibrils were evident.

Based on these observations, it can be inferred that the major aggregates formed at pH 1.6- 2.2 were long semi-flexible fibrils, although they did not appear to be the same. Clear difference occurred at pH 2.4, where short worm-like fibrils were the predominant aggregates. This difference suggests that the fibril morphology is pH dependent.

5.1.4 Discussion

The difference in fibrillation process and fibril morphology at pH 1.6 – 2.4 might be a combination of many reasons, such as structure transitions, the molecular association states, the electrostatic repulsive forces or the rate of denaturation or the hydrophobic reaction.

The pH-induced structural transitions were investigated by Sakurai & Goto (2007), who found that between pH 2 and 8 β-lactoglobulin exhibited a number of pH-induced structural transitions as well as changes in the association state and stability. So it is possible that some structural transitions occured under the experimental conditions used in this study.

It is widely believed (See the literature review in Chapter 2) that β-lactoglobulin presents as a dimer at physiological pH and it begins to dissociate to monomer at pH <3.5 (Aymard *et al.*, 1996). This monomer-dimer equilibrium is dynamic (Sakurai *et al.*, 2001). Therefore the β-lactoglobulin association state may change by varying pH from 1.6 to 2.4.

At pH 1.6 – 2.4 , β-lactoglobulin molecules only bear positive charges (+21e/ monomer at pH 2, 17+e/ monomer at pH 2.5) (Aymard *et al.*, 1996; Basch & Timashef, 1967; Kavanagh *et al.*, 2000b; Rogers *et al.*, 2006). Hence, the strong repulsive electrostatic interactions inhibit the formation of random aggregates and permit the formation of fibrilar aggregates. The electrostatic repulsive forces are dependent on the molecular charge which is related to the pH value; therefore, the electrostatic force would be different at different pH values.

In comparison with the TEM image of pH 1.6 at 4h (Figure 5.1.5, panels A), ThT fluorescence data at 3h were rather low (Figure 5.1.1). One explanation is that the measurements at this time point may be lower than the real value. In this case, the value of k_1, which based on the ThT florescence measurements, should be higher.

5.1.5 Conclusions

The present study investigated the formation and morphology of the heat-induced β-lactoglobulin aggregates formed at 80 °C without adding salt at various pH values (1.6-2.4).

Regardless the variation of pH from 1.6 to 2.4, β-lactoglobulin fibrillation pattern of all samples exhibited a sigmoidal behaviour. This suggests that no change in mechanism occurred as pH was varied. However, the lag time and growth rate were influenced by varying pH from 1.6- 2.4. The fibrillation pattern at pH 1.6 was unique compared to the others, in that it had the lowest k_1 and the highest k_2. The model did not fit the experimental data well at pH 1.6.

The whole fibril assembling process was much faster at pH 1.6 than that at pH 1.8-2.4. The yield of fibrils after 24 hours incubation was slightly influenced by the variation of pH; a significant decrease was found for the sample incubated at pH 2.4.

TEM observations suggest that the fibril morphology was dependent on pH. A clear change in fibril morphology occurred from pH 2.2 to 2.4, with the short worm-like fibrils were the predominant aggregates at pH 2.4, whereas below this pH the majority aggregates were long and semiflexible fibrils.

The overall results obtained in this study suggest that fibril formation was sensitive to pH and even small variations can affect the fibrillation pattern and morphology.

It is not clear at this stage as to what caused the difference in fibrillation pattern and morphology when varying pH from 1.6 to 2.4. For a clearer view of these, more methods and techniques, such as X-ray diffraction and NMR spectroscopy are needed.

A ThT fluorescence assay from 0 to 24h and more TEM images at earlier times for the pH 1.6 sample are recommended in future studies.

5.2 Effect of ionic strength on fibril formation

5.2.1 Introduction

The kinetics of heat-induced aggregation of β-lactoglobulin and the structure of the aggregates formed at pH 2.0 have been studied intensively (Arnaudov *et al.*, 2003; Aymard *et al.*, 1999; Kavanagh *et al.*, 2000b; Veerman *et al.*, 2002). According to earlier research, ionic strength not only influences the morphology of the aggregates but also affects the aggregation rate (Aymard *et al.*, 1999).

At constant β-lactoglobulin concentration and heating temperature (80°C), aggregation is slow at low ionic strength at pH 2.0 (Aymard *et al.*, 1999). Using size-exclusion chromatography, multi-angle laser light scattering and other techniques, Schokker *et al.* (2000) found that the rate of disappearance of native-like β-lactoglobulin increased with increasing the ionic strength at pH 2.5.

Light, neutron and X-ray scattering studies have been used to study the structure of β-lactoglobulin aggregates produced by heat-induced denaturation at pH 2.0 (Aymard *et al.*, 1999; Durand *et al.*, 2002). Rod-like aggregates were observed at low ionic strength, while a fractal structure was suggested for solutions at higher ionic strength (Durand *et al.*, 2002). The dependence of the morphology on the ionic strength was also examined by AFM and light scattering experiments (Arnaudov & de Vries, 2006). It was noted that fibrils became shorter and curlier with increasing ionic strength.

Most of the studies on the impact of ionic strength on β-lactoglobulin fibril formation were performed in widely-spaced NaCl concentrations, and nearly no comparison of the effect of NaCl and $CaCl_2$ on fibril kinetics and fibril morphology has been made. Therefore, a detailed study of the effect of salt (NaCl and $CaCl_2$) on fibrilar aggregation of β-lactoglobulin at pH 2.0, 80°C was undertaken. The salts were NaCl (0 - 100 mM) and $CaCl_2$ (0 – 100 mM). The fibrilar kinetics were studied by ThT fluorescence and the morphology of the aggregates was examined by TEM.

5.2.2 Experimental

Sample preparation

0.5844 g NaCl and 1.4702g $CaCl_2 \cdot 2H_2O$ were dissolved in 10 mL Milli-Q water to obtain 1M NaCl and $CaCl_2$ standard solutions. Based on Table 5.2.1 and 5.2.2, different volumes of the standard NaCl and $CaCl_2$ solutions were added to the prepared β-lactoglobulin solutions (prepared as described in Section 3.1.3) and mixed well to obtain the desired protein working solutions. The protein solutions used were slightly higher than 1% w/v, to ensure that the final protein concentration of each sample was approximately 1 % w/v.

Table 5.2.1 Sample preparation for NaCl experiments

Sample	NaCl concentration [mM]	1M NaCl solution [mL]	HCl of pH 2.0 [mL]	protein solution [mL]	Ionic strength* [mM]
Control	0	0.00	0.00	10.00	0
A	10	0.10	0.00	9.90	10
B	20	0.20	0.00	9.80	20
C	30	0.30	0.00	9.70	30
D	40	0.40	0.10	9.50	40
E	50	0.50	0.00	9.50	50
F	60	0.60	0.40	9.00	60
G	80	0.80	0.20	9.00	80
H	100	1.00	0.00	9.00	100

Table 5.2.2 Sample preparation for $CaCl_2$ experiments

Sample	$CaCl_2$ concentration [mM]	1M $CaCl_2$ solution [mL]	HCl of pH 2.0 [mL]	protein solution [mL]	Ionic strength* [mM]
Control	0	0.00	1.00	9.00	0
A	3	0.03	0.97	9.00	9
B	10	0.10	0.90	9.00	30
C	33	0.33	0.67	9.00	100
D	40	0.40	0.60	9.00	120
E	50	0.50	0.50	9.00	150
F	60	0.60	0.40	9.00	180
G	80	0.80	0.20	9.00	240
H	100	1.00	0.00	9.00	300
I	20	0.20	0.80	9.00	60
J	5	0.05	0.95	9.00	15

*: $I = \frac{1}{2}\sum_{i=1}^{n} m_i z_i^2$

Sample A: $I = ½ \times (3\times 2^2 + 3\times 2\times(-1)^2) = 9$ mM

ThT fluorescence assay

2 mL of each solution at desired salt concentration was put into the sealed glass tube (the cap screwed tightly to minimise water evaporation) and heated in a water bath at 80 ± 0.1 ºC. The tubes were taken out at designated times shown in Table 5.2.3 and cooled with ice-water for 10 minutes, then used for ThT fluorescence assay. ThT fluorescence assays were performed as described in Section 3.2.1. For both NaCl and $CaCl_2$ ThT fluorescence assays, a sample without added salt was included as a control.

TEM

After finishing the ThT fluorescence assay, the 6h protein samples (except the control sample) were kept at 4°C overnight. The samples were then processed and examined with TEM as described in Section 3.2.2.

Table 5.2.3 Sample treatments for the ionic strength experiments

Salt [mM]		**Heating times [h]**	**TEM times [h]**	**ThT fluorescence assay times [h]**
NaCl	10-100	0, 3, 4, 6, 8	6	all heating times
$CaCl_2$	3, 10, 33-100	0, 2, 4, 6, 8	6	all heating times
$CaCl_2$	5, 20	0, 2, 4, 6, 8	No data	all heating times

5.2.3 Results

Effect of NaCl concentration on β-lactoglobulin fibril formation

- **Appearance of sample solutions in tubes**

The appearance of small gel particles was first observed in the solutions heated foraround 3 hours, and tthe quantity of gel particles increased with increasing heating time. These phenomena were also observed by other researchers but at higher protein concentrations (Aymard *et al.*, 1999; Kavanagh *et al.*, 2000a).

- **ThT fluorescence assay**

In order to study the effect of NaCl on the kinetics of β-lactoglobulin fibril formation, the fibril formation processes at various NaCl concentrations at pH 2.0, 80°C, were monitored using ThT fluorescence.

Figure 5.2.1 shows the time evolution of β-lactoglobulin fluorescence intensity (FI**) during the aggregation process at different NaCl concentrations. All samples exhibited an increase in ThT fluorescence indicative of the formation of amyloid structures. However during the first 3 hours there was no large increase in ThT fluorescence of solutions containing 0 - 80 mM NaCl. These results suggest that the lag time of β-lactoglobulin fibril formation may not be significantly influenced by increasing NaCl concentration up to 80 mM. These results are consistent with the visual observations that no gel particles were found during the initial 3 hours incubation.

After heating for 3 hours, ThT fluorescence increased rapidly, which indicates that the fibrillation process entered the growth phase. In the growth phase, ThT fluorescence increased directly with increasing NaCl concentration from 0 – 40 mM (Figure 5.2.1a). When NaCl concentration was increased to high or NaCl concentrations (50 – 100 mM), the influence of NaCl concentration on ThT fluorescence became weaker (Figure 5.2.1b).

A sigmoidal increase in ThT fluorescence was observed for the 100 mM NaCl sample, which means only this sample completed fibrillation process within 8 hours.

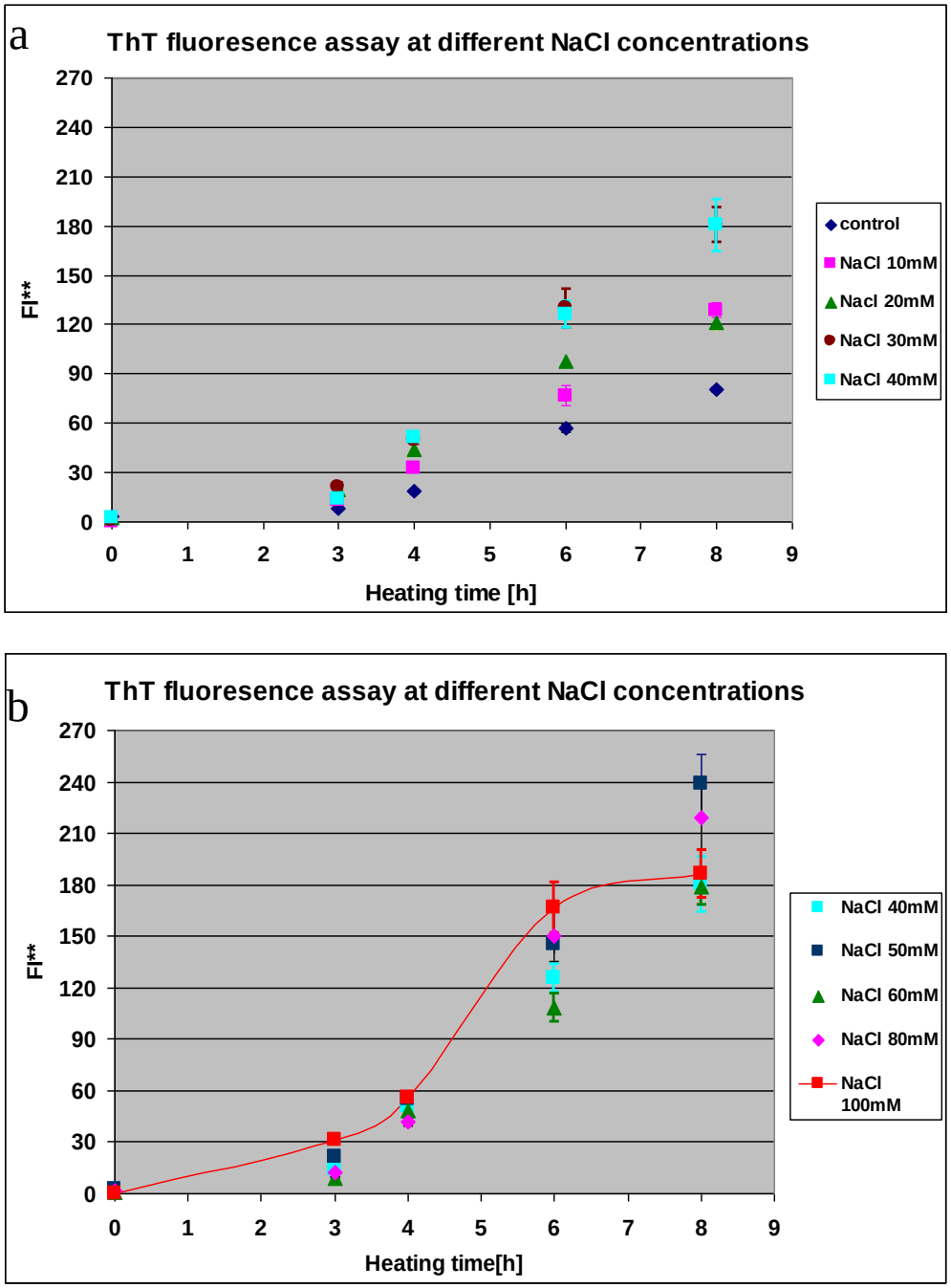

Figure 5.2.1 FI** as a function of NaCl concentration and heating time. The 40mM sample was plotted in a and b. All the samples were incubated at pH 2.0, 80°C. Samples were measured in triplicate. Error bars indicate the standard error of mean (SEM).

Effect of NaCl on β-lactoglobulin fibril growth rate

The ThT fluorescence data were not sufficient to fit the two-step autocatalytic reaction model. Therefore the slope of the growth curve (rapidly increasing part of the ThT fluorescence data shown in Figure 5.2.1) of each sample was estimated by linear regression and described as growth rate (FI**/h) of fibril formation. The growth phase

was from 3 to 8 h for all samples except the 100 mM NaCl sample, which was from 3 - 6 h (The detailed calculations are shown in Appendix 5.2).

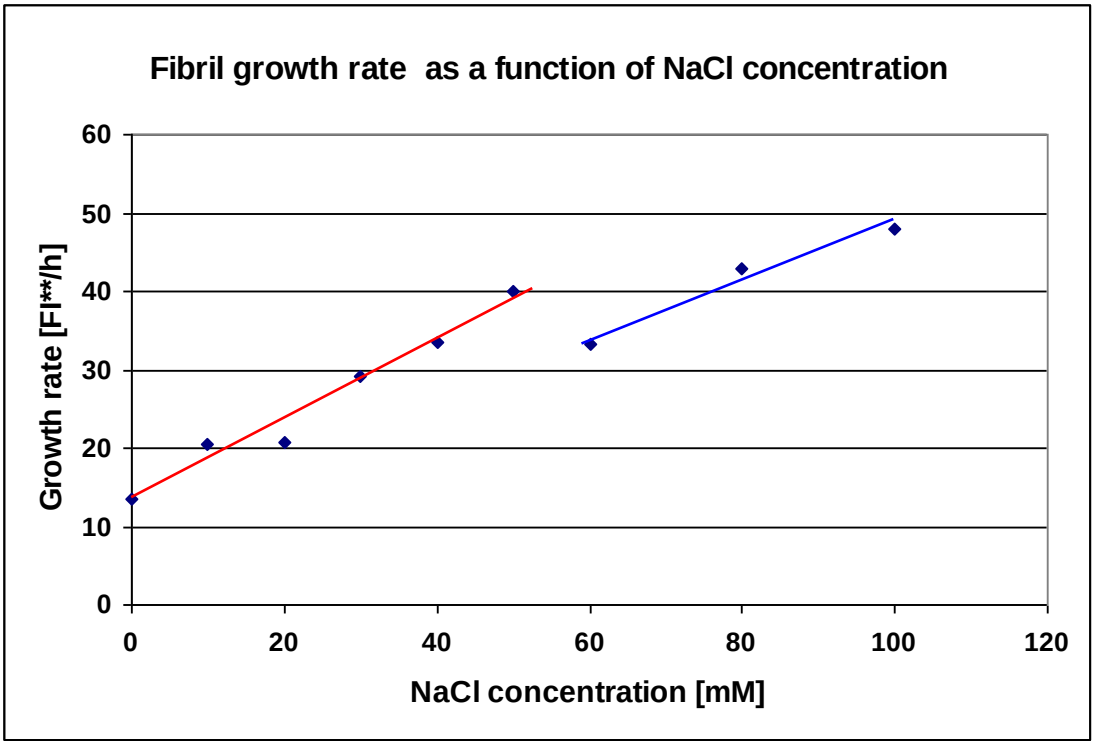

Figure 5.2.2 Fibril growth rate as a function of NaCl concentration.

Figure 5.2.2 shows that an increase in NaCl concentration resulted in faster growth rate of fibrils, a clear correlation between the NaCl concentration and the rate of fibril growth was observed from 0 to 50 mM (the red line) and from 60 to 100 mM (the blue line) respectively. A distinctive turning point appeared at 60mM. A possible explanation for the drop at 60 mM is that the significant change in fibril shape influenced the ThT fluorescence. From 60 mM to 100 mM, the growth rate increased steadily with increasing NaCl concentration.

- **TEM**

The TEM images (Figure 5.2.3) reveaedl that these aggregates were unbranched fibrils. As expected, the samples at low NaCl concentration (Figure 5.2.3, A-B) showed long straight amyloid fibrils which were similar to those formed under control conditions (pH 2.0, low ionic strength, 80°C). Interestingly, some wavy, long, unbranched fibrils with diameters similar to those formed at lower NaCl concentrations were observed for samples at 30 – 50 mM NaCl (Figure 5.2.3, C - E).

Curly fibrils first appeared when the NaCl concentration increased to 60 mM; the fraction of curly fibrils and the extent of curvy were increased as a result of increasing NaCl concentration (Figure 5.2.3, F - H).

TEM images showed three distinctive types of fibrils:

- Straight fibrils: long straight fibrils and short straight fibrils (<500 nm)
- Wavy fibrils: straight fibrils with slight curves (blue arrow)
- Curly fibrils: curly (red arrow)

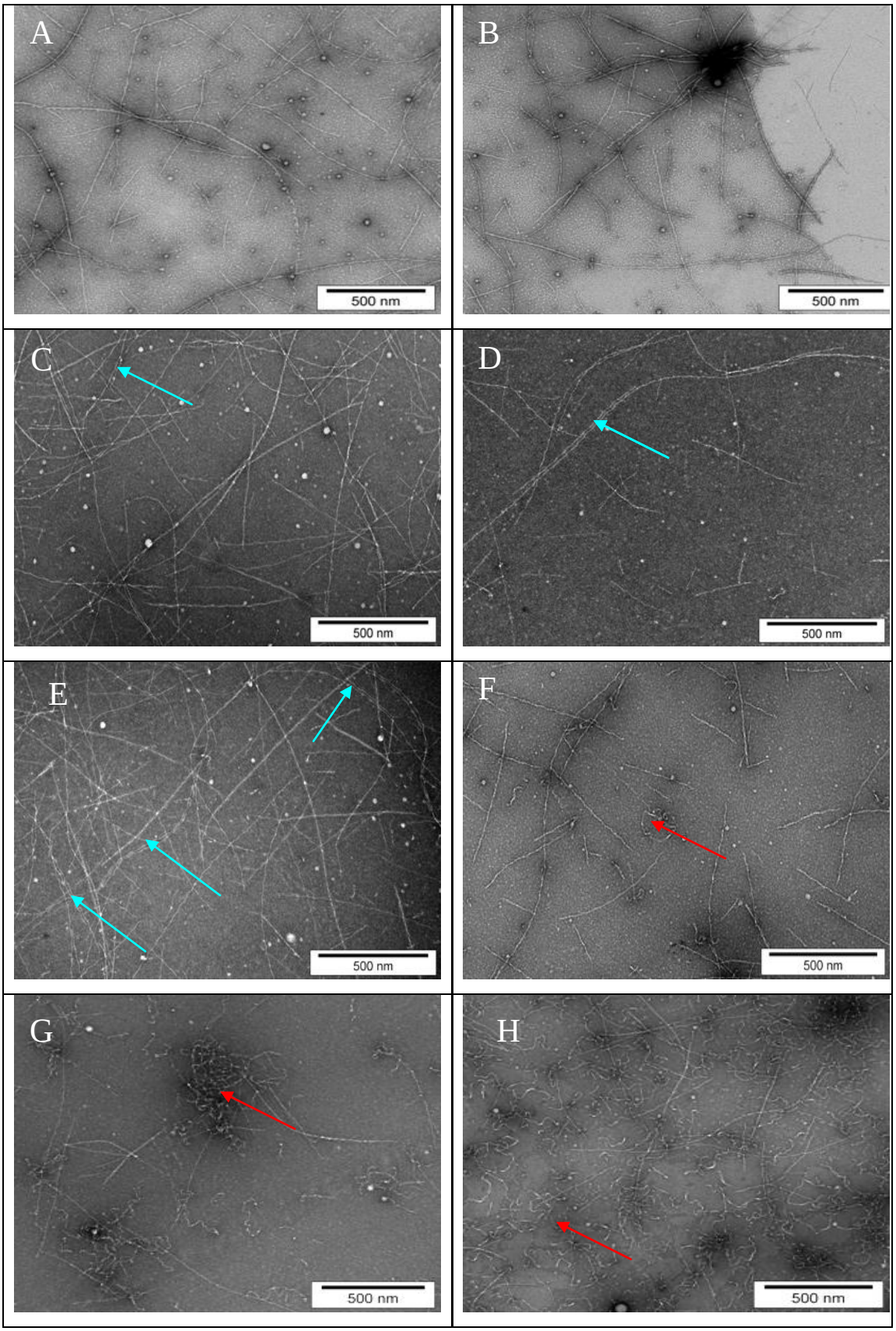

Figure.5.2.3 Negatively stained TEM images for β-lactoglobulin (approximate 1% w/v) at pH 2.0, 80 °C and various NaCl concentrations (A.) 10 mM; (B.) 20 mM; (C.) 30mM; (D.) 40 mM; (E.) 50 mM; (F.) 60 mM; (G.) 80 mM; (H.) 100 mM. All samples were incubated for 6 hours.

The morphological variations of β-lactoglobulin fibrils formed at different NaCl concentrations are summarised in Table 5.2.4.

Table 5.2.4 Morphology of fibrils formed at different NaCl concentrations

Sample	**NaCl [mM]**	**Fibril Morphology**
A B	10, 20	Long and short straight semi-flexible fibrils
C D E	30, 40, 50	Long and short straight semi-flexible fibrils A few wavy semi-flexible fibrils
F	60	Long and short semi-flexible fibrils (straight and wavy) Some curly fibrils
G	80	Curly fibrils Small number of straight fibrils
H	100	Curly fibrils A few straight fibrils

The experimental results indicate that at pH 2.0, the heated β-lactoglobulin forms aggregates with a range of lengths and a variety of shapes, both of which depend on NaCl concentration.

Effect of $CaCl_2$ concentration on β-lactoglobulin fibril formation

- **Appearance of sample solutions in tubes**

The appearance of the samples incubated with $CaCl_2$ was similar to that of the samples in the presence of NaCl. The main difference was that gel particles formed eariler in the $CaCl_2$ samples than with NaCl. Small gel particles appeared after heating for 2 hours when incubated with 80 - 100 mM $CaCl_2$. The quantity of gel particles also increased with increasing heating time and $CaCl_2$ concentration.

- **ThT fluorescence assay**

Figure 5.2.4 shows the ThT fluorescence profile of the samples (1 % w/v β-lactoglobulin solution at various of $CaCl_2$ concentrations).

The lag phase is around 2 hours for the samples in the presence of 0 - 60 mM $CaCl_2$. As the time point interval is long, the lag time is an approximate value. On the other hand, in the presence of 80 and 100 mM $CaCl_2$, fluorescence increased without a lag phase and proceeded to equilibrium within 8 hours. These observations suggest that the nucleation time was reduced or even eliminated by adding sufficient $CaCl_2$.

Comparing the fibrillation pattern of all samples, sigmoidal increase appeared in the 80 and 100 mM $CaCl_2$ samples. The ThT data indicate that the fibrillation process of these two samples was completed within 6 and 4 hours respectively, which was much faster than the others. Hence, the fibrillation process was promoted by increasing $CaCl_2$ concentration.

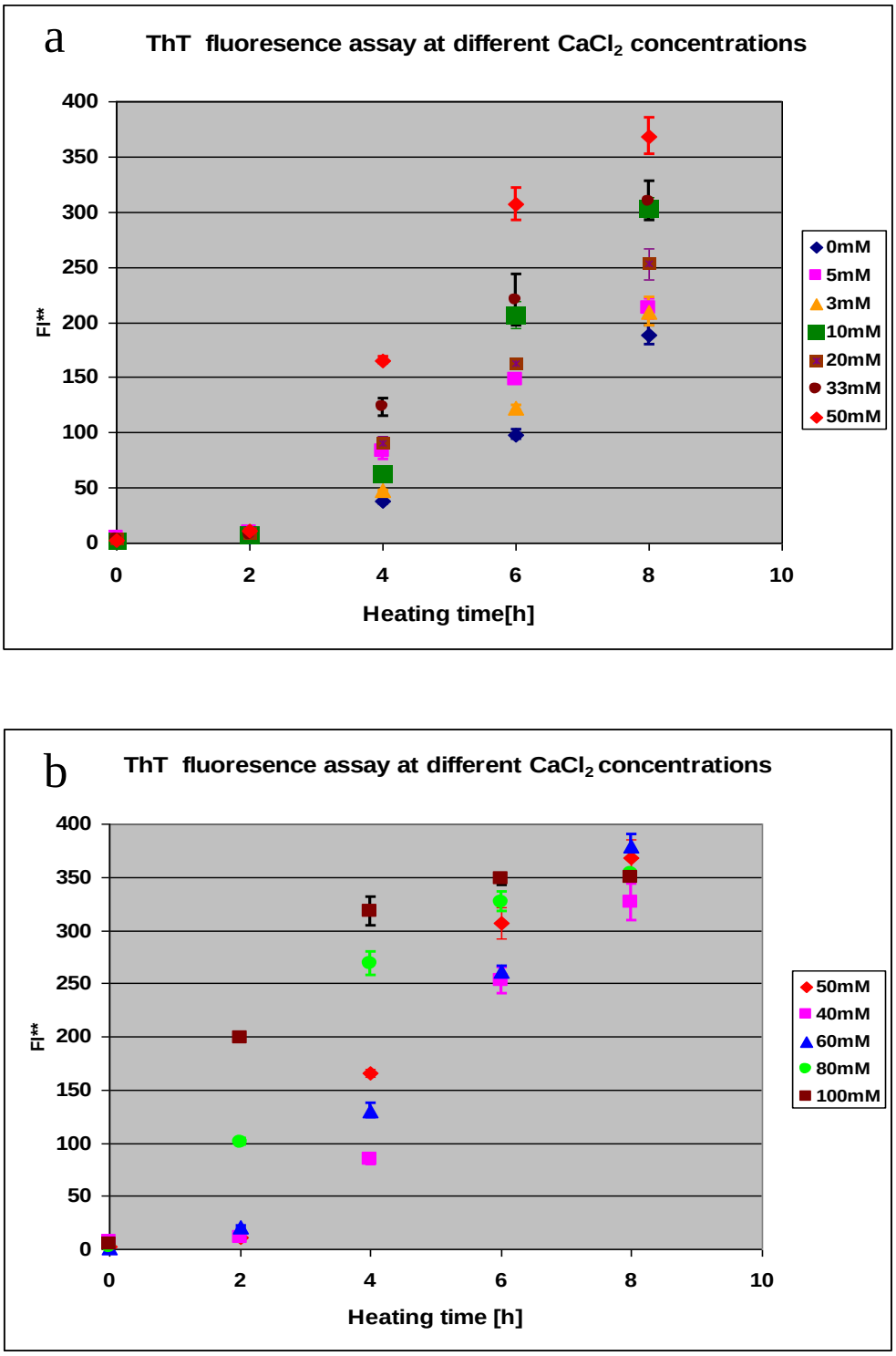

Figure 5.2.4 FI** as a function of $CaCl_2$ concentration and heating time. The fluorescence intensities were measured after changing the lamp of the fluorescence meter (RF-1501 SHIMADZU). All samples were incubated at pH 2.0, 80±1°C. Samples were measured in triplicate**.** Error bars represents standard error of mean (SEM) of three independent measurements, respectively. The 50 mM sample is plotted in both a and b.

Effect of $CaCl_2$ on β-lactoglobulin fibril growth rate

The effects of $CaCl_2$ on β-lactoglobulin fibril growth rate were analysed in the same way as for NaCl. The apparent growth rates for fibril formation are estimated from the ThT fluorescence assay data shown in Figure 5.2.4. The fibril growth phase is considered from 2 to 8h for the samples incubated with 0 – 60 mM $CaCl_2$, and changes to 2 - 4h for the 80 and 100 mM $CaCl_2$ samples (The detailed calculations are shown in Appendix 5.2).

An increasing growth rate (FI**/h) with increasing $CaCl_2$ concentration was observed, except in the 10 mM $CaCl_2$ sample. This result indicated that the growth rate of β-lactoglobulin fibrillation was linearly correlated with $CaCl_2$ concentration. Increased $CaCl_2$ concentration led to a faster growth of β-lactoglobulin fibrils.

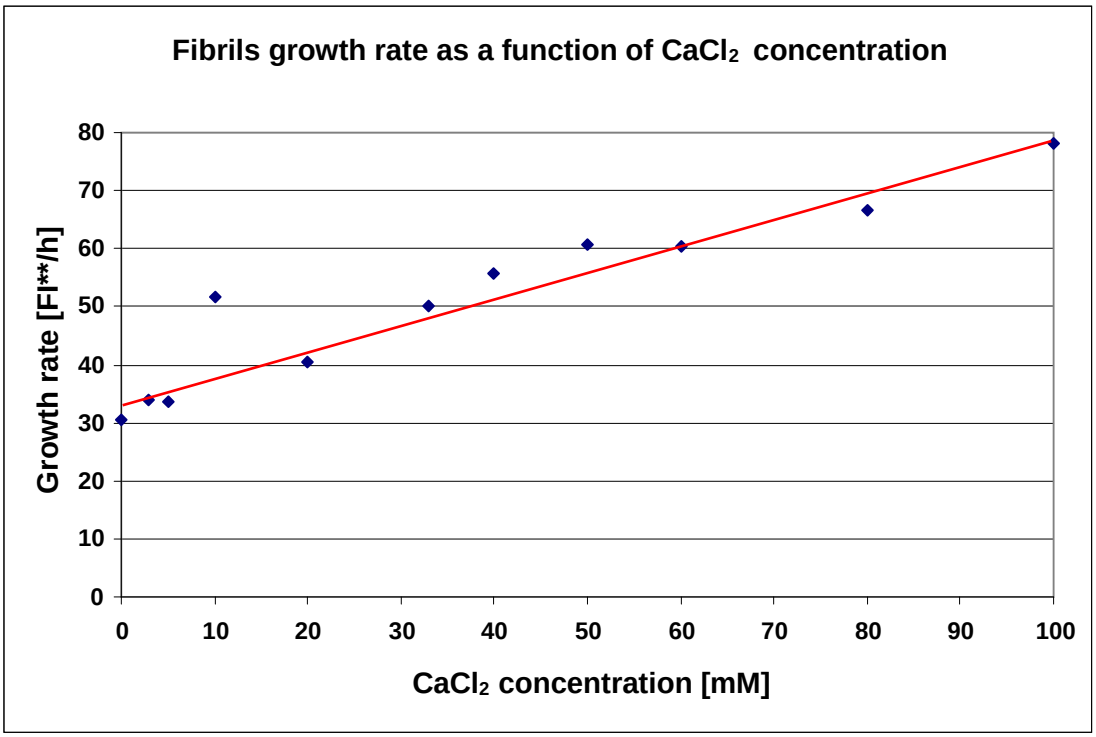

Figure 5.2.5 Fibril growth rate as a function of $CaCl_2$ concentration. The linear growth phases of all samples were from 2 - 8h, except the sample at 80mM and 100 mM $CaCl_2$, which were from 0 - 4h. Linear regression was calculated (R^2 = 0.9705), except the 10 mM $CaCl_2$ sample.

- **TEM**

Figure 5.2.6 shows TEM images for β-lactoglobulin at pH 2.0 and varying $CaCl_2$ concentration (3 – 100 mM). The images clearly showed that fibrils were formed in all samples investigated, and most of the aggregates were presented as long, thin structures, rather than small spherical particles.

The morphology of the fibrils was strongly affected by the amount of $CaCl_2$ present in the solutions, similar to the effect of NaCl. Straight, wavy, and curly fibrils were also observed.

Long straight fibrils were observed for $CaCl_2$ concentrations of 3 - 10 mM (Figure 5.2.6, A - B). Straight fibrils and curly fibrils were observed co-existing in the samples with 30 – 40 mM $CaCl_2$ (Figure 5.2.6, C - D). With increasing $CaCl_2$ concentration to 50 mM, curly fibrils dominated the aggregates (Figure 5.2.6, E - F). With ≥ 80 mM $CaCl_2$ only curly fibrils could be observed. The morphological variation of β-lactoglobulin fibrils are summarised in Table 5.2.5.

Table 5.2.5 Shapes of fibrils formed at different $CaCl_2$ concentration

Sample	**$CaCl_2$ [mM]**	**Fibril Morphology**
A, B	3, 10	Long and short straight semi-flexible fibrils
C, D	33, 40	Long and short semi-flexible fibrils (straight and wavy) Some curly fibrils
E, F	50, 60	A few semi-flexible straight fibrils Many curly fibrils
G, H	80, 100	All curly fibrils. Fibrils twisted more compactly in sample H.

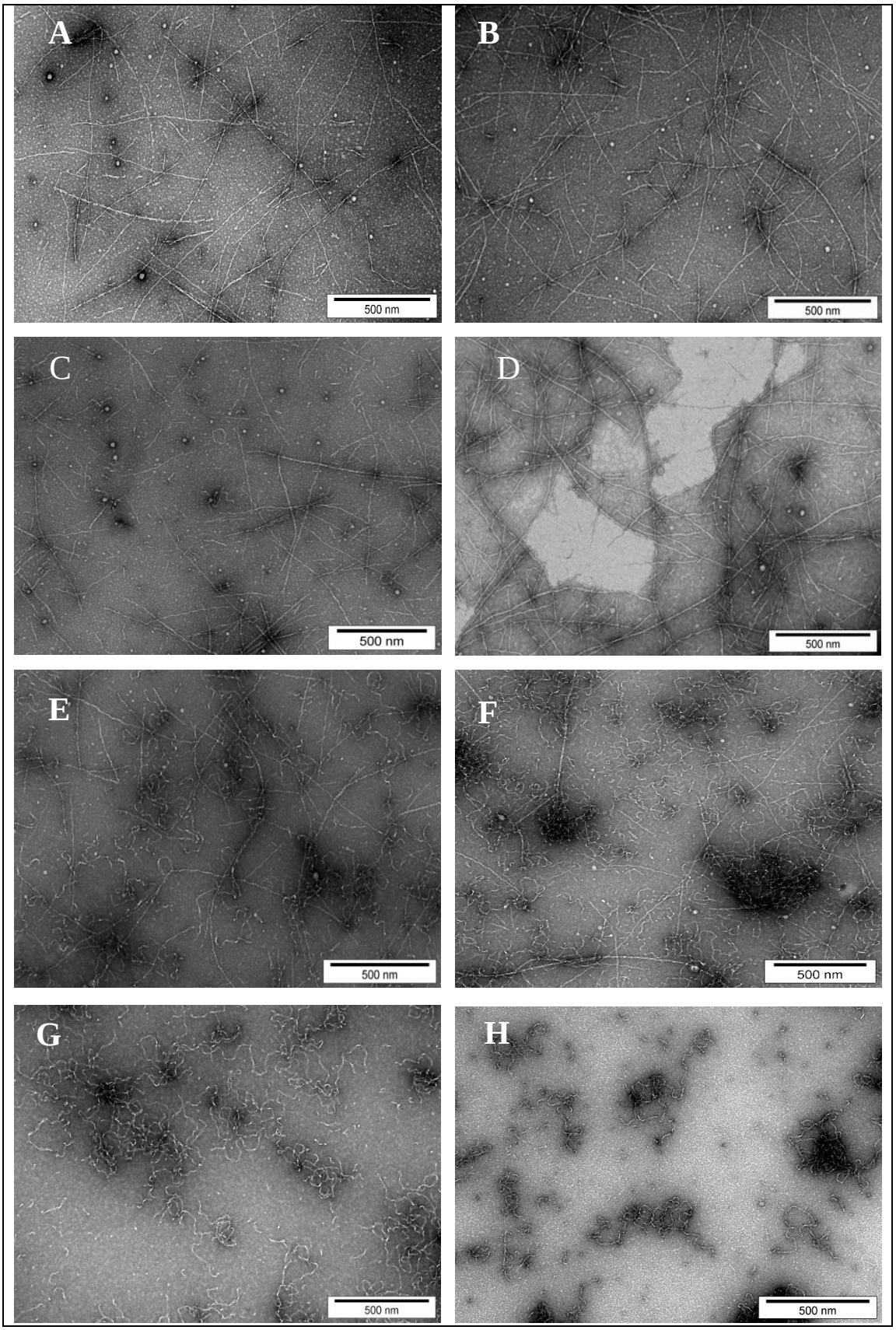

Figure 5.2.6 Negatively stained TEM images for β-lactoglobulin (approximate 1% w/v) at pH 2.0, 80 °C and various $CaCl_2$ concentrations (A.) 3 mM; (B.) 10 mM; (C.) 33mM; (D.) 40 mM; (E.) 50 mM; (F.) 60 mM; (G.) 80 mM; (H.) 100 mM. All samples were incubated for 6 hours.

Comparison of the effects of NaCl and $CaCl_2$

In summary, together with the results obtained from ThT fluorescence assay, TEM imaging and visual observations are summarised in Table 5.2.6. On an equimolar basis, $CaCl_2$ is more effective than NaCl in the induction of fibrillation and altering the morphology of the fibrils.

Table 5.2.6 Summary of the effects of NaCl and $CaCl_2$ on fibrils formation

Salt Concentration [mM]		**0-20**	**30-40**	**50**	**60**	**80**	**100**
NaCl	ThT fluorescence assay Fibrillation	Uncompleted within 8h					Completed within 8h
	Fibril morphology TEM	LS[1]	LS, LW[2]	LW, LS	LW, SV[3], curly	Curly LW	curly
	gel particle appearance time	Around 3 hours					Less than 3 hours
$CaCl_2$	ThT fluorescence assay Fibrillation	Uncompleted within 8h				Completed within 8h	
	Fibril morphology TEM	LS	SW, LS	Curly, LW	Curly, LW	Curly	Curly wormlike
	gel particle appearance time	2-3 hours				2 hours	2 hours

[1] LS: long straight fibrils
[2] LW: long wavy fibrils
[3] SW: short wavy fibrils

The effects of the two salts on the kinetics of fibrillation were also compared at the same ionic strength (I= 30/ 60/ 100) (Figure 5.2.7). The effects of NaCl and $CaCl_2$ on β-lactoglobulin fibrillation were very similar when compared at the same ionic strength.

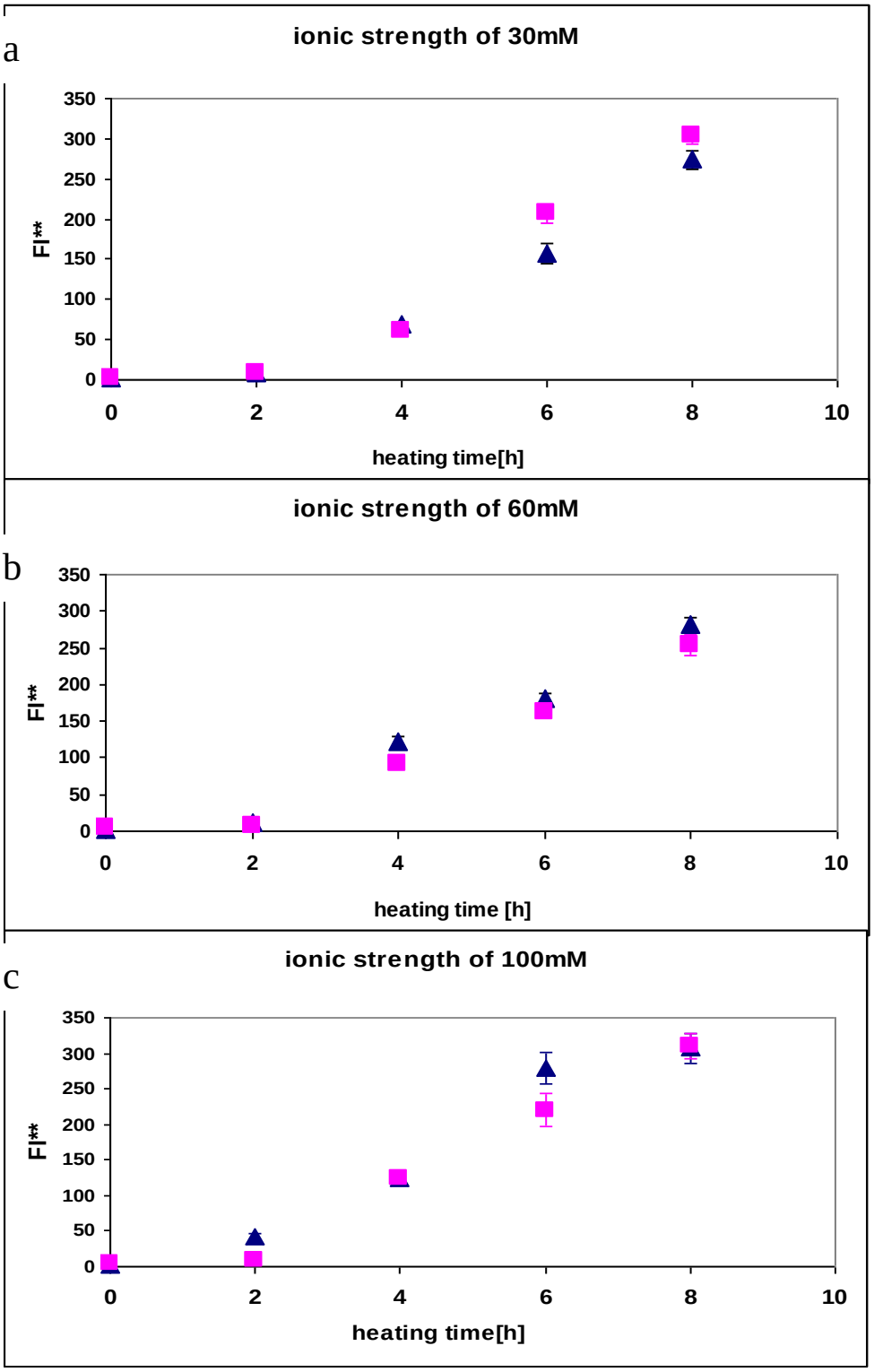

Figure 5.2.7 ThT fluorescence assay for $CaCl_2$ and NaCl at same ionic strength. $CaCl_2$ (■), NaCl (▲). Fluorescence intensities were measured for all samples after changing the lamp of the fluorescence meter (RF-1501 SHIMADZU). The same batch protein solutions were used for preparing all samples (1 % w/v). All samples were incubated at pH 2.0 and 80°C.

5.2.4 Discussion

Strong effects of ionic strength on β-lactoglobulin fibril formation kinetics were found using ThT fluorescence assay (0 - 8h). Fibril formation process was accelerated by increasing salt (NaCl, $CaCl_2$) concentration. Fibrillation process was completed within 8 hours only at high salt concentrations (100 mM NaCl or 80 – 100 mM $CaCl_2$). High salt concentrations not only shortened the lag time but also accelerated the growth rate. The estimated fibril growth rate showed a strong positive correlation with salt concentration.

TEM study showed that fibril morphology was strongly dependent on ionic strength. The morphological variations of fibrils formed at pH 2.0, 80ºC with various salt concentrations are summarised in Figure 5.2.8. This figure highlights the critical dependence of fibril morphology on ionic strength; fibrils become shorter and curvier with the increasing of ionic strength.

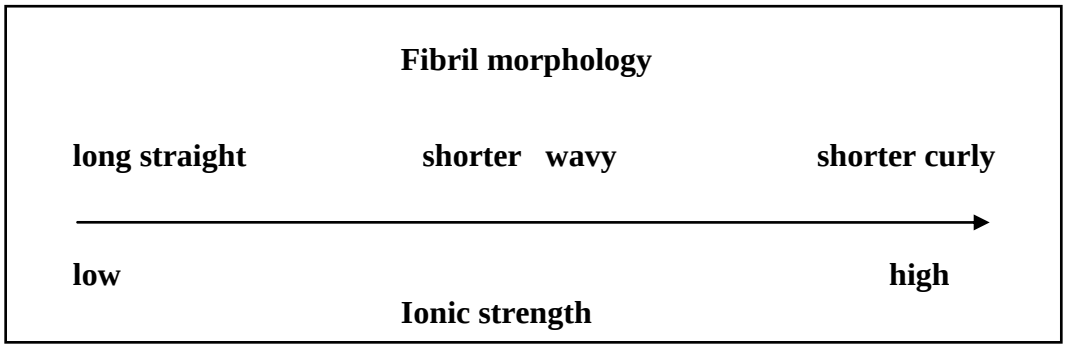

Figure 5.2.8 Schematic representation of the morphological variation of fibrils as a function of ionic strength

In general, the results obtained in this study are consistent with the results of other researchers. At pH 2.0 linear aggregates are formed which are very rigid at low ionic strength (13 mM) and flexible at high ionic strength (0.2 M) (Durand *et al.*, 2002). Arnaudov *et al.* (2006) obtained similar results using AFM: at ionic strength from 13 to 100 mM, shorter and tighter curve fibrils were formed at higher ionic strength. Therefore, the results suggest that the ionic strength conditions in which the aggregates grow are a determining factor for their structure (Aymard *et al.*, 1999).

Kavanagh *et al.* (2000) reported that long fibrils were not observed in the presence of 50 mM NaCl, while Veerman *et al.* (2002) observed long fibrils up to ionic strength of 80 mM (Veerman *et al.*, 2002). The results obtained in this study agree with theirs in that the higher salt concentrations lead to curvier fibrils. However, a few long straight fibrils are also present (at NaCl 100 mM and $CaCl_2$ 60 mM).

The kinetics of fibril formation and the morphology of fibrils were highly dependent on ionic strength, thus pointing to the role of electrostatic interactions in the aggregation process. Several studies have focused on the effect of ionic strength on β-lactoglobulin fibril formation (Arnaudov & de Vries, 2006; Aymard *et al.*, 1996). At pH 2.0, β-lactoglobulin bears only positive charges (Basch & Timashef, 1967), so the electrostatic repulsion becomes more or less important, depending on the extent to which positive charges are screened by negatively-charged ions.

A possible explanation of the lower growth rate at low salt concentration is that the aggregates are inhibited from further association, due to strong electrostatic repulsion at low ionic strength (Durand *et al.*, 2002). On the other hand, the faster growth rate at higher ionic strength is probably due to the large reduction of electric repulsion, as the net charge of β-lactoglobulin can be screened by added salts (Aymard *et al.*, 1996).

In this study, the effects of NaCl and $CaCl_2$ were nearly the same when compared at the same ionic strength level (30, 60, 100 mM respectly). One would expect that the effect of $CaCl_2$ would be stronger than that of NaCl, which was not shown by the data presented in this work. At pH above the isoelectric point, calcium ions promote protein aggregation of β-lactoglobulin by forming protein-Ca^{2+} -protein complexes, while a monovalent ion (Na+) is unable to perform such a role (Simons *et al.*, 2002). The disappearance of the special function of calcium may be due to the positively charged β-lactoglobulin at pH 2.0, as β-lactoglobulin was positively charged, the protein-Ca^{2+}-protein complexes could not form.

5.2.5 Conclusions

The formation of β-lactoglobulin fibril in the presence of NaCl and $CaCl_2$ was monitored by using ThT fluorescence and TEM. Large quantities of fibrils were formed under the experimental conditions used.

The kinetics of fibril formation are strongly dependent on ionic strength. At the same temperature (80°C), pH (pH 2.0) and protein concentration (1% w/v), higher ionic strength results in a faster fibrillation. The lag phase can be reduced or eliminated by adding sufficient amount of salts (NaCl 100mM and $CaCl_2 \geq 80$ mM).

TEM results demonstrate that the morphology of the fibrils is strongly affected by the ionic strength of the solutions. The shape of the fibrils changed significantly from long and straight at low salt concentration to curly and even worm-like at high salt concentration. The electrostatic repulsion between the proteins is an important factor in determining the rate of fibrillation and the morphology of the fibrils.

5.3 Effect of temperature on fibril formation

5.3.1 Introduction

The dependence of β-lactoglobulin fibril formation on ionic strength and pH has been studied intensively in recent years (Arnaudov & de Vries, 2006; Aymard *et al.*, 1999; Durand *et al.*, 2002; Schokker *et al.*, 2000; Veerman *et al.*, 2002), and yet, a study of the effect of temperature on fibril formation of β-lactoglobulin at acidic pH has not been examined in detail.

The effect of temperature on the dimerisation of β-lactoglobulin has been studied by Aymard *et al.*, (1996). They found that the dissociation of dimer increased with increasing temperature (5 - 76°C). A distinctive feature of nucleation-dependent polymerization is a sigmoidal time-course curve (Nilsson, 2004; Sabate *et al.*, 2003). The nucleation step is believed to be thermodynamically unfavourable; the reaction is strongly temperature dependent (Sabate *et al.*, 2005).

In this study, the effect of temperature on β-lactoglobulin fibril formation was determined by heating the 1 % w/v β-lactoglobulin (low ionic strength) solutions, at 75, 80, 90, 100, 110, and 120°C at pH 2.0. ThT fluorescence was used to monitor the kinetics of fibril formation, and transmission electron microscopy (TEM) was used to provide direct observation of the aggregates formed.

5.3.2 Experimental

Water loss test

2 mL of water was added to each glass tube and the cap screwed tightly. The tubes were weighed before heating. The three heating blocks (DB-3D, OB-3D, TECHNE, and DB16525, THERMOLYNE) were preheated to 75, 110 and 120 °C and then the glass tubes were put into them. The test tubes were weighed and put back immediately at each designed time points. The sample series were measured in duplicate. The detailed treatments are shown in Table 5.3.1.

Table 5.3.1 Sample treatments for water loss test

Temperature [°C]	Heating time [h]
75	0, 1, 2, 4, 6, 27
110	0, 1, 2, 3, 4, 5
120	0, 1, 2, 3, 4, 5

ThT fluorescence assay

A 2 mL 1 % w/v β-lactoglobulin solution (prepared as described in Section 3.1.3) was added to each of the sealed glass tubes and the caps screwed tightly. The heat blocks (Dri-Block® DB-3D, OB-3D TECHNE and Dri-Bath®, THERMOLYNE) were preheated to designated temperature (all temperature were ±1ºC unit), the tubes were then placed in these block heaters. After specific heating times (from 0 to 24h), each tube was taken out and cooled with ice-water for 10 minutes, then used for ThT fluorescence assay. ThT measurements were performed as described in Section 3.2.1.

TEM

The heated β-lactoglobulin samples after ThT fluorescence assay were stored overnight at 4°C. Selected samples were then processed and examined using TEM as described in Section 3.2.2. The sample treatments are summarised in Table 5.3.2.

Table 5.3.2 Sample treatments for the temperature experiments

Temperature °C	Heating times [h]	ThT fluorescence assay times	TEM times [h]
75	0, 2, 3, 4, 6, 8,14,16, 24	all heating times	4
80	0, 1, 2, 3, 4, 6, 8, 9, 10, 12, 16, 24	all heating times	2
90	0, 0.5, 1, 1.5, 2, 3, 4, 6, 8, 9, 10, 12	all heating times	2
100	0, 0.5, 1, 1.5, 2, 3, 4, 6 ,7, 8, 9, 10, 12	all heating times	1
110	0, 0.5, 1, 2, 3, 4, 4.5, 5, 6, 7, 8	all heating times	2, 6
120	0, 0.5, 1, 2.25, 3.3, 4, 4.5, 5, 6, 7, 8	all heating times	2, 8

5.3.3 Results

Water loss test

In order to determine how much water was evaporated from the sample solution in sealed tubes, the water loss experiment was carried out. The results are summarised in Table 5.3.3. The detailed experimental data are shown in Appendix 5.3.1. The results shown in Table 5.3.3 indicate that the water loss rate increased with increasing temperature. The water loss will become considerable when heating at 110 and 120°C for a long time. Water loss from sample solutions will influence the measurements of ThT fluorescence, the data obtained from ThT fluorescence assay should be adjusted by water loss.

Table 5.3.3 Results of water loss test

Temperature	**75°C**	**110°C**	**120°C**
Average water loss rate [g/h]	0.0029	0.0064	0.0254

ThT fluorescence assay

In this study, ThT fluorescence was used to monitor the kinetics of aggregation at different temperatures at pH 2.0. The ThT fluorescence measurements at various temperatures from 75 to 120°C were plotted in Figure 5.3.2. The experimental data of 110 and 120°C samples were adjusted for water loss before plotting. The directly measured data and the data after water loss modification for 110 and 120°C were plotted in Figure 5.3.1. It can be easily seen that the ThT fluorescence measurements decreased after water loss adjustment.

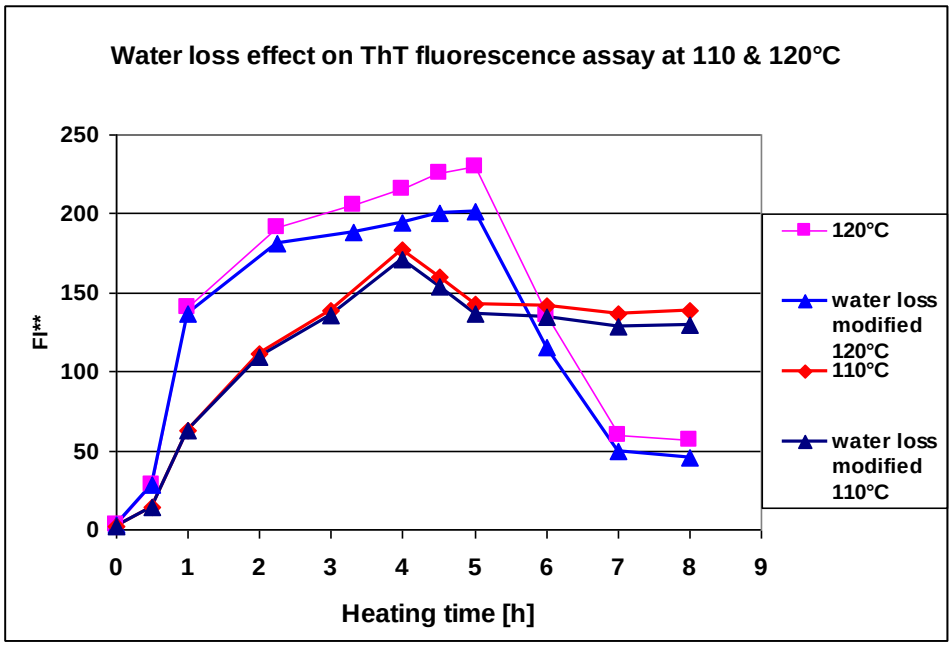

Figure 5.3.1 Influence of water loss on ThT fluorescence data at 110 and 120°C (average values).

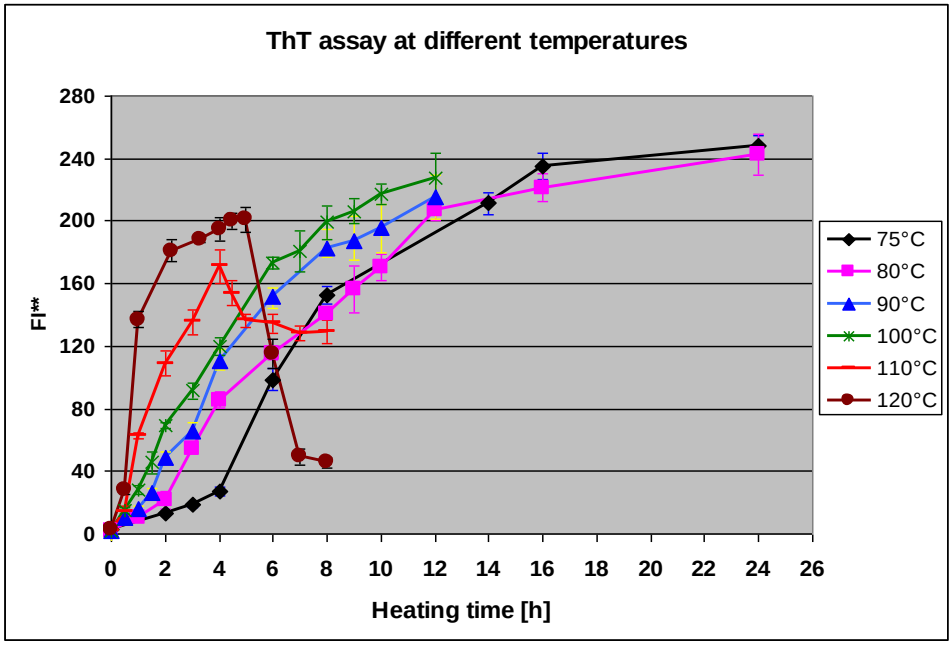

Figure 5.3.2 Effect of temperature on fibril formation of β-lactoglobulin (1 % w/v). All samples were incubated at pH 2.0 ± 0.05 without added salt. Samples were measured in triplicate, error bars indicate the standard error of mean (SEM). The data at 110 and 120 °C were already adjusted of water loss.

The enhanced fluorescence emissions of ThT indicate the presence of amyloid fibrils at all the temperatures. From Figure 5.3.2 it can be seen that the length of lag phase was sensitive to temperature, the lag time decreased from 3 - 4 hours at 75°C to less than 0.5 hour at higher than 100°C. The growth rate was also accelerated by increasing temperature; the slope of growth curve became deeper with increasing

temperature. Therefore, the whole fibril formation process was accelerated by increasing temperature; at 110 and 120°C, the fibrillation process was nearly completed after heating for 4 and 2 hours respectively, while this time extended to 10-16 hours when heating at 100-75°C.

Interestingly, the ThT fluorescence of 110 and 120 °C samples dropped rapidly after reaching their peak values at 4 and 6 h, indicating the decrease of amyloid structures by prolonged heating. In order to see the effect of prolonged heating on fibril formation at 110 and 120°C, TEM images were taken at different heating times (Figure 5.3.3).

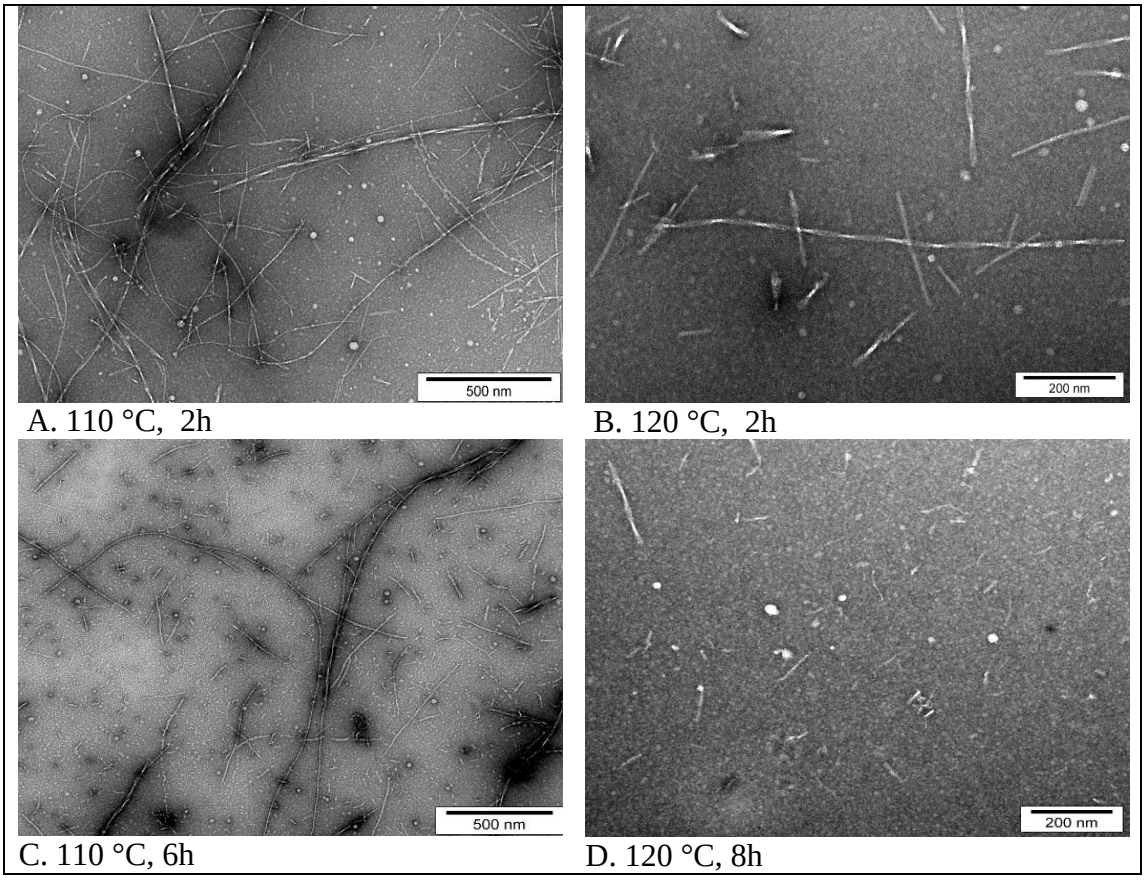

A. 110 °C, 2h B. 120 °C, 2h

C. 110 °C, 6h D. 120 °C, 8h

Figure 5.3.3 Negatively stained TEM image of β-lactoglobulin (1 % w/v) at 110 and 120°C, pH 2.0, low ionic strength, for 6 and 8 hours.

Figure 5.3.3, A and C show the aggregates formed at 110 °C after heating for 2 and 6 hours respectively. Comparing these two images, it can be seen that the percentage of long fibrils reduced and more short fibrils appeared. When heating at 120 °C for 8 hours, (Figure 5.3.4, D), fibrils became much shorter and thinner in comparison to the

fibrils at 2 h (Figure 5.3.4, B). Such drop might be caused by the destruction of the earlier formed fibrils which decreased the ThT fluorescence emission.

TEM

The effect of temperature on the morphology of β-lactoglobulin aggregates was studied using TEM. The presence of fibril at all temperatures was confirmed by direct observation with TEM images (Figure 5.3.4).

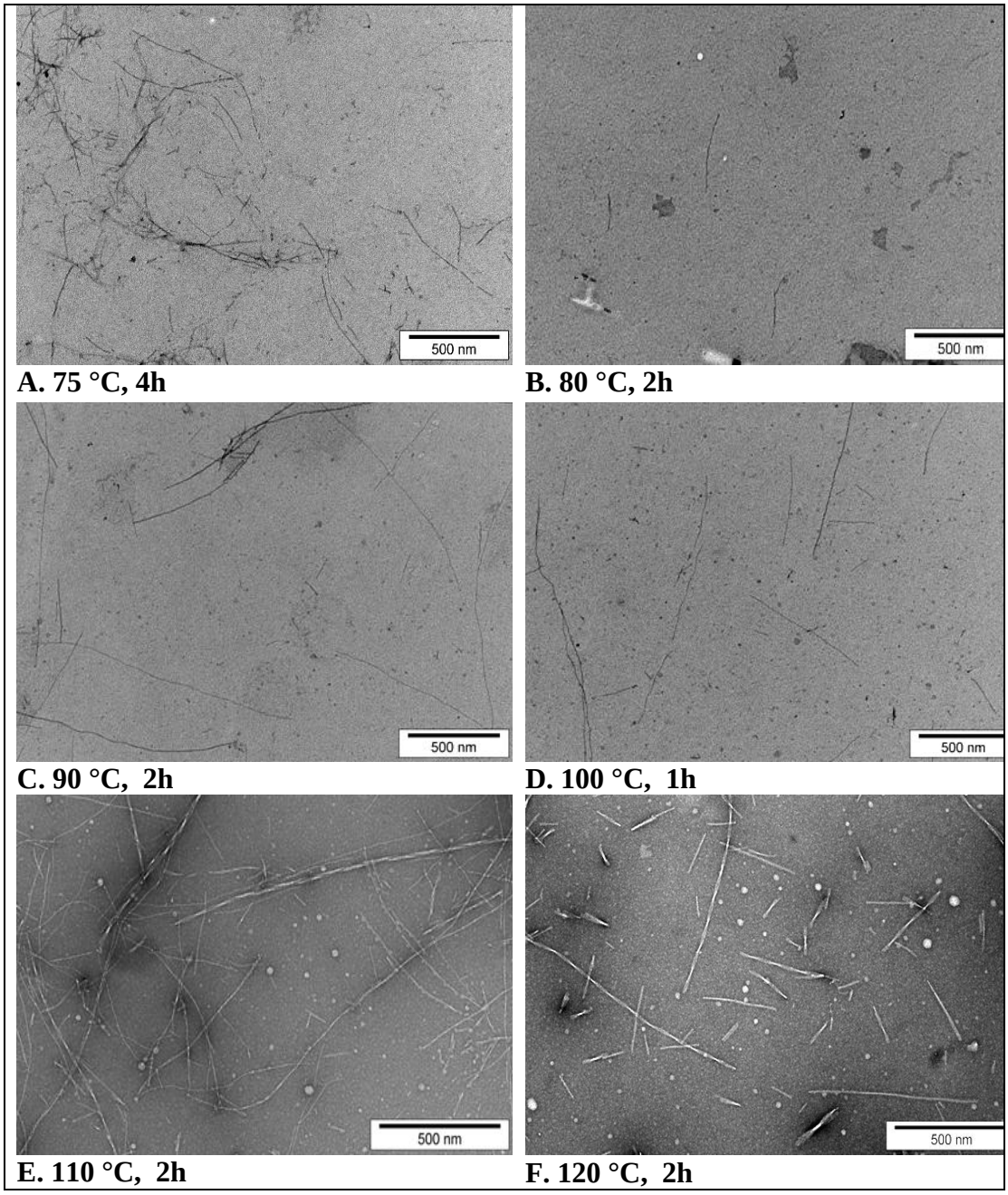

Figure 5.3.4 Negatively stained TEM image of β-lactoglobulin (1 % w/v) at various temperatures, at pH 2.0 and low ionic strength.

The TEM results suggest that the fibrils formed immediately and grew up rapidly when incubating at 110 - 120°C, as indicated by the appearance of large fibrils (bundle- like fibrils) in Figure 5.3.4, E-F. On the other hand, the fibril formation was slow at low temperature (Figure 5.3.4, A). The observations from the TEM study are in excellent agreement with the results of ThT fluorescence assay. The results from ThT fluorescence assay and TEM study are summarised in Table 5.3.4.

Table 5.3.4 Results of ThT fluorescence and TEM

Sample	[1]Fibril Morphology (at observed time point)	[2]Lag phase time [h]	[2]Time to beginning of stationary phase [h]
75°C	Short and intermediate thin	3 - 4	16
80°C	short and thin	2	12
90°C	long and short thin	1 - 1.5	9 - 10
100°C	long and short thin	0.5	8 - 9
110°C	long and short thick , bundle-like	No lag phase	4
120°C	short, thick and bundle-like		2

[1] Short fibril is less than 500 nm, intermediate fibril is between 500 and 1000 nM, long fibril is longer than 1000 nm.
[2] The times are approximate values

Two-step autocatalytic reaction model fitting

The temperature dependence of β-lactoglobulin fibril formation kinetics was analysed by fitting the ThT fluorescence data with Eq. (3), using SigmaPlot 10.0 software. This equation represents a two-step autocatalytic reaction mechanism.

$$[B]_t = [A]_0 - \frac{\frac{k_1}{k_2} + [A]_0}{1 + \frac{k_1}{k_2[A]_0}\exp[t(k_1 + k_2[A]_0)]} \quad (3)$$

The obtained nucleation reaction rate, k_1 and elongation reaction-rate, k_2 for samples at all temperatures are shown in Table 5.3.5. The detailed analytical results are shown in Appendix 5.3.2.

Table 5.3.5 Model fitting results for fibril formation at various temperatures

Temperature [°C]	k_1 **[h^{-1}]**	k_2 **[$RFU^{-1}h^{-1}$]**	**Rsqr**
75	1.55E-02	2.02E-03	0.984
80	6.45E-02	6.54E-04	0.976
90	8.24E-02	1.66E-03	0.970
100	1.27E-01	8.42E-04	0.980
110	1.53E-01	4.96E-03	0.964
120	6.97E-02	2.89E-02	0.993

The results in Table 5.3.5 demonstrate that the nucleation rate, k_1, increased with increasing temperature from 75 to 110°C but reduced at 120°C. There was no clear correlation between the elongation rate, k_2, and temperature. The low value of k_1 of the 120°C sample was inconsistent with the results of ThT fluorescence and TEM study. According to the model analytical results of 110 and 120°C, the VIF values were very high (>32 and >10 respectively), which means the two parameters were highly dependent on each other. Furthermore, the decrease of k_1 at 120°C was not in agreement with the results from ThT fluorescence assay and TEM imaging.

The two-step autocatalytic reaction model fitted plots of all samples are shown in Figure 5.3.5. It shows the model predictions and the ThT fluorescence assay data. From the plots, it can be seen that at high temperature (100-120°C) the predicted value did not fit the experimental data very well. This is possibly due to the very short or even lack of a lag phase when heating at high temperatures.

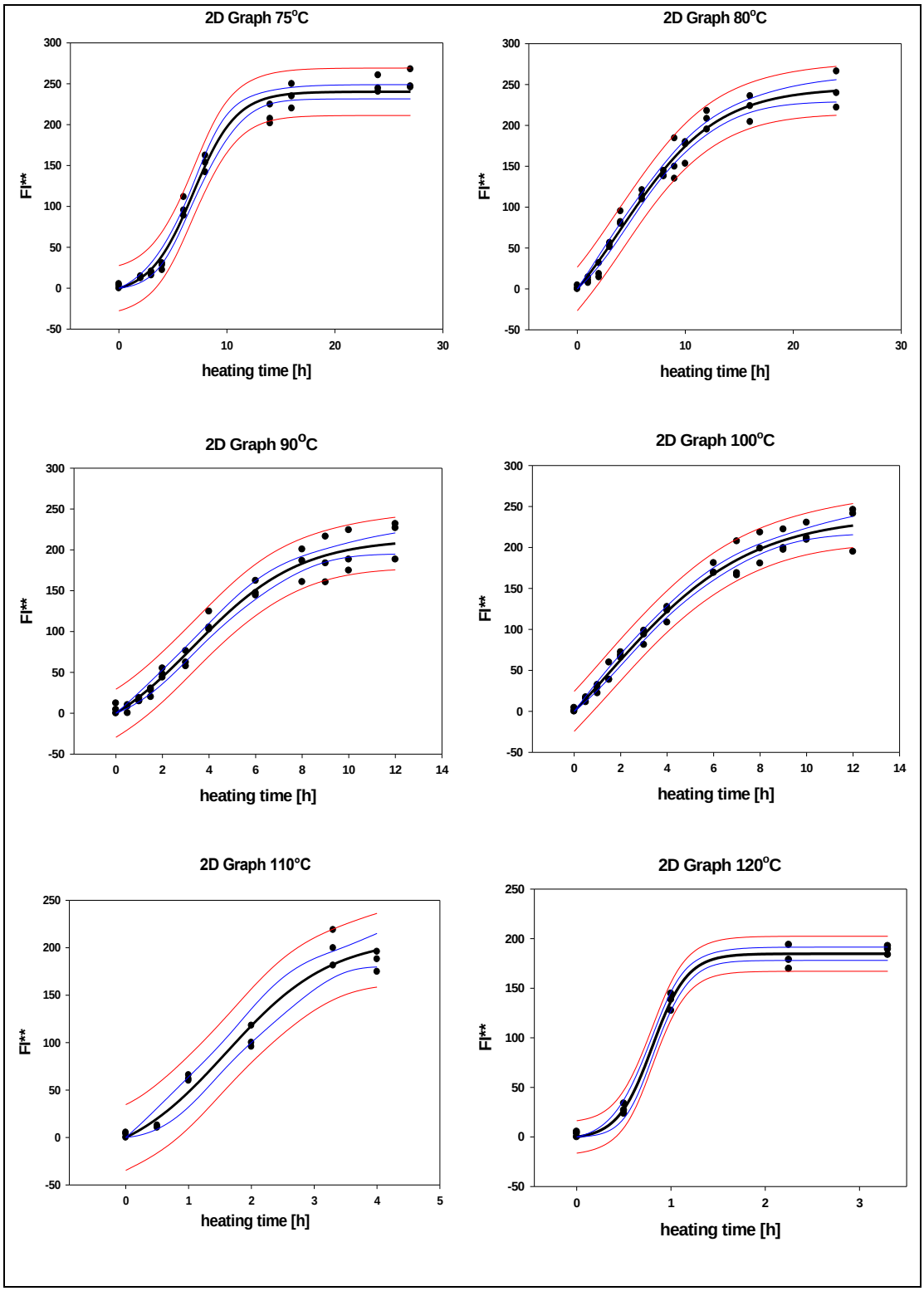

Figure 5.3.5 Two-step autocatalytic reaction model fitting of β-lactoglobulin (1 % w/v) at different temperatures using SigmaPlot 10.0.

5.3.4 Discussion

The fibril formation process of β-lactoglobulin appears strongly dependent on temperature. The lag phase time was significantly reduced by increasing temperature and the rate of the fibril growth increased more steeply with increasing temperature. Similar results were obtained by Vetri and Militello (2005). The similar effects of temperature on fibril formation were also found for other proteins such as, ovalbumin, crude egg white, and BSA (Pearce *et al.*, 2007).

The reduction of lag phase time at higher temperatures could be caused by the faster association of monomers in the nucleation step, which is thermodynamically unfavourable (Sabate *et al.*, 2003). In addition, higher temperature can increase the denaturation and hydrolysis rate of β-lactoglobulin, therefore shorten the lag time.

The rapid formation of shorter fibrils at higher temperature, compared to the slow formation of long fibrils at lower temperature, is very interesting. It has been reported that the aggregation rate is correlated to fibril length (Smith & Radford, 2001). Fast aggregation is associated with short fibrils, whereas conditions favouring slower growth lead to longer fibrils. The increase of short fibrils and decrease of the long fibrils at 110 and 120 °C (the majority fibrils are short fibrils at 120°C) are probably caused by the rapidly formed large number of nuclei during fibril formation process. Thus, not many monomers remain to elongate the nucleus to form long fibrils. The ratio of long and short fibrils is influenced by the relative rates of nucleation and growth reactions. The population of each fibril type depends on the relative rates of assembly along each pathway and, eventually, on the stability of each fibril type under the incubation conditions.

The observations of TEM suggest that the morphology of the fibrils can be altered by higher temperatures (110-120°C), in comparison with the well defined fibrils formed at lower temperatures. Bundle-like fibrils which look like the initial formed species intertwined together can be observed in Figure 5.3.4, E-F. As the TEM method is invasive, the twisted appearance of the fibrils observed at 110 and 120 °C may be caused from the variance in height along the fibril length.

The significant drop in ThT fluorescence observed after heating for 4 or 6 hours may reflect the conversion of β-lactoglobulin fibrils from well defined long and thick to poor defined short and thin, which may have a lower affinity toward ThT. Similar phenomena were also observed by other researchers (Khurana *et al.*, 2001a; Nilsson, 2004). They believe such a drop is caused by the decrease of ThT binding sites of the fibrillar aggregates formed by prolonged heating.

5.3.5 Conclusions

The fibril formation process was accelerated by increasing temperature. The acceleration is due to the decrease of lag phase time and the faster growth in the growth phase. The lag phase can be reduced or even eliminated by heating at sufficiently high temperature, such as > 100 °C in this study.

A significant drop in ThT fluorescence was found for the 110 and 120°C samples after heating for 4 to 5 hours. Therefore, prolonged incubation at 110 or 120 °C resulted in the decrease of fibril yield.

The morphology of the fibrillar aggregates was also altered by varying temperature. Long and thin fibrils formed at lower temperature (<100°C), while short and thick fibrils were predominant at higher temperature (110 and 120°C). It is apparent that the ratio of long and short fibrils is partly determined by kinetic competition between the pathways leading to nucleation and elongation.

The ThT fluorescence data were analysed with the two-step autocatalytic reaction model. The analytical results suggest that this model cannot fit the data very well at higher temperatures.

CHAPTER 6

EFFECTS OF MULTI-FACTORS ON β-LACTOGLOBULIN FIBRIL FORMATION

6.1 Introduction

From the early studies on the individual effects of the environmental factors (Section 4.2, 4.3, 4.4), it was found that pH, NaCl, $CaCl_2$ and temperature, have a strong impact on fibril formation of β-lactoglobulin. They influence both the kinetics of fibrillation and the morphology of the fibrils. The consensus of these experimental results derived by the independent experiments leads to proposing new incubation conditions for amyloid formation.

This experiment was set out to investigate the interaction and non-linear effects of the four factors on β-lactoglobulin fibril formation. β-Lactoglobulin (1% w/v) solution was incubated under a variety of different solution conditions (pH, temperature, and ionic strength) which induce fibril formation. These factors were pH (1.0 - 3.0), temperature (80 - 120°C), NaCl (0 - 100 mM), $CaCl_2$ (0 – 80 mM). The fibrillation process was monitored by ThT fluorescence; some special samples were examined for the presence of fibrils by TEM.

The experimental strategy chosen for the optimization of incubation conditions was a central composite circumscribed design (CCC), which is the original form of Central Composite Design (CCD). CCD is a popular design for modelling and analysis in applications where a response of interest is influenced by several variables and the objective is to optimize this response (Montgomery *et al.*, 2004).

The CCC design consists of a combination of a factorial design and an additional design (star design) in which the centre of both designs coincide. The star points are at α distance from the centre and establish new extremes for the low and high settings for both factors. This design has circular symmetry and requires five levels for each factor. To maintain rotatability, the α value based on the properties desired for the

design and the number of factors in the design (Greenfield & Metcalfe, 2007). Figure 6.1 illustrates the position of star points on a CCC design.

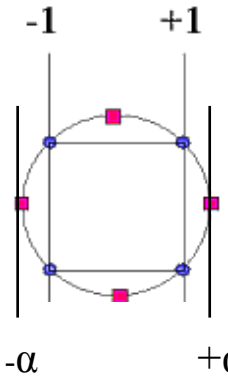

Figure 6.1 Positions of star points (■) on CCC designs. (http://www.itl.nist.gov/div898/handbook/pri/section3/pri3361.htm)

6.2 Experimental

Central Composite Circumscribed (CCC) Design

The parameter settings in the design are provided in Table 6.1, while the design is reproduced in Table 6.2. The design runs were carried out in a randomized sequence. The experimental block design is shown in Appendix 6.1. The whole experimental design consists of a 2^4 full factorial design (16 trials), a centre points design (3 trials), and a 2×4 runs of the "start" point design.

Table 6.1 Factor settings in the CCC design

Factor	Code	Level				
		$-\alpha^1$	-1	0	1	α^1
NaCl [mM]	A	0	25	50	75	100
$CaCl_2$ [mM]	B	0	20	40	60	80
Temperature [°C]	C	80	90	100	110	120
pH	D	1	1.5	2	2.5	3

[1] α= [number of factorial runs]$^{1/4}$ α=[16]$^{1/4}$ = 2

Table 6.2 CCC experimental design used in this study

Trial order	Treatment				Coded Variables			
	NaCl [mM]	$CaCl_2$ [mM]	Temp [C°]	pH	A	B	C	D
1	50	40	100	2.0	0	0	0	0
2	25	20	90	1.5	-1	-1	-1	-1
3	75	20	90	1.5	+1	-1	-1	-1
4	25	60	90	1.5	-1	+1	-1	-1
5	75	60	90	1.5	+1	+1	-1	-1
6	25	20	110	1.5	-1	-1	+1	-1
7	75	20	110	1.5	+1	-1	+1	-1
8	25	60	110	1.5	-1	+1	+1	-1
9	75	60	110	1.5	+1	+1	+1	-1
10	25	20	90	2.5	-1	-1	-1	+1
11	75	20	90	2.5	+1	-1	-1	+1
12	25	60	90	2.5	-1	+1	-1	+1
13	75	60	90	2.5	+1	+1	-1	+1
14	25	20	110	2.5	-1	-1	+1	+1
15	75	20	110	2.5	+1	-1	+1	+1
16	25	60	110	2.5	-1	+1	+1	+1
17	75	60	110	2.5	+1	+1	+1	+1
18	50	40	100	2	0	0	0	0
19	0	40	100	2	-2	0	0	0
20	100	40	100	2	+2	0	0	0
21	50	0	100	2	0	-2	0	0
22	50	80	100	2	0	+2	0	0
23	50	40	80	2	0	0	-2	0
24	50	40	120	2	0	0	+2	0
25	50	40	100	1	0	0	0	-2
26	50	40	100	3	0	0	0	+2
27	50	40	100	2	0	0	0	0

: centre points
: factorial points
: star points

Sample preparation

The protein sample solutions were prepared according to the CCC design shown in Table 6.2. The original 1.2 % w/v β-lactoglobulin solutions (prepared as described in Section 3.1.3) were adjusted to the desired pH values (± 0.05) with a 6 M HCl solution. Different volumes of 1M salt solutions were added to the protein solutions and mixed well to achieve the desired salt concentrations (protein concentration decreased slightly, by adding 1M NaCl and $CaCl_2$ standard solutions and pH adjustment).

ThT fluorescence assay

2 mL of each prepared sample solution was put into the sealed glass tube (the cap screwed tightly to prevent water evaporation) and heated in the heat blocks at designated temperatures (treatments are shown in Table 6.2). The tubes were taken out at designated times shown in Table 6.3 and cooled with ice-water for 10 minutes, then used for ThT fluorescence assay. ThT fluorescence measurements were performed as described in Section 3.2.1.

TEM

After finishing the ThT fluorescence assay, the selected protein samples shown in Table 6.3 were kept at 4°C overnight. The samples were then processed and examined with TEM as described in Section 3.2.2.

Table 6.3 Sample treatments for the CCC design experiment

Sample Trial #	ThT fluorescence assay times [h]	TEM times [h]
8, 9	0, 1, 2, 3, 4, 6, 8, 9, 10, 16, 24	1
1, 7, 13,15, 16, 17, 18, 8, 22, 25, 26	0, 1, 2, 3, 4, 6, 8, 9, 10, 16, 24	2
16	0, 1, 2, 3, 4, 6, 8, 9, 10, 16, 24	4
19	0, 1, 2, 3, 4, 6, 8, 9, 10, 16, 24	2
24	0, 1, 2, 3, 4, 6, 8, 9, 10, 16, 24	2
27	0, 1, 2, 3, 4, 6, 8, 9, 10, 16, 24	6
2, 3, 4, 5, 6, 10, 11, 12, 14	0, 1, 2, 3, 4, 6, 8, 9, 10, 16, 24	No data

6.3 Results

6.3.1 ThT fluorescence, TEM and the samples appearance

All samples in each variant incubation conditions were monitored by ThT fluorescence. The fibril growth curves were quite different to each other; most of them did not show the typical sigmoidal shape (results shown in Appendix 6.2), for example, the time-course curve of trial 7# decreased continually after heating for 2h without lag and stationary phase. This observation indicates that the rate of fibril formation of β-lactoglobulin was found to be very sensitive to the treatment.

Based on the results obtained from ThT fluorescence assays, some samples were selected for the TEM examination. During the incubation time, each sample was visually examined for its viscosity, gel formation, and the appearance of white colour. The visually observed results together with the results obtained from ThT fluorescence assay and TEM are summarised in Table 6.4.

Table 6.4 Results of ThT fluorescence assay, TEM and the observation of sample solutions

Trial #	Temp [°C]	NaCl [mM]	$CaCl_2$ [mM]	pH	Peak time[1] [h]	FI**$_{peak}$ [RFU][2]	Gel[3]	Solution colour white[4]	Fibril shape [5]	Ionic strength [mM]
1	100	50	40	2	4	132.32	*	+	most curly M+S+L	170
2	90	25	20	1.5	4	205.3	*	no	No TEM	85
3	90	75	20	1.5	4	254.7	*	+	No TEM	135
4	90	25	60	1.5	3	247.7	*	++	No TEM	205
5	90	75	60	1.5	2	319.8	***	+++	No TEM	255
6	110	25	20	1.5	1	132.5	*	no	No TEM	85
7	110	75	20	1.5	1	274.38	*	+	most curly S	135
8	110	25	60	1.5	2	260.06	*	++	curly S	205
9	110	75	60	1.5	1	369.42	**	+++	curly S	255
10	90	25	20	2.5	10	112.55	*	no	No TEM	85
11	90	75	20	2.5	6	265.45	*	no	No TEM	135
12	90	25	60	2.5	6	256.76	*	+	No TEM	205
13	90	75	60	2.5	4	339.79	***	+++	curly L+M	255
14	110	25	20	2.5	3	95.52	*	no	No TEM	85
15	110	75	20	2.5	4	146.56	*	+	curly L+M+S	135
16	110	25	60	2.5	4	207.45	*	++	most curly S	205
17	110	75	60	2.5	3	291.73	**	+++	curly M + S	255
18	100	50	40	2	4	103.07	*	+	most curly M+S+L	170
19	100	0	40	2	4	234.57	***	no	straight L+M+S	120
20	100	100	40	2	4	263.04	**	++	curly M+ S	220
21	100	50	0	2	10	169.93	**	no	straight L+M+S	50
22	100	50	80	2	3	210.73	*	+++	curly S	290
23	80	50	40	2	10	173.39	*	+	most curly M+L	170
24	120	50	40	2	1	221.15	*	+	Straight M+S	170
25	100	50	40	1	2	255.53	**	++	curly S	170
26	100	50	40	3	2	662.8	**	+++	curly S	170
27	100	50	40	2	4	117.29	*	+	most curly M+S+L	170

[1] Peak time: the time when the ThT fluorescence data starts to level off.
[2] FI^{**}_{peak} : the FI** value at peak time.
[3] * : the quantity of gel particles appeared in the sample solution.
[4] +: the intensity of white colour of the sample solution.
[5] S: short fibrils <500 nm; M: intermediate fibrils 500-1000 nm;
L: long fibrils >1000 nm.

Fibril shape and solution whiteness versus ionic strength

The fibril shape observed from TEM study and the solution colour of the heating protein samples were compared against the ionic strength (Table 6.5).

Table 6.5 Fibril shape and solution whiteness as a function of ionic strength

Ionic strength [mM]	**Fibril shape**			**Solution whiteness**[2]			
	straight	straight and curly mix	curly	no	+	++	+++
50	√[1]			√			
85	√			√ √√√			
120	√			√			
135		√√		√	√√√		
170	√	√√√	√√√		√√√√√	√	√
205		√	√		√	√√√	
220			√			√	
255			√√√				√√√√
290			√				√

[1] √ represents one trial
[2] + the intensity of white colour of the sample solution

From the results shown in Table 6.5, it can be seen that fibril shape changed from straight to curly by increasing ionic strength, which is in agreement with the observation obtained in Section 5.3.

The intensity of whiteness of the heated protein solution was estimated visually. It can be seen from Table 6.5 that the basic trend is that the intensity of whiteness of the solution increased with increasing ionic strength. The white colour of the solution is due to the scattering of light by the dispersed phase of colloidal particles. The intensity of colour is directly proportional to the size and number of the particles (Chandan *et al.*, 2006). As large linear aggregates produce transparent gel particles, the white colour is likely due to the presence of large random aggregates.

These observations suggest that more random aggregates were formed when the amount of added salt was increased. Under the pH range 1.0 - 3.0, β-lactoglobulin has a net positive charge; the electrostatic repulsion between the protein molecules is strong. When adding salts, the net positive charge was shielded by anions (Cl^-). Therefore, the electrostatic repulsion between protein molecules was reduced and random aggregates were formed. According to Nielsen *et al.* (2001) such random aggregates could be the β-lactoglobulin–Cl complexes.

6.3.2 Sample selection

The optimum conditions were selected according to the large peak value, FI^{**}_{peak} and short peak time. According to the results shown in Table 6.4, the samples which give both a high peak value (FI^{**}_{peak} >200 RFU) and short peak time (<=4 hours) were selected and divided into three groups (Table 6.6). Their TEM images are shown in Figure 6.2.

Table 6.6 The selected samples (three groups)

	Trial #	**TEM image**	**Temp [°C]**	**NaCl [mM]**	**$CaCl_2$ [mM]**	**pH**
Group 1 peak time 1- 2 hours FI^{**}_{peak} >300 RFU	9	A	100	50	40	3
	26	B	110	75	60	1.5
	5	No data	90	75	60	1.5
Group 2 peak time 1- 2 hours FI^{**}_{peak} >200 RFU	7	C	110	75	20	1.5
	8	D	110	25	60	1.5
	24	E	120	50	40	2
	25	F	100	50	40	1
Group 3 peak time 3- 4 hours FI^{**}_{peak} >200 RFU	13	G	90	75	60	2.5
	16	H	110	25	60	2.5
	17	I	110	75	60	2.5
	19	J	100	0	40	2
	22	K	100	50	80	2

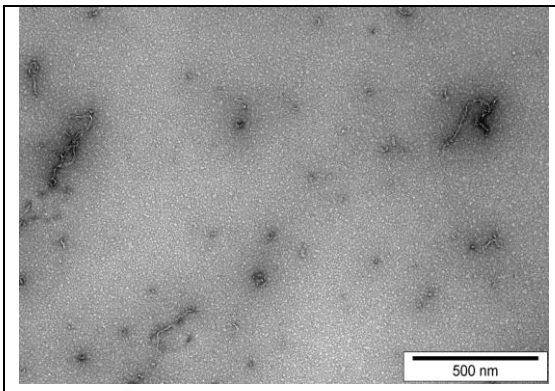

A. 9#-1h

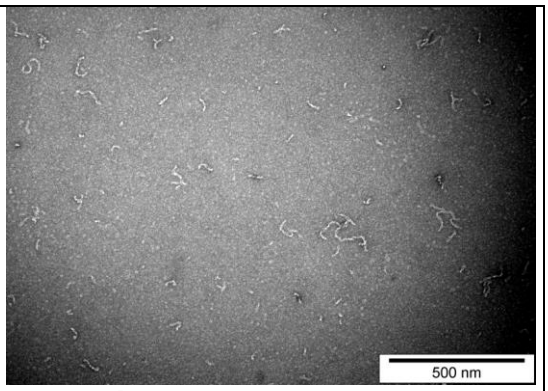

B.26#-2h

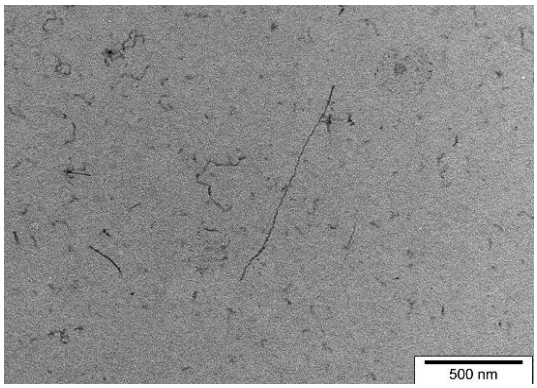

C. 7#-2h

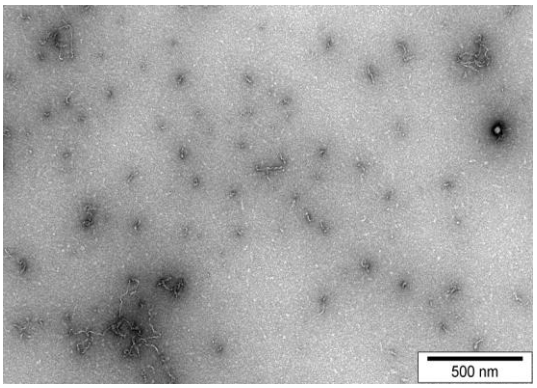

D. 8#-1h

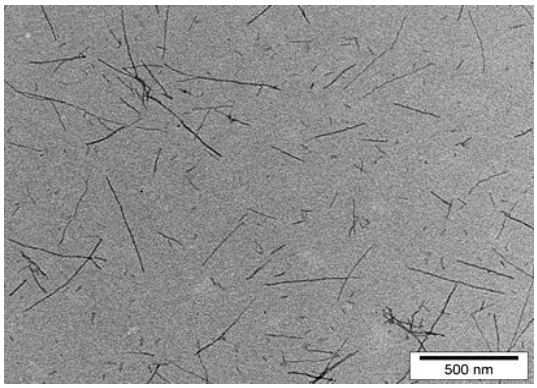

E. 24#-2h

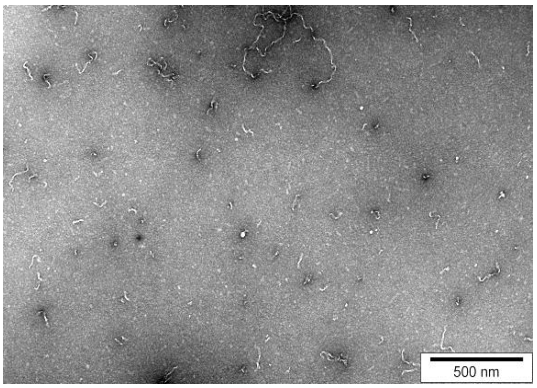

F. 25#-2h

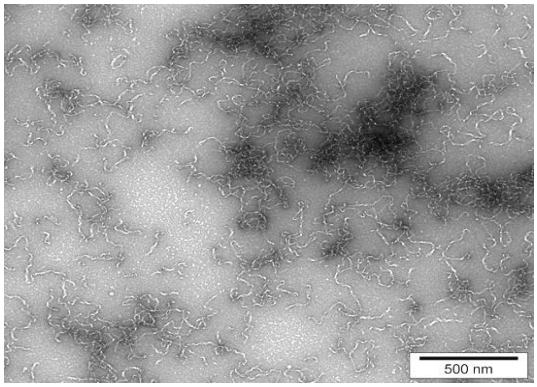

G. 13#-2h

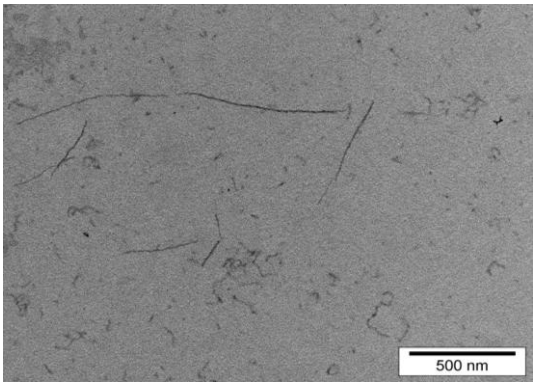

H. 16#-4h

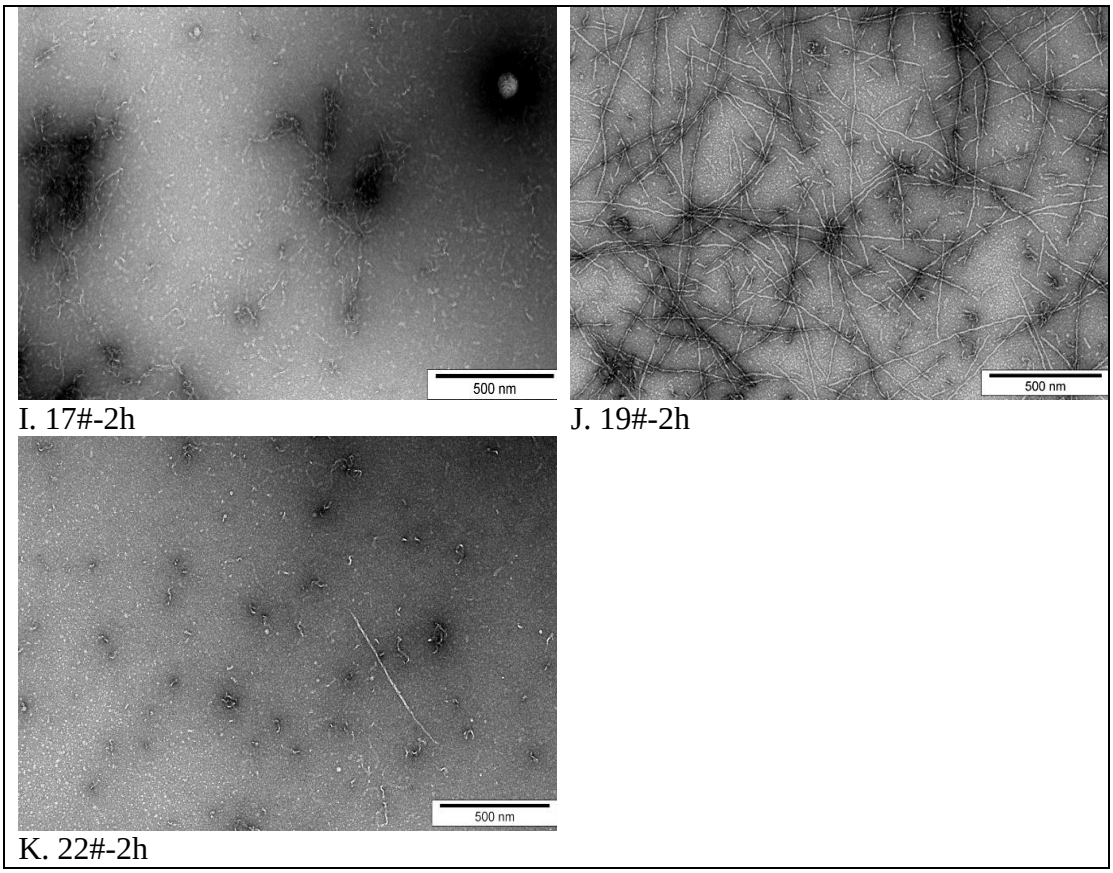

I. 17#-2h J. 19#-2h

K. 22#-2h

Figure 6.2 Negatively stained TEM images of selected samples. β-Lactoglobulin (approximately 1 % w/v). The relative incubation conditions are shown in Table 6.6.

6.3.3 Statistical analysis using Minitab 15.0

- **ANOVA:** FI^{**}_{peak} **versus treatment**

The FI^{**}_{peak} of the 25 treatments (total 27 trials, 1#, 18# and 27# were under the same treatment) were analysed with ANOVA. The detailed analytical results are shown in Appendix 6.3.

The results indicate that treatment has a significant effect ($P<0.0005$) on FI^{**}_{peak}**.** These results suggest the incubation conditions (combination of the four factors) significantly influenced the quantity of fibril yield at peak time.

- **Response Surface Regression: FI^{**}_{peak} vs. NaCl, $CaCl_2$, temperature and pH**

The peak value, FI^{**}_{peak} , was analysed as a function of the four factors with Response Surface Regression using Minitab 15.0. The results are shown in Table 6.7. The detailed analytical results are shown in Appendix 6.3.

Table 6.7 The effects of the four environmental factors on peak FI^{**}_{peak}

Response Surface Regression: FI^{**}_{peak} versus A-NaCl, B-$CaCl_2$, C-temp, D-pH

The analysis was done using coded units.
Estimated Regression Coefficients for FI**

Term	Coef	SE Coef	T	P
Constant	117.563	23.16	5.077	0.000
A-NaCl	61.641	16.37	3.765	0.000
B-$CaCl_2$	68.983	16.37	4.213	0.000
C-temp	-15.846	16.37	-0.968	0.337
D-pH	43.973	16.37	2.686	0.009
A-NaCl*A-NaCl	108.615	34.73	3.127	0.003
B-$CaCl_2$*B-$CACl_2$	50.554	34.73	1.455	0.150
C-temp*C-temp	57.084	34.73	1.643	0.105
D-pH*D-pH	318.978	34.73	9.183	0.000
A-NaCl*B-$CACl_2$	3.701	40.11	0.092	0.927
A-NaCl*C-temp	22.586	40.11	0.563	0.575
A-NaCl*D-pH	-15.677	40.11	-0.391	0.697
B-$CaCl_2$*C-temp	53.704	40.11	1.339	0.185
B-$CaCl_2$*D-pH	21.073	40.11	0.525	0.601
C-temp*D-pH	-75.849	40.11	-1.891	0.063

S = 69.4676 PRESS = 490285
R-Sq = 67.20% R-Sq(pred) = 49.51% R-Sq(adj) = 60.25%

Based on the analytical results, the three main effects of NaCl, $CaCl_2$, pH, the quadratic items of NaCl and pH were statistically significant ($P<0.01$, shown with yellow colour in Table 6.7). All the interaction effects were not statistically significant ($P>0.05$).

The significant positive effects of NaCl, $CaCl_2$ and pH suggests that increasing the value of these three individual factors within the investigated range will lead to a significant increase of FI^{**}_{peak}, which means a significant increase of fibril yield at the peak time. In addition, the significant effects of quadratic items of NaCl and pH indicate that the increase of fibril yield is even bigger. The positive effect of pH on fibril yield is not consistent with the results from individual study of pH (Section 5.1); this inconsistency might be due to the wider pH range and the effects of interactions in this experiment.

The coefficient of the temperature on FI^{**}_{peak} was -15.846, indicating that the quantity of fibril yield decreased with increasing temperature. However, the P value was 0.337, indicating that the effect of temperature was not significant. The negative effect of temperature on fibril yield is in agreement with the results obtained from earlier individual study (Section 5.3).

- **Response Surface Regression: Peak time vs. NaCl, $CaCl_2$, temperature and pH**

The peak time was the time when the increase in ThT fluorescence started to level off, which means fibrillation starts to enter its stationary phase. Response Surface Regression was used to analyse the effect of the four factors (Table 6.8).

Table 6.8 The effects of the four environmental factors on peak time

Response Surface Regression: peak time versus A-NaCl, B-$CaCl_2$, C-temp, D-pH

The analysis was done using coded units.
Estimated Regression Coefficients for peak time

Term	Coef	SE Coef	T	P
Constant	4.0000	0.8022	4.986	0.000
A-NaCl	-0.6667	0.5672	-1.175	0.263
B-$CaCl_2$	-0.6667	0.5672	-1.175	0.263
C-temp	-3.1667	0.5672	-5.583	0.000
D-pH	1.8333	0.5672	3.232	0.007
A-Nacl*A-NaCl	-0.1667	1.2033	-0.139	0.892
B-$CaCl_2$*B-$CaCl_2$	-0.1667	1.2033	-0.139	0.892
C-temp*C-temp	1.3333	1.2033	1.108	0.290
D-pH*D-pH	-2.1667	1.2033	-1.801	0.097
A-NaCl*B-$CaCl_2$	-0.5000	1.3894	-0.360	0.725
A-NaCl*C-temp	1.5000	1.3894	1.080	0.302
A-NaCl*D-pH	-1.0000	1.3894	-0.720	0.485
B-$CaCl_2$*C-temp	2.5000	1.3894	1.799	0.097
B-$CaCl_2$*D-pH	-1.0000	1.3894	-0.720	0.485
C-temp*D-pH	-1.0000	1.3894	-0.720	0.485

S = 1.38944 PRESS = 133.44
R-Sq = 82.61% R-Sq(pred) = 0.00% R-Sq(adj) = 62.31%

The analytical results indicate that only the effect of temperature and pH are significant ($P<0.01$, shown with yellow colour in Table 6.8). All the interaction and non-linear effects are not significant.

NaCl, $CaCl_2$ and temperature had negative effects on peak time, which means increasing the concentration of salt (NaCl, $CaCl_2$) and temperature could reduce the time needed for β-lactoglobulin fibrillation, but only the effect of temperature was

significant. In contrast, pH had a significant positive effect, which indicates that increasing pH will significantly prolong the fibrillation time. The main effect results obtained from the CCC experiment are consistent with the results obtained from the previous individual studies reported in Chapter 5.

6.4 Discussion

From the results of ThT fluorescence assay and TEM study, some interesting observations were found. Some of the samples, for example 9# and 26#, gave very high values of FI^{**}_{peak} (Table 6.4), but the fibrils observed in their TEM images did not appear higher than the others (Figure 6.2). On closer inspection, much smaller and meandering or wormlike fibrils were evident, these being typically 100-500 nm in length and highly compact (Figure 6.2, A and B). So the high ThT fluorescence value of these two samples could be caused by the presence of a large quantity of such short and compact fibrils. However, the high ThT fluorescence signals may not be accurate due to the interference of the random aggregates which cause turbid solutions. These phenomena need to be investigated in the later study.

Several factors have been shown to influence the process of amyloid fibril formation. The individual effects of pH, NaCl, $CaCl_2$ and temperature on β-lactoglobulin fibril formation were investigated in the earlier experiments and strong effects were found (see Chapter 5). This CCD experiment investigated interactions between factors and non-linear effects of individual factors. The analytical results show that NaCl, $CaCl_2$, pH have significant effects on FI^{**}_{peak} while temperature and pH have significant effects on peak time. The interactions and non-linear effects do not significant on FI^{**}_{peak} (except "D-pH*D-pH" on FI^{**}_{peak}) and peak time.

To interpret these results only using simple terms such as "inhibition" or "promotion" are inadequate (Lomakin *et al.*, 1996). These factors are not necessary work in the same direction. For example, lower temperature inhibits nucleation, since the total number of fibrils will be small, but on the other hand it promotes elongation, since longer fibrils will be formed.

The samples were prepared in batches; a single batch was used for all of the time points, further sources of variation would be introduced if each sample was made up separately. The trials were performed in different days and it was assumed that the day would have no effect on the outcome.

Considering the individual effect and the interaction effect of the factors, it is a challenge to explain all the results obtained. There is no doubt that the four factors are important for determining the fibrillation kinetics and the fibril morphology, but if people want to have a clear view of the intact system, more research is needed.

6.5 Conclusions

The individual items of NaCl, $CaCl_2$, pH and the non-linear items of pH and NaCl had statistical significant positive effects (95%) on fibril yield at peak time (FI^{**}_{peak}), but the other non-linear and the interaction effects were not. Only the main effects of pH and temperature are statistically significant (95%) on peak time. The significant negative effect of temperature and the significant positive effect of pH on peak time are consistent with the results from the early studies of their individual effect on fibril formation (Chapter 5).

The fibrillation process can be accelerated under designated treatments in comparison to the control conditions (pH 2.0, 80°C and low ionic strength); most of the peak times obtained in this CCD experiment were less than 6h, while under the control conditions the peak time was around 12h. Unsurprising, the morphologies of fibrils were different by altering the incubation conditions studied.

Although recent work has demonstrated that the environmental factors (pH, temperature, NaCl and $CaCl_2$) have strong effects on β-lactoglobulin fibril formation *in vitro*, the underlying reasons are not clear at this stage. More detailed knowledge of the kinetic and structural changes caused by incubation conditions will provide the mechanistic understanding needed to develop future application strategies in food industry.

CHAPTER 7

GENERAL DISCUSSION AND CONCLUSIONS

7.1 Discussion

The ability of β-lactoglobulin to form amyloid fibrils *in vitro* has been used to investigate how including pH, temperature, and salt concentrations (NaCl and $CaCl_2$) influence the fibril formation process and the morphology of the fibrils.

7.1.1 Effect of the environmental factors on fibril formation

Strong effects of the four factors have been shown on fibrillation kinetics and the morphology of fibrils. As the kinetics of the linear aggregation are quite complex (Arnaudov *et al.*, 2003), the molecular mechanisms are poorly understood (Khurana *et al.*, 2001a). Early studies have shown that decreasing pH will promote destabilizing of the native states or increasing the denaturation rates of protein (Khurana *et al.*, 2001a), while increasing temperature can accelerate rate of protein denaturation and hydrolysis (Calamai *et al.*, 2005; Sabate *et al.*, 2005). These effects were strongly related to the lag time of fibril formation. Ionic strength will influence the electrostatic interaction during fibril formation due to the screening of net charge on β-lactoglobulin molecules (Arnaudov & de Vries, 2006; Aymard *et al.*, 1996).

Competition in nucleation and elongation

At higher temperature, the fibrils were shorter and the fibrillation process was fast, while at lower temperature, the fibrils were long and the fibrillation process was slow. A similar trend was found from the ionic strength experiments; at a higher salt concentration, the fibrillation process was faster and the fibrils were shorter in comparison to those at a lower salt concentration. A possible explanation for these phenomena is that there is competition between nucleation and elongation. A similar effect of the balance between nucleation and elongation rate is observed in amyloid β-protein aggregation (Lomakin *et al.*, 1996).

The effect of inhibition or promotion

Fibrillization of β-lactoglobulin is controlled by two kinetic parameters: the nucleation rate and the growth rate (Sabate *et al.*, 2003). Simple terms like inhibition or promotion are inadequate to describe the effect of the external factors on fibril formation, as they can play different roles at different fibrillation phases (Lomakin *et al.*, 1996). Conditions inhibiting nucleation, such as low temperature, might promote elongation, since fewer but longer fibrils were formed at low temperature. Similarly, conditions promoting nucleation could inhibit elongation, for example, many short fibrils were formed at high salt concentrations. Furthermore, these factors (pH, ionic strength and salt concentration) interact to each other during the incubation process, which make the explanation of the effect of each factor more complicated.

7.1.2 The application of two-step autocatalytic reaction model

In general, the reaction rates of β-lactoglobulin fibril formation are assumed to follow the two-step autocatalytic reaction model which consists of nucleation and elongation. According to the results obtained from this study, this model provided an accurate fit for the experimental data under control conditions (pH 2.0, 80°C and low ionic strength). Questions appeared when applying the model under other incubation conditions. For example, at lower pH (1.6) and at higher temperatures (110 and 120°C), the model did not fit the experimental data well and gave unreliable values of the reaction constantans. The two-step autocatalytic reaction equation should be considered as an empirical approximation of the real underlying kinetic scheme. It can only be used to predict the reaction constants when it gives very good fit to the experimental data.

7.1.3 Experimental noise

It is important to note that there was some experimental noise in the ThT fluorescence data. The enhanced fluorescence emission of ThT in association with amyloid fibrils provides a very convenient method to monitor the kinetics of amyloid fibril formation (Naiki *et al.*, 1989). However, the fluorescence signal is very sensitive to many factors, such as temperature, purity of solution. In order to reduce the influence of experimental noise, the same apparatus was used and same laboratory procedure was

followed for all experiments. Triplicate measurements were performed for all samples. In addition, care was taken to eliminate all forms of solid interference (such as dust and fibres).

Light scattering can be a problem, when a fluorescence spectrophotometer is used; so particle-free solution is an advantage. In this study, the big variation of fluorescence readings occurred in this two situations:

1. The initially clear solutions become opaque white when incubated as in the case of sample with high salt concentrations. This may due to the formation of random particles.
2. Prolonged heating, when gel clumps appear in the sample solution.

These findings suggest that the above two kinds of protein solutions are not suitable to be used as the ThT fluorescence measurements. So the ThT fluorescence method is not recommended for the experiments when protein solution becomes opaque and many gel particles are present in the sample solution.

The control trials from different batches were compared (data are shown in Appendix 7.1). The differences are likely to be due to small fluctuations in pH, protein concentrations and the ThT fluorescence equipments.

There might be some artefacts appeared on the TEM images, due to the negative staining technique (Kavanagh *et al.*, 2000b). For example, the dark areas of the TEM images are caused by the salts which interfer with the staining technique. The other disadvantage is that using TEM it is very difficult to obtain reliable information on the fibril length, since in the images, fibrils may overlap or extend across several fields of view and it may be difficult to obtain enough images.

7.2 Conclusions

β-Lactoglobulin fibril formation kinetics exhibit a sigmoidal behaviour, consisting of a short lag phase followed by a growth phase then eventually a stationary phase under most of the incubation conditions. The two-step autocatalytic reaction model can be used to predict the nucleation and elongation rate of fibril formation under control conditions. WPI shows a similar ThT fluorescence time-course curve as β-lactoglobulin, but not WPH1-5, which indicates that WPI can be used as a source to produce protein fibrils.

In this study, the investigated factors showed strong effects on fibrillation kinetics. In the investigated range, lower pH, higher ionic strength and higher temperature increased the fibril formation process individually. The results obtained from the CCD experiments suggest that pH, NaCl and $CaCl_2$ and the quadratic items of pH and NaCl have significant (95%) positive effect on the quantity of fibril yield (FI^{**}_{peak}). The effects of pH (positive) and temperature (negative) were significant (95%) on peak time, all the non-linear and interaction effects were not significant.

The investigated factors also showed a strong impact on the morphology of the fibrils. Under low pH conditions (pH 1.6 - 2.2, 80°C, low ionic strength), the fibrils were long and straight, very different from those formed at pH 2.4 (80°C and low ionic strength). At 80°C and pH 2.0, the fibrils became shorter and more curved on increasing the ionic strength. Temperature is also a major factor influencing the length of fibrils; at pH 2.0 and low ionic strength, long and thin fibrils were formed at lower temperature, short and thick fibrils were appeared at higher temperature.

At this stage, it is clear that the four factors can be used to accelerate the fibrillation process of β-lactoglobulin and alter the morphology of the fibrils. However, these factors interact to each other and influence the system of fibril formation in different ways, which makes this system rather complex.

7.3 Recommendations

As the understanding of the underlying molecular mechanisms of protein fibril formation is an essential step for control of the formation of protein fibrils and food application strategies, a detailed study on fibril formation mechanisms is recommended for the whole project. It is recommended to use NMR spectroscopy to study the structural constraints in fibrils and to quantify the fibrils with flow-induced birefringence and ThT fluorescence. Flow-induced birefringence is a proportional measure of the length concentration of fibrils.

New incubation conditions of amyloid formation can be proposed according to the results derived from the different experiments; however such conditions frequently results in alteration in fibril morphology. As the fibril shape has great effect on in the functional properties, such as rheological properties (Veerman *et al.*, 2002), it is recommended to study the functional properties of the different kinds of fibrils before further selecting the incubation conditions. In addition, the stability of the amyloid fibrils is a key property that needs to be explored before further applications.

REFERENCES

Akkermans, C., van der Goot, A. J., Venema, P., Gruppen, H., Vereijken, J. M., van der Linden, E., & Boom, R. M. (2007). Micrometer-sized fibrillar protein aggregates from soy glycinin and soy protein isolate. *Journal of Agricultural and Food Chemistry, 55*(24), 9877-9882.

Akkermans, C., Venema, P., Rogers, S., Van der Goot, A., Boom, R., & van der Linden, E. (2006). Shear Pulses Nucleate Fibril Aggregation. *Food Biophysics, 1*(3), 144-150.

Akkermans, C., Venema, P., Van Der Goot, A. J., Gruppen, H., Bakx, E. J., Boom, R. M., & Van der Linden, E. (2008). Peptides are building blocks of heat-induced fibrillar protein aggregates of β-lactoglobulin formed at pH 2. *Biomacromolecules, 9*, 1474-1479.

Arnaudov, L. N., & de Vries, R. (2005). Thermally induced fibrillar aggregation of hen egg white lysozyme. *Biophysical Journal, 88*(1), 515-526.

Arnaudov, L. N., & de Vries, R. (2006). Strong impact of ionic strength on the kinetics of fibrilar aggregation of bovine β-lactoglobulin. *Biomacromolecules, 7*(12), 3490-3498.

Arnaudov, L. N., de Vries, R., Ippel, H., & van Mierlo, C. P. M. (2003). Multiple steps during the formation of β-lactoglobulin fibrils. *Biomacromolecules, 4*(6), 1614-1622.

Arnaudov, L. N., de Vries, R., & Stuart, M. A. C. (2006). Time-resolved small-angle neutron scattering during heat-induced fibril formation from bovine β-lactoglobulin. *Journal of Chemical Physics, 124*(8).

Aymard, P., Durand, D., & Nicolai, T. (1996). The effect of temperature and ionic strength on the dimerisation of β-lactoglobulin *International Journal of Biological Macromolecules, 19*(3), 213-221.

Aymard, P., Nicolai, T., Durand, D., & Clark, A. (1999). Static and dynamic scattering of β-lactoglobulin aggregates formed after heat-induced denaturation at pH 2. *Macromolecules, 32*(8), 2542-2552.

Basch, J. J., & Timashef, S. N. (1967). Hydrogen Ion Equilibria of Genetic Variants of Bovine β-lactoglobulin. *Archives of Biochemistry and Biophysics, 118*(1), 37-47.

Bolder, S. G., Hendrickx, H., Sagis, L. M. C., & van der Linden, E. (2006). Fibril assemblies in aqueous whey protein mixtures. *Journal of Agricultural and Food Chemistry, 54*(12), 4229-4234.

Bolder, S. G., Sagis, L. M. C., Venema, P., & van der Linden, E. (2007a). Thioflavin T and birefringence assays to determine the conversion of proteins into fibrils. *Langmuir, 23*(8), 4144-4147.

Bolder, S. G., Sagis, L. M. C., Venema, P., & van der Linden, E. (2007). Effect of stirring and seeding on whey protein fibril formation. *Journal of Agricultural and Food Chemistry, 55*(14), 5661-5669.

Bolder, S. G., Vasbinder, A. J., Sagis, L. M. C., & van der Linden, E. (2007b). Heat-induced whey protein isolate fibrils: Conversion, hydrolysis, and disulphide bond formation. *International Dairy Journal, 17*(7), 846-853.

Bollag, D. M., Rozycki, M. D., & Edelstein, S. J. (1996). *Protein Methods* (2nd ed.). New York: Wiley-Liss.

Boye, J. I., Ma, C. Y., & Ismail, A. (2004). Thermal stability of beta-lactoglobulins A and B: effect of SDS, urea, cysteine and N-ethylmaleimide. *Journal of Dairy Research, 71*(2), 207-215.

Bromley, E. H. C., Krebs, M. R. H., & Donald, A. M. (2004). Aggregation across the length-scales in β-lactoglobulin. *Faraday Discussions, 128*, 13–27.

Caessens, P., Daamen, W. F., Gruppen, H., Visser, S., & Voragen, A. G. J. (1999). β-lactoglobulin hydrolysis. 2. Peptide identification, SH/SS exchange, and functional properties of hydrolysate fractions formed by the action of plasmin. *Journal of Agricultural and Food Chemistry, 47*(8), 2980-2990.

Calamai, M., Chiti, F., & Dobson, C. M. (2005). Amyloid fibril formation can proceed from different conformations of a partially unfolded protein. *Biophysical Journal, 89*(6), 4201-4210.

Carrotta, R., Bauer, R., Waninge, R., & Rischel, C. (2001). Conformational characterization of oligomeric intermediates and aggregates in β-lactoglobulin heat aggregation. *Protein Science, 10*(7), 1312-1318.

Chandan, R. C., White, C. H., Kilara, A., & Hui, Y. H. (2006). *Manufacturing yogurt and fermented milks* (1st ed.). Ames, Iowa Blackwell.

Damodaran, S. (1996). *Food Chemistry* (3rd ed.). New York: Marcel Dekker.

Dumay, E. M., Kalichevsky, M. T., & Cheftel, J. C. (1998). Characteristics of pressure-induced gels of β-lactoglobulin at various times after pressure release. *Food Science and Technology-Lebensmittel-Wissenschaft & Technologie, 31*(1), 10-19.

Durand, D., Christophe Gimel, J., & Nicolai, T. (2002). Aggregation, gelation and phase separation of heat denatured globular proteins. *Physica A: Statistical Mechanics and its Applications, 304*(1-2), 253-265.

Eisert, R., Felau, L., & Brown, L. R. (2006). Methods for enhancing the accuracy and reproducibility of Congo red and thioflavin T assays. *Analytical Biochemistry, 353*(1), 144-146.

Euston, S. R., Ur-Rehman, S., & Costello, G. (2007). Denaturation and aggregation of β-lactoglobulin—a preliminary molecular dynamics study. *Food Hydrocolloids, 21*(7), 1081-1091.

Farrell, H. M., Cooke, P. H., Wickham, E. D., Piotrowski, E. G., & Hoagland, P. D. (2003). Environmental influences on bovine kappa-casein: Reduction and conversion to fibrillar (amyloid) structures. *Journal of Protein Chemistry, 22*(3), 259-273.

Galani, D., & Apenten, R. K. O. (1997). The comparative heat stability of bovine β-lactoglobulin in buffer and complex media. *Journal of the Science of Food and Agriculture, 74*(1), 89-98.

Gosal, W. S., Clark, A. H., Pudney, P. D. A., & Ross-Murphy, S. B. (2001, Nov 24-28). *Novel amyloid fibrillar networks derived from a globular protein:β-lactoglobulin.* Paper presented at the 2nd International Conference on Self-Assembled Fibrillar Networks, Autrans, France.

Gosal, W. S., Clark, A. H., & Ross-Murphy, S. B. (2004). Fibrillar β-lactoglobulin gels: Part 1. Fibril formation and structure. *Biomacromolecules, 5*(6), 2408-2419.

Gosal, W. S., Morten, I. J., Hewitt, E. W., Smith, D. A., Thomson, N. H., & Radford, S. E. (2005). Competing pathways determine fibril morphology in the self-assembly of β2-microglobulin into amyloid. *Journal of Molecular Biology, 351*(4), 850-864.

Greenfield, T., & Metcalfe, A. (2007). *Design and analyse your experiment with MINITAB*. London: Hodder Arnold.

Hamada, D., & Dobson, C. M. (2002). A kinetic study of β-lactoglobulin amyloid fibril formation promoted by urea. *Protein Science, 11*(10), 2417-2426.

Havea, P., Carr, A. J., & Creamer, L. K. (2004). The roles of disulphide and non-covalent bonding in the functional properties of heat-induced whey protein gels. *Journal of Dairy Research, 71*(3), 330-339.

Hawe, A., Sutter, M., & Jiskoot, W. (2008). Extrinsic fluorescent dyes as tools for protein characterization. *Pharmaceutical Research, 25*(7), 1487-1499.

Ikeda, S., & Morris, V. J. (2002). Fine-stranded and particulate aggregates of heat-denatured whey proteins visualized by atomic force microscopy. *Biomacromolecules, 3*(2), 382-389.

Ionescu-Zanetti, C., Khurana, R., Gillespie, J. R., Petrick, J. S., Trabachino, L. C., Minert, L. J., Carter, S. A., & Fink, A. L. (1999). Monitoring the assembly of Ig light-chain amyloid fibrils by atomic force microscopy. *Proceedings of the National Academy of Sciences of the United States of America, 96*(23), 13175-13179.

Jung, J. M., Savin, G., Pouzot, M., Schmitt, C., & Mezzenga, R. (2008). Structure of heat-induced β-lactoglobulin aggregates and their complexes with sodium-dodecyl sulfate. *Biomacromolecules, 9*(9), 2477-2486.

Kavanagh, G. M., Clark, A. H., Gosal, W. S., & Ross-Murphy, S. B. (2000a). Heat-Induced Gelation of β-Lactoglobulin/α-Lactalbumin Blends at pH 3 and pH 7. *Macromolecules, 33*(19), 7029-7037.

Kavanagh, G. M., Clark, A. H., & Ross-Murphy, S. B. (2000b). Heat-induced gelation of globular proteins: part 3. Molecular studies on low pH β-lactoglobulin gels. *International Journal of Biological Macromolecules, 28*(1), 41-50.

Khurana, R., Coleman, C., Ionescu-Zanetti, C., Carter, S. A., Krishna, V., Grover, R. K., Roy, R., & Singh, S. (2005). Mechanism of thioflavin T binding to amyloid fibrils. *Journal of Structural Biology, 151*(3), 229-238.

Khurana, R., Gillespie, J. R., Talapatra, A., Minert, L. J., Ionescu-Zanetti, C., Millett, I., & Fink, A. L. (2001a). Partially folded intermediates as critical precursors of light chain amyloid fibrils and amorphous aggregates. *Biochemistry, 40*(12), 3525-3535.

Khurana, R., Uversky, V. N., Nielsen, L., & Fink, A. L. (2001b). Is Congo Red an Amyloid-specific Dye? *Journal of Biological Chemistry, 276*(25), 22715-22721.

Krebs, M. R. H., Bromley, E. H. C., & Donald, A. M. (2005a). The binding of thioflavin-T to amyloid fibrils: localisation and implications. *Journal of Structural Biology, 149*(1), 30-37.

Krebs, M. R. H., Bromley, E. H. C., Rogers, S. S., & Donald, A. M. (2005b). The mechanism of amyloid spherulite formation by bovine insulin. *Biophysical Journal, 88*(3), 2013-2021.

Krebs, M. R. H., Devlin, G. L., & Donald, A. M. (2007). Protein particulates: Another generic form of protein aggregation? *Biophysical Journal, 92*(4), 1336-1342.

Krebs, M. R. H., Morozova-Roche, L. A., Daniel, K., Robinson, C. V., & Dobson, C. M. (2004). Observation of sequence specificity in the seeding of protein amyloid fibrils. *Protein Science, 13*(7), 1933-1938.

Langton, M., & Hermansson, A. M. (1992). Fine-Stranded and Particulate Gels of β-Lactoglobulin and Whey-Protein at Varying pH. *Food Hydrocolloids, 5*(6), 523-539.

Lencki, R. W. (2007). Evidence for fibril-like structure in bovine casein micelles. *Journal of Dairy Science, 90*(1), 75-89.

LeVine III, H. (1999). Quantification of β-sheet amyloid fibril structures with thioflavin T. *Methods Enzymol, 309*, 274-284.

Lomakin, A., Chung, D. S., Benedek, G. B., Kirschner, D. A., & Teplow, D. B. (1996). On the nucleation and growth of amyloid β-protein fibrils: Detection of nuclei and quantitation of rate constants. *Proceedings of the National Academy of Sciences of the United States of America, 93*(3), 1125-1129.

Makin, O. S., & Serpell, L. C. (2005). Structures for amyloid fibrils. *FEBS Journal, 272*(23), 5950-5961.

Malisauskas, M., Zamotin, V., Jass, J., Noppe, W., Dobson, C. M., & Morozova-Roche, L. A. (2003). Amyloid protofilaments from the calcium-binding protein equine lysozyme: Formation of ring and linear structures depends on pH and metal ion concentration. *Journal of Molecular Biology, 330*(4), 879-890.

Merz, P. A., Wisniewski, H. M., Somerville, R. A., Bobin, S. A., Masters, C. L., & Iqbal, K. (1983). Ultrastructural Morphology of Amyloid Fibrils from Neuritic and Amyloid Plaques. *Acta Neuropathologica, 60*(1-2), 113-124.

Mishra, R., Sorgjerd, K., Nystrom, S., Nordigarden, A., Yu, Y.-C., & Hammarstrom, P. (2007). Lysozyme Amyloidogenesis Is Accelerated by Specific Nicking and Fragmentation but Decelerated by Intact Protein Binding and Conversion. *Journal of Molecular Biology, 366*(3), 1029-1044.

Modler, A. J., Gast, K., Lutsch, G., & Damaschun, G. (2003). Assembly of amyloid protofibrils via critical oligomers - A novel pathway of amyloid formation. *Journal of Molecular Biology, 325*(1), 135-148.

Montgomery, D. C., Runger, G. C., & Hubele, N. F. (2004). *Engineering Statistics* (3rd ed.). New York: John Wiley & Sons, Inc.

Morris, A. M., Watzky, M. A., Agar, J. N., & Finke, R. G. (2008). Fitting neurological protein aggregation kinetic data via a 2-step, Minimal/"Ockham's Razor" model: The Finke-Watzky mechanism of nucleation followed by autocatalytic surface growt. *Biochemistry, 47*(8), 2413-2427.

Naiki, H., Higuchi, K., Hosokawa, M., & Takeda, T. (1989). Fluorometric-Determination of Amyloid Fibrils Invitro Using the Fluorescent Dye, Thioflavine-T. *Analytical Biochemistry, 177*(2), 244-249.

Nelson, R., Sawaya, M. R., Balbirnie, M., Madsen, A. O., Riekel, C., Grothe, R., & Eisenberg, D. (2005). Structure of the cross-beta spine of amyloid-like fibrils. *Nature, 435*(7043), 773-778.

Nicolai, T., & Durand, D. (2007). Protein aggregation and gel formation studied with scattering methods and computer simulations. *Current Opinion in Colloid & Interface Science, 12*(1), 23-28.

Nielsen, L., Khurana, R., Coats, A., Frokjaer, S., Brange, J., Vyas, S., Uversky, V. N., & Fink, A. L. (2001). Effect of environmental factors on the kinetics of insulin fibril formation: Elucidation of the molecular mechanism. *Biochemistry, 40*(20), 6036-6046.

Nilsson, M. R. (2004). Techniques to study amyloid fibril formation in vitro. *Methods, 34*(1), 151-160.

Padrick, S. B., & Miranker, A. D. (2002). Islet amyloid: Phase partitioning and secondary nucleation are central to the mechanism of fibrillogenesis. *Biochemistry, 41*(14), 4694-4703.

Pearce, F. G., Mackintosh, S. H., & Gerrard, J. A. (2007). Formation of Amyloid-like Fibrils by Ovalbumin and Related Proteins under Conditions Relevant to Food Processing. *Journal of Agricultural and Food Chemistry, 55*(2), 318-322.

Quintas, A., Vaz, D. C., Cardoso, I., Saraiva, M. J. M., & Brito, R. M. M. (2001). Tetramer dissociation and monomer partial unfolding precedes protofibril formation in amyloidogenic transthyretin variants. *Journal of Biological Chemistry, 276*(29), 27207-27213.

Rogers, S. S., Venema, P., Van der Ploeg, J. P. M., Van der Linden, E., Sagis, L. M. C., & Donald, A. M. (2006). Investigating the permanent electric dipole moment of β-lactoglobulin fibrils, using transient electric birefringence. *Biopolymers, 82*(3), 241-252.

Sabate, R., Gallardo, M., & Estelrich, J. (2003). An autocatalytic reaction, as a model for the kinetics of the aggregation of β-amyloid. *Biopolymers, 71*(2), 190-195.

Sabate, R., Gallardo, M., & Estelrich, J. (2005). Temperature dependence of the nucleation constant rate in β amyloid fibrillogenesis. *International Journal of Biological Macromolecules, 35*(1-2), 9-13.

Sabate, R., & Saupe, S. J. (2007). Thioflavin T fluorescence anisotropy: An alternative technique for the study of amyloid aggregation. *Biochemical and Biophysical Research Communications, 360*(1), 135-138.

Sakurai, K., & Goto, Y. J. (2007). Principal component analysis of the pH-dependent conformational transitions of bovine β-lactoglobulin monitored by heteronuclear NMR. *Proceedings of the National Academy of Sciences of the United States of America, 104*(39), 15346-15351.

Sakurai, K., Oobatake, M., & Goto, Y. (2001). Salt-dependent monomer-dimer equilibrium of bovine β-lactoglobulin at pH 3. *Protein Science, 10*(11), 2325-2335.

Schokker, E. P., Singh, H., Pinder, D. N., & Creamer, L. K. (2000). Heat-induced aggregation of β-lactoglobulin AB at pH 2.5 as influenced by ionic strength and protein concentration. *International Dairy Journal, 10*(4), 233-240.

Simons, J., Kosters, H. A., Visschers, R. W., & de Jongh, H. H. J. (2002). Role of calcium as trigger in thermal β-lactoglobulin aggregation. *Archives of Biochemistry and Biophysics, 406*(2), 143-152.

Sittikijyothin, W., Sampaio, P., & Goncalves, M. P. (2007). Heat-induced gelation of β-lactoglobulin at varying pH: Effect of tara gum on the rheological and structural properties of the gels. *Food Hydrocolloids, 21*(7), 1046-1055.

Smith, D. P., & Radford, S. E. (2001). Role of the single disulphide bond of β(2)-microglobulin in amyloidosis in vitro. *Protein Science, 10*(9), 1775-1784.

Takata, S., Norisuye, T., Tanaka, N., & Shibayama, M. (2000). Heat-induced gelation of β-lactoglobulin. 1. Time-resolved dynamic light scattering. *Macromolecules, 33*(15), 5470-5475.

Thakur, A. K., & Rao, C. M. (2008). UV-Light Exposed Prion Protein Fails to Form Amyloid Fibrils. *PLoS ONE, 3*(7,), 9.

Tycko, R. (2004). Progress towards a molecular-level structural understanding of amyloid fibrils. *Current Opinion in Structural Biology, 14*(1), 96-103.

van der Linden, E., & Venema, P. (2007). Self-assembly and aggregation of proteins. *Current Opinion in Colloid & Interface Science, 12*(4-5), 158-165.

Veerman, C., Baptist, H., Sagis, L. M. C., & van der Linden, E. (2003a). A new multistep Ca2+-induced cold gelation process for β-lactoglobulin. *Journal of Agricultural and Food Chemistry, 51*(13), 3880-3885.

Veerman, C., Ruis, H., Sagis, L. M. C., & van der Linden, E. (2002). Effect of electrostatic interactions on the percolation concentration of fibrillar β-lactoglobulin gels. *Biomacromolecules, 3*(4), 869-873.

Veerman, C., Sagis, L. M. C., Heck, J., & van der Linden, E. (2003b). Mesostructure of fibrillar bovine serum albumin gels. *International Journal of Biological Macromolecules, 31*(4-5), 139-146.

Veerman, C., Sagis, L. M. C., & van der Linden, E. (2004, Apr 18-21). *Properties of fibrillar food protein assemblies and their percolating networks.* Paper presented at the Conference on Food Colloids, Harrogate, ENGLAND.

Vetri, V., & Militello, V. (2005). Thermal induced conformational changes involved in the aggregation pathways of β-lactoglobulin. *Biophysical Chemistry, 113*(1), 83-91.

Volkova, K. D., Kovalska, V. B., Balanda, A. O., Vermeij, R. J., Subramaniam, V., Slominskii, Y. L., & Yarmoluk, S. M. (2007). Cyanine dye-protein interactions: Looking for fluorescent probes for amyloid structures. *Journal of Biochemical and Biophysical Methods, 70*(5), 727-733.

Waugh, D. F., Wilhelmson, D. F., Commerford, S. L., & Sackler, M. L. (1953). Studies of the Nucleation and Growth Reactions of Selected Types of Insulin Fibrils. *Journal of the American Chemical Society, 75*(11), 2592-2600.

Appendix 3.1 Calibration of the protein concentration

Prepare standard protein solution: 50 mg β-lactoglobulin powder (SIGMA, L0130-5G, lot. no. 078K7430 and 095K7006) into 5 mL HCl pH 2.0 solution then stirred for overnight until totally dissolved (10mg protein powder /mL). The experiment buffer (HCl of Ph 2.0) was used as blank and the reading at 278 nm was reset to zero.

Table 3.1.A A_{278} for the first β-lactoglobulin bottle 078K7430

Tube	Standard protein solution	HCl (pH2.0)	Protein powder	Protein *90%	Absorbance at 278 nm
No.	mL	mL	mg/mL	mg/mL	
1	0.0	5.0	0.0	0.0	0.0
2	0.2	4.8	0.4	0.36	0.288
3	0.4	4.6	0.8	0.72	0.578
4	0.6	4.4	1.2	1.08	0.868
5	0.8	4.2	1.6	1.44	1.18
6	1.0	4.0	2.0	1.8	1.52

*: The β-lactoglobulin powder was 90% pure as stated by Sigma.

Table 3.1.B A_{278} for the second β-lactoglobulin bottle 095K7006

Tube	Standard protein solution	HCl (pH2)	Protein powder	Protein *90%	Absorbance at 278 nm
No.	mL	mL	mg/mL	mg/mL	
1	0.0	5.0	0.0	0.0	0.0
2	0.2	4.8	0.4	0.36	0.304
3	0.4	4.6	0.8	0.72	0.608
4	0.6	4.4	1.2	1.08	0.9
5	0.8	4.2	1.6	1.44	1.195
6	1.0	4.0	2.0	1.8	1.504

Appendix 3.2 Two ways of improving TEM imaging quality

- **Centrifugal method**

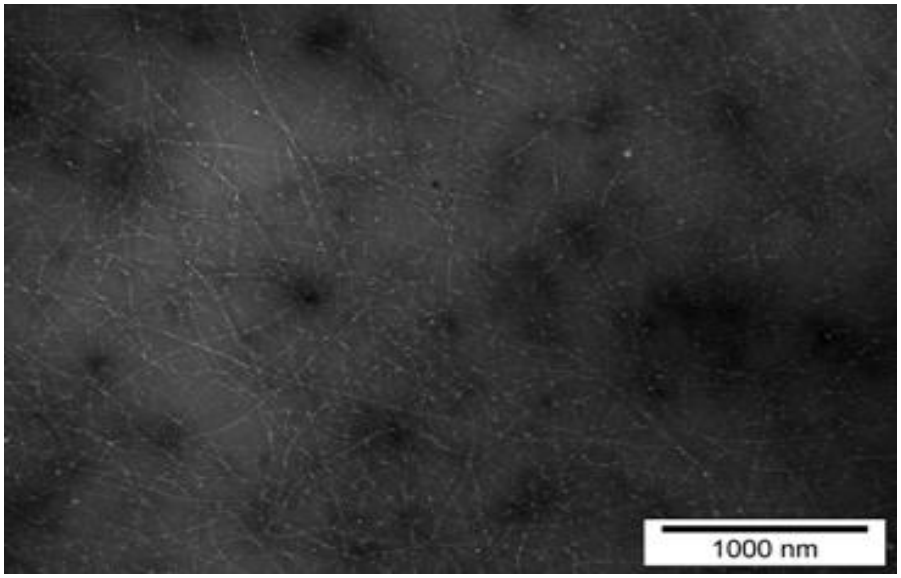

A. Retentate 1

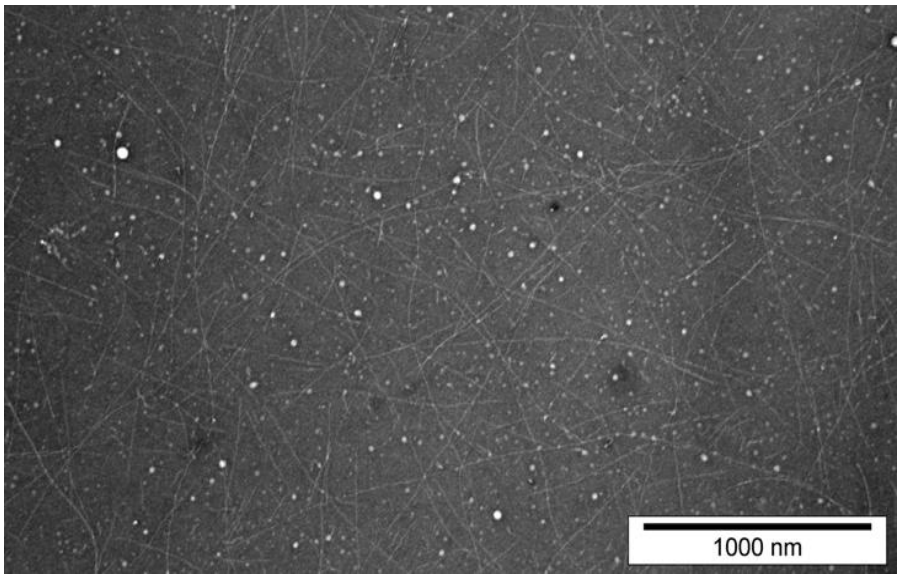

B. Retentate 2

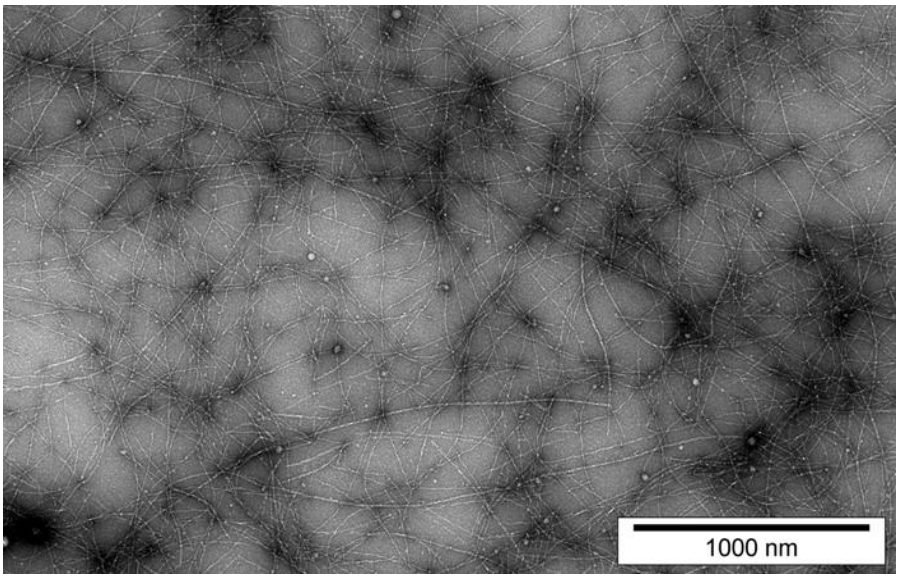

C. Retentate 3

Figure 3.2.A.TEM image of the β-lactoglobulin (2.5% w/v) retantaes obtained after subsequent centrifuge runs. Each centrifugal filtration step was centrifuged with 100 kDa centrifuge filter for 15min). The sample was heated for 10 hours at pH2, 80°C.

- **Dilution method**

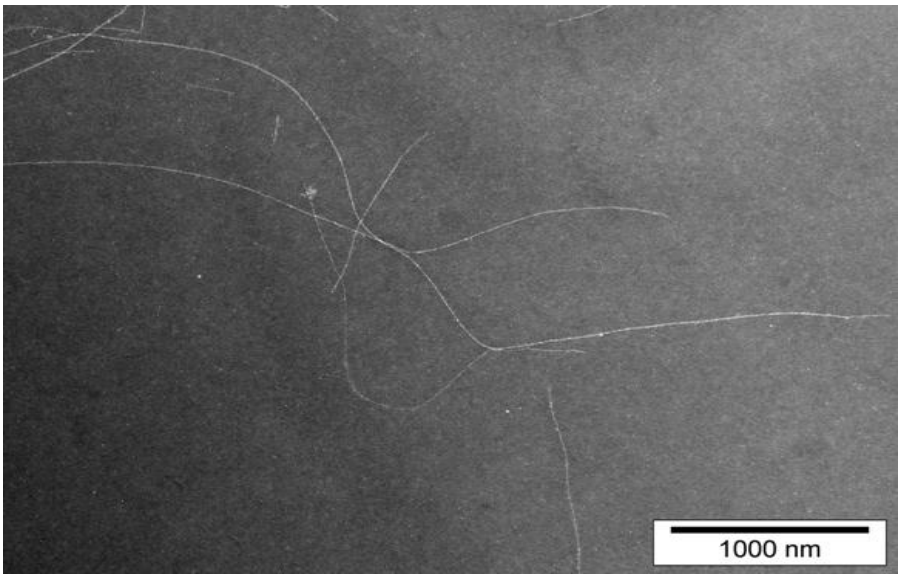

Figure 3.2.B TEM images of the 50 fold directly diluted β-lactoglobulin sample (0.05 % w/v). The sample was heated for 10 hours at pH2, 80°C.

In Figure 3.2.A, TEM images are shown of retentates obtained after subsequent centrifugation runs for a 2.5 % w/v protein sample that was heated for 10 hour. In the retentates, long semi-flexible fibrils were observed. This indicates that fibrils can be separated from non-assembled material using centrifugal filtration. After repeated centrifugal filtration steps the darkness of the image background was reduced due to

the wash out of the non-assembled protein (<100 kDa). It's clear that the quality of the TEM image improved with the subsequent wash out steps.

The same protein sample was diluted to 0.05 wt % with HCl of pH 2.0, shown in Figure 3.2.B. form this image, a few long semi-flexible fibrils can be observed. Compare this image with the images of Figure 3.3.A, the quantity of fibrils was largely reduced and the other species of aggregates were barely visible. The morphology of the fibrils observed from Figure 3.3A and Figure 3.3.B were all long, thin and semi-flexible. These results means the fibrils remained stable during this process, so the triple centrifugal filtration process can be used for preparing TEM specimen.

Appendix 3.3 Variable and parameter settings of two-step autocatalytic reaction model equation using SigmaPlot 10.0

Two-step autocatalytic reaction model Eq.(3) (Finke-Watzky2)

$$[B]_t = [A]_0 - \frac{\frac{k_1}{k_2} + [A]_0}{1 + \frac{k_1}{k_2[A]_0}\exp[t(k_1 + k_2[A]_0)]} \quad (3)$$

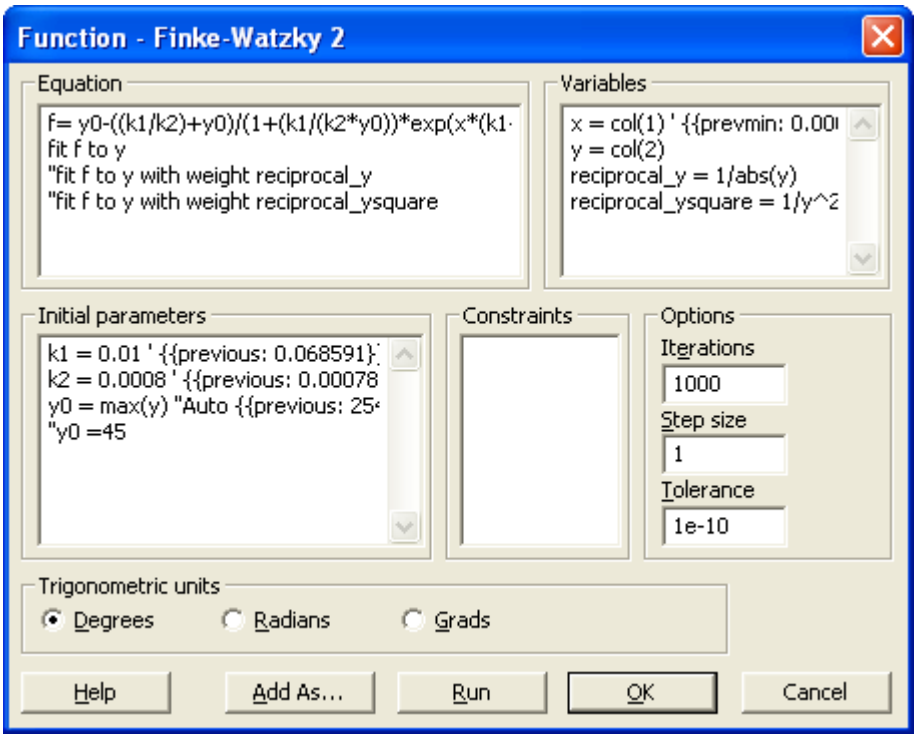

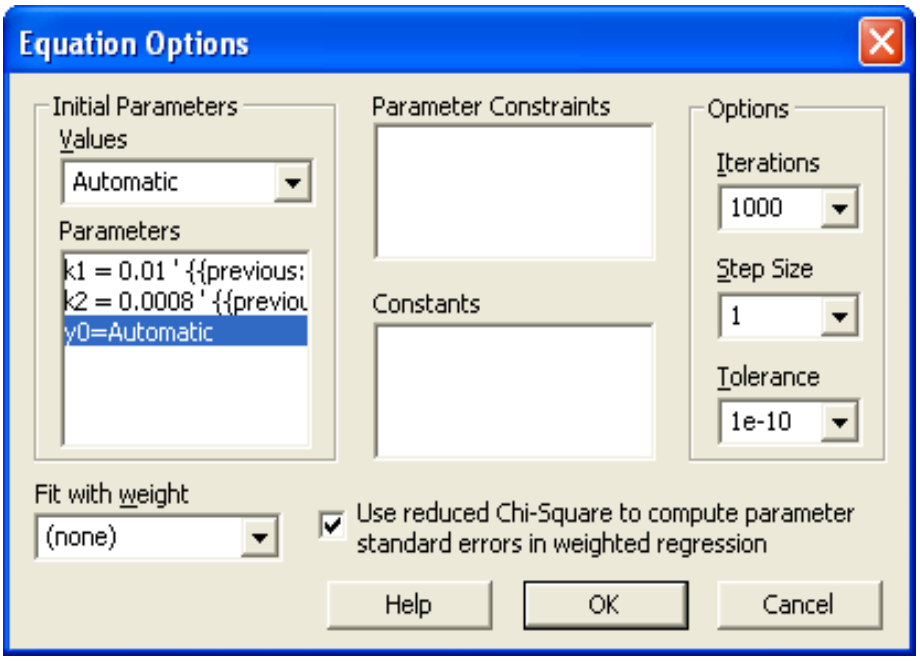

Appendix 4.1 TEM images of the gel particles

Gel particles of β-lactoglobulin (4 % w/v) that formed under control conditions (pH 2.0, 80 °C, low ionic strength) for 9h were studied by TEM.

Gel Particle Specimen Processing for TEM

Drop of gels were fixed in primary fixative (3% Glutaraldehyde, 2% formaldehyde in 1M phosphate buffer, pH 7.2) to coagulate the gel.
The gel was sliced with razor blade into primary fixative for 2-3h in fume cupboard.
Replace the fix after vacuum infiltration and fix for 2-3 hours at RT.
3x buffer washes, same buffer at RT. [10-15 minutes each.]
1% OsO4 in PO4 buffer for half to 1 hour at RT.
Buffer washes as above.
Dehydration through a graded acetone series, 25%, 50%, 75%, 95%, 2x 100%.
10 to 15 minutes each and 1 hour in last 100% step.
Infiltration with an acetone/resin mixture [Procure 812 resin, or similar.] 50/50 on a stirrer over-night, then change to 100% resin for 8 hours on stirrer.
Embed in fresh resin in silicone rubber moulds and cured at 60 degrees centigrade for 48 hours.
1 micron sections are cut from trimmed blocks, using glass knives, heat mounted on to glass slides, stained with 0.05% Toluidine Blue on the hot-plate, and viewed using the light microscope to chose an area of interest.
Trim the block down to approx. half by half a millimetre square to include the area of interest, and cut approx. 100nm thin sections [pale gold interference colour] using a diamond knife and the Ultra-microtome. [Block size varies with different and more difficult samples.]
'Stretch' the sections using chloroform vapour from a drop of chloroform on an old grid 'waved' above the sections.
Sections picked up on copper grids, [using sellotape-chloroform cement to 'stick' the thin sections to the grid.] double stained with saturated Uranyl Acetate in 50% ethanol [4 minutes.] followed by Lead Citrate. [4 minutes.]

Two types of gel structure were observed.

- **Fine stranded gels**

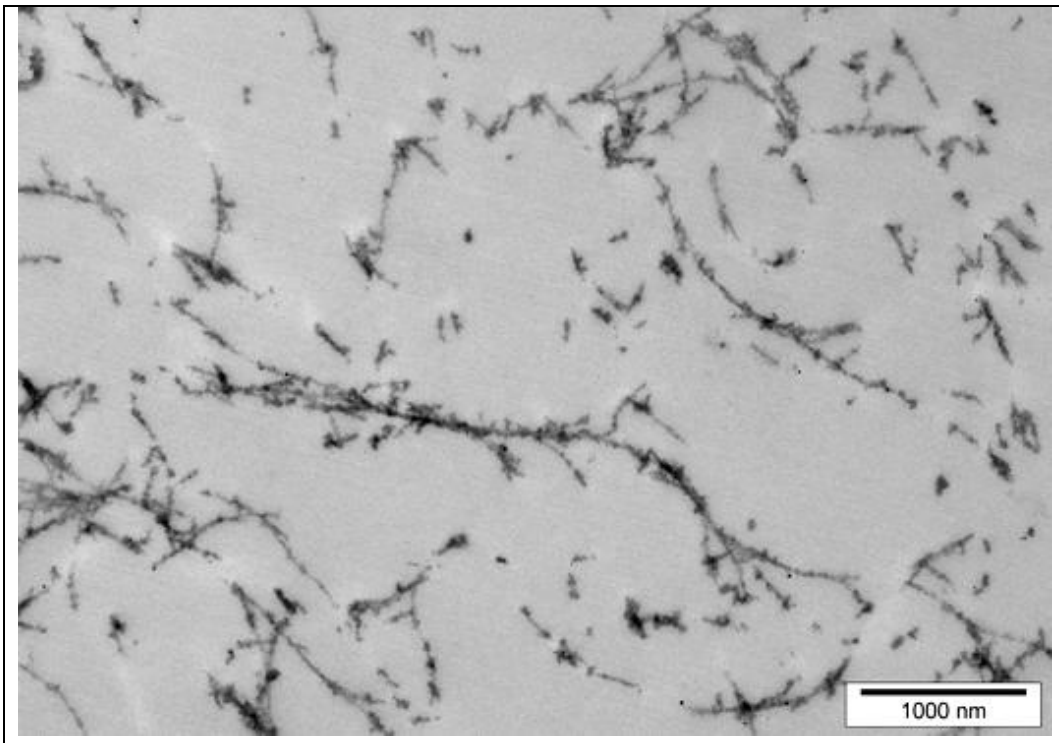

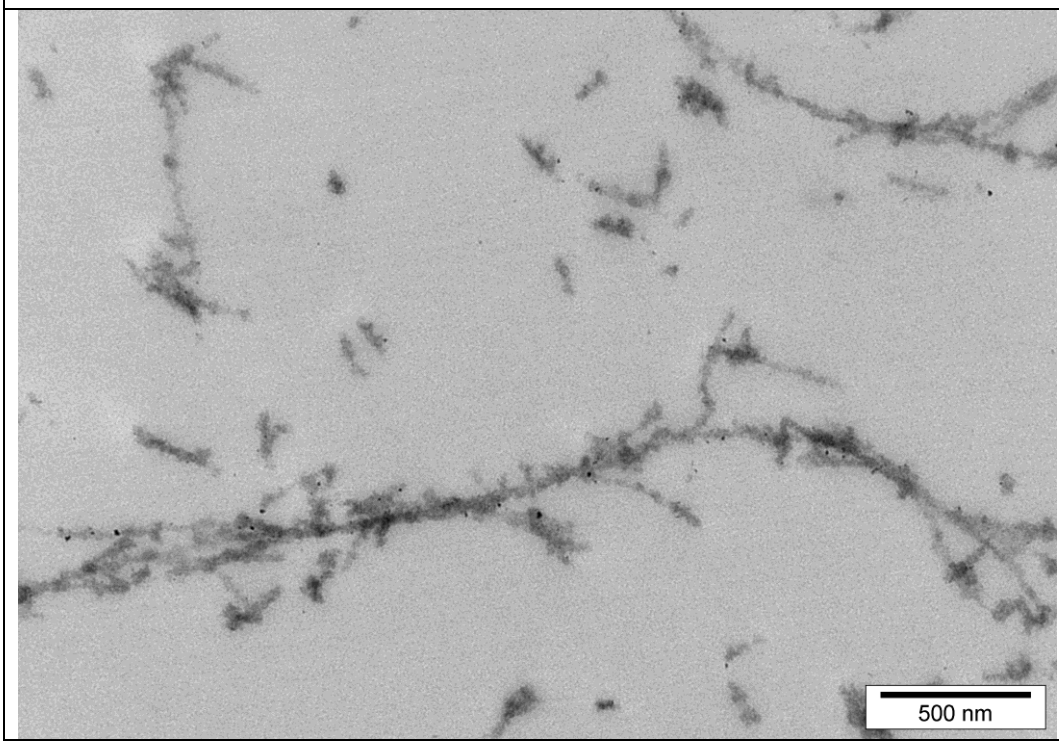

- **Particulate gels**

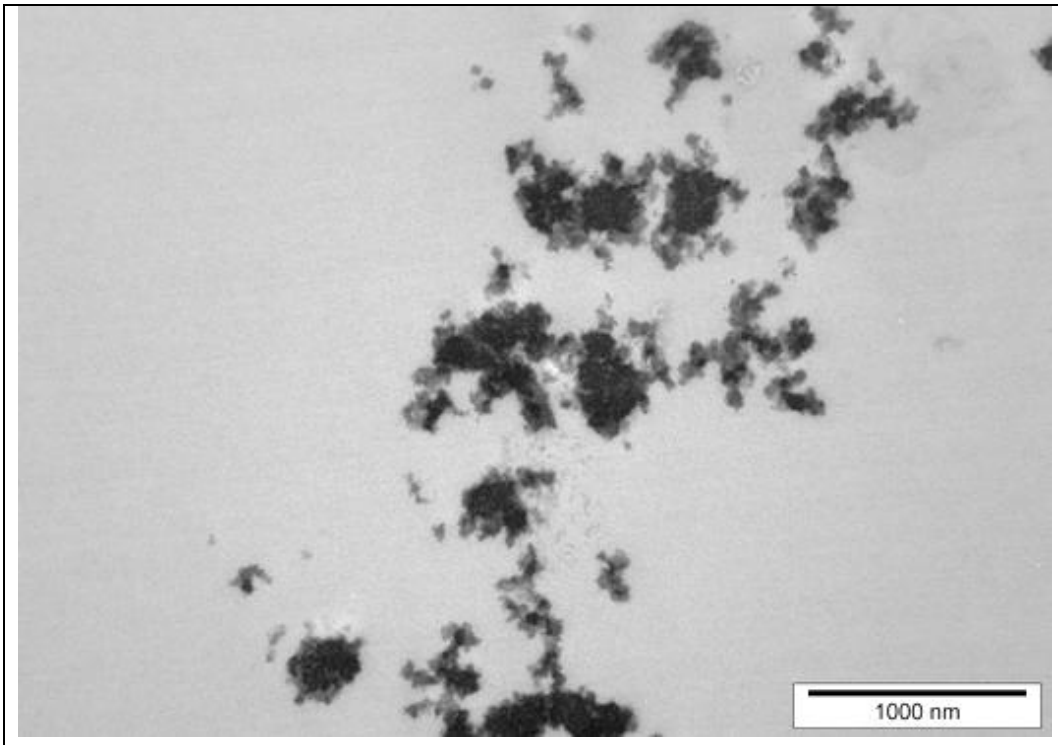

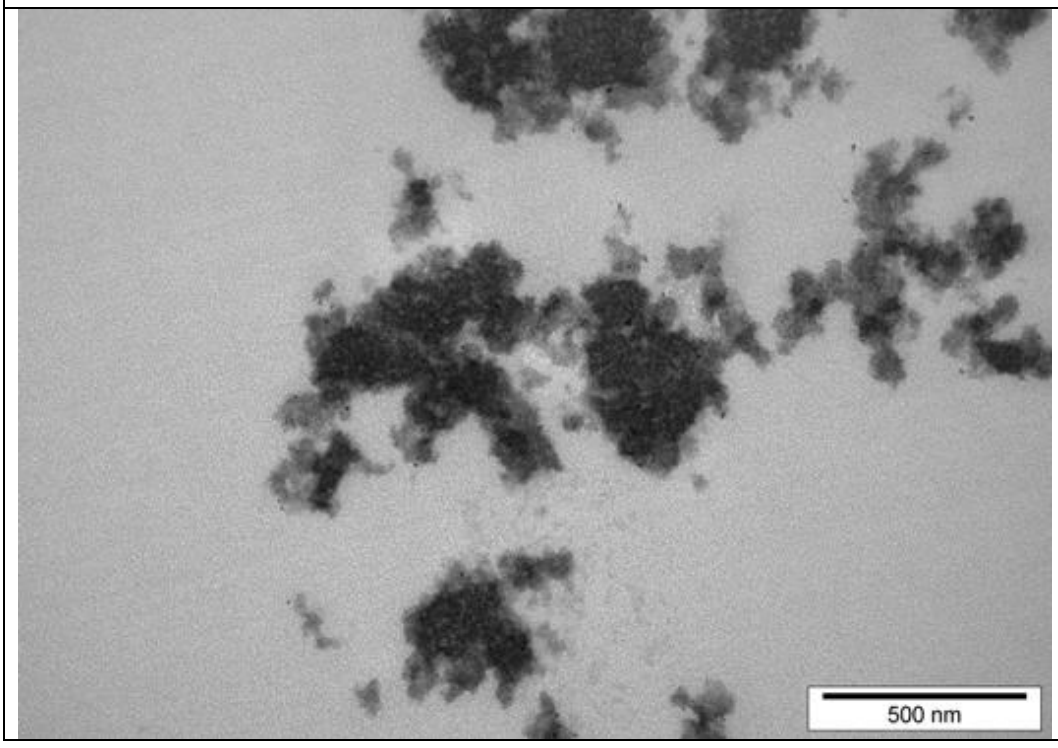

Appendix 4.2 Two-step autocatalytic reaction model analysis under control conditions

The ThT fluorescence data (Fibril formation under control conditions in Chapter 4), FI** vs. heating time, were analysed using SigmaPlot 10.0.

Fibril formation under control conditions

Nonlinear Regression
Data Source: Data 2 in formation curve.JNB
Equation: Sigmoidal, Finke-Watzky 2 in Simon.JFL
f= y0-((k1/k2)+y0)/(1+(k1/(k2*y0))*exp(x*(k1+k2*y0)))

R	Rsqr	Adj Rsqr	Standard Error of Estimate
0.9904	0.9810	0.9789	13.5077

	Coefficient	Std. Error	t	P	VIF
k1	0.0686	0.0109	6.3083	<0.0001	7.5433<
k2	0.0008	0.0002	3.3490	0.0036	12.7248<
y0	254.2524	8.6777	29.2994	<0.0001	4.4011<

Analysis of Variance:

Uncorrected for the mean of the observations:

	DF	SS	MS
Regression	3	481262.8586	160420.9529
Residual	18	3284.2220	182.4568
Total	21	484547.0805	23073.6705

Corrected for the mean of the observations:

	DF	SS	MS	F	P
Regression	2	169425.7112	84712.8556	464.2900	<0.0001
Residual	18	3284.2220	182.4568		
Total	20	172709.9331	8635.4967		

Statistical Tests:

PRESS 4558.1573

Durbin-Watson Statistic 1.0583 Failed

Normality Test Passed (P = 0.4758)

K-S Statistic = 0.1784 Significance Level = 0.4758

Constant Variance Test Passed (P = 0.8016)

Power of performed test with alpha = 0.0500: 1.0000

Appendix 5.1 Two-step autocatalytic reaction model analysis report at pH1.6 and summarised results at all pH values

The ThT fluorescence data (Section 5.1), FI** vs. heating time at pH 1.6 at 80 °C and low ionic strength were analysed using SigmaPlot 10.0.

- **Statistic report at pH 1.6**

pH 1.6

Nonlinear Regression

Data Source: Data 6 in pH.JNB
Equation: Sigmoidal, Finke-Watzky 2 in Simon.JFL
f= y0-((k1/k2)+y0)/(1+(k1/(k2*y0))*exp(x*(k1+k2*y0)))

R	Rsqr	Adj Rsqr	Standard Error of Estimate
0.9927	0.9854	0.9843	10.4069

	Coefficient	Std. Error	t	P	VIF
k1	0.0003	0.0002	1.4839	0.1498	93.2593<
k2	0.0084	0.0009	9.1940	<0.0001	151.5812<
y0	212.1654	5.5938	37.9284	<0.0001	18.9060<

Analysis of Variance:

Uncorrected for the mean of the observations:

	DF	SS	MS
Regression	3	437356.4724	145785.4908
Residual	26	2815.8917	108.3035
Total	29	440172.3641	15178.3574

Corrected for the mean of the observations:

	DF	SS	MS	F	P
Regression	2	190412.4239	95206.2120	879.0684	<0.0001
Residual	26	2815.8917	108.3035		
Total	28	193228.3156	6901.0113		

Statistical Tests:

PRESS 4118.0113

Durbin-Watson Statistic 2.4052 Passed

Normality Test Failed (P = 0.0275)

K-S Statistic = 0.2650 Significance Level = 0.0275

Constant Variance Test Failed (P = 0.0132)

Power of performed test with alpha = 0.0500: 1.0000

- **Summary of the statistic results at different pH values**

pH 1.6

Parameter	Value	StdErr	CV(%)	Dependencies	Adj Rsqr
k1	3.20E-04	2.15E-04	6.74E+01	0.989277	0.9843
k2	8.38E-03	9.12E-04	1.09E+01	0.993403	
y0	2.12E+02	5.59E+00	2.64E+00	0.947107	

pH 1.8

Parameter	Value	StdErr	CV(%)	Dependencies	Adj Rsqr
k1	1.26E-02	3.97E-03	3.15E+01	0.9246	0.9644
k2	2.24E-03	3.45E-04	1.54E+01	0.9383	
y0	2.24E+02	8.24E+00	3.68E+00	0.7447	

pH 2.0

Parameter	Value	StdErr	CV(%)	Dependencies	Adj Rsqr
k1	8.97E-03	2.23E-03	2.49E+01	0.9310	0.9814
k2	3.28E-03	3.39E-04	1.03E+01	0.9438	
y0	1.70E+02	4.42E+00	2.61E+00	0.7590	

pH 2.2

Parameter	Value	StdErr	CV(%)	Dependencies	Adj Rsqr
k1	3.03E-03	1.07E-03	3.54E+01	0.9490	0.9816
k2	4.30E-03	4.18E-04	9.72E+00	0.9601	
y0	1.73E+02	4.74E+00	2.74E+00	0.8140	

pH 2.4

Parameter	Value	StdErr	CV(%)	Dependencies	Adj Rsqr
k1	6.93E-04	2.98E-04	4.31E+01	0.9746	0.9899
k2	6.85E-03	5.42E-04	7.92E+00	0.9780	
y0	1.34E+02	2.68E+00	2.00E+00	0.8371	

Appendix 5.2 Growth rate of fibril formation at different salts concentrations

- **Growth rate of fibril formation at different NaCl concentrations using Excel**

NaCl [mM]	Linear Trend Line Equation	Growth phase	Trend Line Slope FI**/h
0	y = 13.457x - 34.162 R^2 = 0.9807	3 - 8h	13.46
10	y = 20.584x - 52.031 R^2 = 0.9826	3 - 8h	20.58
20	y = 20.672x - 37.149 R^2 = 0.9528	3 - 8h	20.67
30	y = 29.165x - 68.317 R^2 = 0.9596	3 - 8h	29.17
40	y = 33.572x - 83.43 R^2 = 0.9562	3 - 8h	33.57
50	y = 40.051x - 106.6 R^2 = 0.9748	3 - 8h	40.05
60	y = 33.353x - 89.072 R^2 = 0.9721	3 - 8h	33.35
80	y = 42.987x - 119.88 R^2 = 0.9508	3 - 8h	42.99
100	y = 47.926x - 126.07 R^2 = 0.927	**3 - 6 h**	47.93

- **Growth rate of fibril formation at different $CaCl_2$ concentrations using Excel**

NaCl [mM]	Linear Trend Line Equation	Growth phase	Trend Line Slope FI**/h
0	y = 30.465x - 69.829 R^2 = 0.9489	2 - 8h	30.47
3	y = 33.836x - 71.954 R^2 = 0.9594	2 - 8h	33.84
5	y = 33.68x - 55.364 R^2 = 0.9851	2 - 8h	33.68
10	y = 51.596x - 112.99 R^2 = 0.9651	2 - 8h	51.60
20	y = 40.329x - 73.166 R^2 = 0.9827	2 - 8h	40.33
33	y = 50.162x - 85.694 R^2 = 0.9618	2 - 8h	50.16
40	y = 55.679x - 109.49 R^2 = 0.9586	2 - 8h	55.68
50	y = 60.718x - 90.489 R^2 = 0.9563	2 - 8h	60.72
60	y = 60.341x - 103.87 R^2 = 0.9941	2 - 8h	60.34
80	y = 66.588x - 9.2857 R^2 = 0.9714	**0-4 h**	66.59
100	y = 78.074x + 17.723 R^2 = 0.9732	**0-4 h**	78.07

Appendix 5.3.1 Water loss test at different temperatures

Water (1mL) was added into glass tube, and screwed the cap tightly, then weighted them and recorded the mass. Preheated the 3 heat blocks to 75, 110 and 120 °C and put the glass tubes into the heat blocks. After designed heating time the tube was weighed and put back into the heat blocker immediately. The mass of the tubes measured at each point was recorded in Table 5.3.1A. The sample series were measured in duplicate (two tubes at each temperature).

Table 5.3.1A. Weighing results of water loss test

Heating time [h]	**75°C**		**110°C**		**120°C**	
	tube [g]	water lose [g]	tube [g]	water lose [g]	tube [g]	water loss [g]
0	16.01	0.00	14.83	0.00	14.80	0.00
1	16.01	0.00	14.82	0.01	14.78	0.02
2	16.00	0.01	14.82	0.01	14.77	0.03
3	16.00	0.01	14.81	0.02	14.76	0.04
4	15.99	0.02	14.81	0.02	14.74	0.06
5	-----	-----	14.8	0.03	14.73	0.07
6	15.98	0.03	-----	-----	-----	-----
27	15.94	0.07	-----	-----	-----	-----
0	16.07	0.00	14.89	0.00	14.74	0.00
1	16.07	0.00	14.88	0.01	14.71	0.03
2	16.06	0.01	14.87	0.02	14.66	0.08
3	16.05	0.02	14.87	0.02	14.62	0.12
4	16.05	0.02	14.86	0.03	14.59	0.15
5	-----	-----	14.85	0.04	14.56	0.18
6	16.04	0.03	-----	-----	-----	-----
27	15.99	0.09	-----	-----	-----	-----

Appendix 5.3.2 Two-step autocatalytic reaction model analysis reports at higher temperatures

The ThT fluorescence data (Section 5.3), FI** vs. heating time at different temperatures (pH 2.0, low ionic strength) were analysed using SigmaPlot 10.0.

- **Statistic report at 90°C**

Nonlinear Regression

Data Source: Data 2 in temp.JNB
Equation: Sigmoidal, Finke-Watzky 2 in Simon.JFL
f= y0-((k1/k2)+y0)/(1+(k1/(k2*y0))*exp(x*(k1+k2*y0)))

R	Rsqr	Adj Rsqr	Standard Error of Estimate
0.9847	0.9696	0.9677	14.4561

	Coefficient	Std. Error	t	P	VIF
k1	0.0824	0.0137	6.0178	<0.0001	6.4820<
k2	0.0017	0.0005	3.2332	0.0028	20.0379<
y0	213.5240	9.9691	21.4185	<0.0001	9.5800<

Analysis of Variance:

Uncorrected for the mean of the observations:

	DF	SS	MS
Regression	3	586998.9801	195666.3267
Residual	33	6896.3149	208.9792
Total	36	593895.2950	16497.0915

Corrected for the mean of the observations:

	DF	SS	MS	F	P
Regression	2	219756.7181	109878.3590	525.7860	<0.0001
Residual	33	6896.3149	208.9792		
Total	35	226653.0330	6475.8009		

Statistical Tests:

PRESS 8709.0794

Durbin-Watson Statistic 2.1795 Passed

Normality Test Passed (P = 0.5886)

K-S Statistic = 0.1259 Significance Level = 0.5886

Constant Variance Test Failed (P = <0.0001)

Power of performed test with alpha = 0.0500: 1.0000

- **Statistic report at 100°C**

Nonlinear Regression

Data Source: Data 3 in temp.JNB
Equation: Sigmoidal, Finke-Watzky 2 in Simon.JFL
f= y0-((k1/k2)+y0)/(1+(k1/(k2*y0))*exp(x*(k1+k2*y0)))

R	Rsqr	Adj Rsqr	Standard Error of Estimate
0.9898	0.9797	0.9785	12.0289

	Coefficient	Std. Error	t	P	VIF
k1	0.1266	0.0125	10.1128	<0.0001	6.8959<
k2	0.0008	0.0003	2.4241	0.0205	29.4095<
y0	238.4966	11.5886	20.5803	<0.0001	18.3279<

Analysis of Variance:

Uncorrected for the mean of the observations:

	DF	SS	MS
Regression	3	823040.3047	274346.7682
Residual	36	5208.9663	144.6935
Total	39	828249.2710	21237.1608

Corrected for the mean of the observations:

	DF	SS	MS	F	P
Regression	2	250893.8909	125446.9454	866.9839	<0.0001
Residual	36	5208.9663	144.6935		
Total	38	256102.8571	6739.5489		

Statistical Tests:

PRESS 6815.8341

Durbin-Watson Statistic 1.7036 Passed

Normality Test Passed (P = 0.6500)

K-S Statistic = 0.1154 Significance Level = 0.6500

Constant Variance Test Failed (P = <0.0001)

Power of performed test with alpha = 0.0500: 1.0000

- **Statistic report at 110°C**

Nonlinear Regression

Data Source: Data 9 in temp.JNB
Equation: Sigmoidal, Finke-Watzky 2 in Simon.JFL
f= y0-((k1/k2)+y0)/(1+(k1/(k2*y0))*exp(x*(k1+k2*y0)))

R	Rsqr	Adj Rsqr	Standard Error of Estimate
0.9817	0.9637	0.9589	16.2316

	Coefficient	Std. Error	t	P	VIF
k1	0.1532	0.0491	3.1177	0.0071	10.6518<
k2	0.0050	0.0024	2.0261	0.0609	32.6377<
y0	210.3767	19.2963	10.9025	<0.0001	15.3054<

Analysis of Variance:

Uncorrected for the mean of the observations:

	DF	SS	MS
Regression	3	266318.7817	88772.9272
Residual	15	3951.9729	263.4649
Total	18	270270.7546	15015.0419

Corrected for the mean of the observations:

	DF	SS	MS	F	P
Regression	2	104975.0167	52487.5083	199.2201	<0.0001
Residual	15	3951.9729	263.4649		
Total	17	108926.9895	6407.4700		

Statistical Tests:

PRESS 6275.4790

Durbin-Watson Statistic 2.9236 Failed

Normality Test Passed (P = 0.9856)

K-S Statistic = 0.1038 Significance Level = 0.9856

Constant Variance Test Passed (P = 0.1433)

Power of performed test with alpha = 0.0500: 1.0000

- **Statistic report at 120°C**

Nonlinear Regression

Data Source: Data 6 in temp.JNB
Equation: Sigmoidal, Finke-Watzky 2 in Simon.JFL
f= y0-((k1/k2)+y0)/(1+(k1/(k2*y0))*exp(x*(k1+k2*y0)))

R	Rsqr	Adj Rsqr	Standard Error of Estimate
0.9963	0.9925	0.9913	7.5068

	Coefficient	Std. Error	t	P	VIF
k1	0.0697	0.0231	3.0182	0.0107	11.7028<
k2	0.0289	0.0028	10.1718	<0.0001	13.4086<
y0	184.7385	3.0722	60.1318	<0.0001	2.3422

Analysis of Variance:

Uncorrected for the mean of the observations:

	DF	SS	MS
Regression	3	263237.8036	87745.9345
Residual	12	676.2300	56.3525
Total	15	263914.0336	17594.2689

Corrected for the mean of the observations:

	DF	SS	MS	F	P
Regression	2	89970.3266	44985.1633	798.2816	<0.0001
Residual	12	676.2300	56.3525		
Total	14	90646.5566	6474.7540		

Statistical Tests:

PRESS 1119.8213

Durbin-Watson Statistic 1.0707 Failed

Normality Test Passed (P = 0.6959)

K-S Statistic = 0.1764 Significance Level = 0.6959

Constant Variance Test Passed (P = 0.1541)

Power of performed test with alpha = 0.0500: 1.0000

Appendix 6.1 Block design of the CCC design experiment

Block	**Trials #**
1	2, 3, 4, 5
2	6, 7, 8, 9
3	1, 19, 20, 21
4	10, 11, 12, 13
5	18, 22, 25
6	23, 24
7	14, 15, 16, 17
8	26, 27

Appendix 6.2 ThT fluorescence results of the CCC design experiment

(The peak values, F^{**}_{peak}, were marked with dark arrows, the times corresponded to the peak values were the peak time)

Block1 Trial 2#, 3#, 4# and 5#

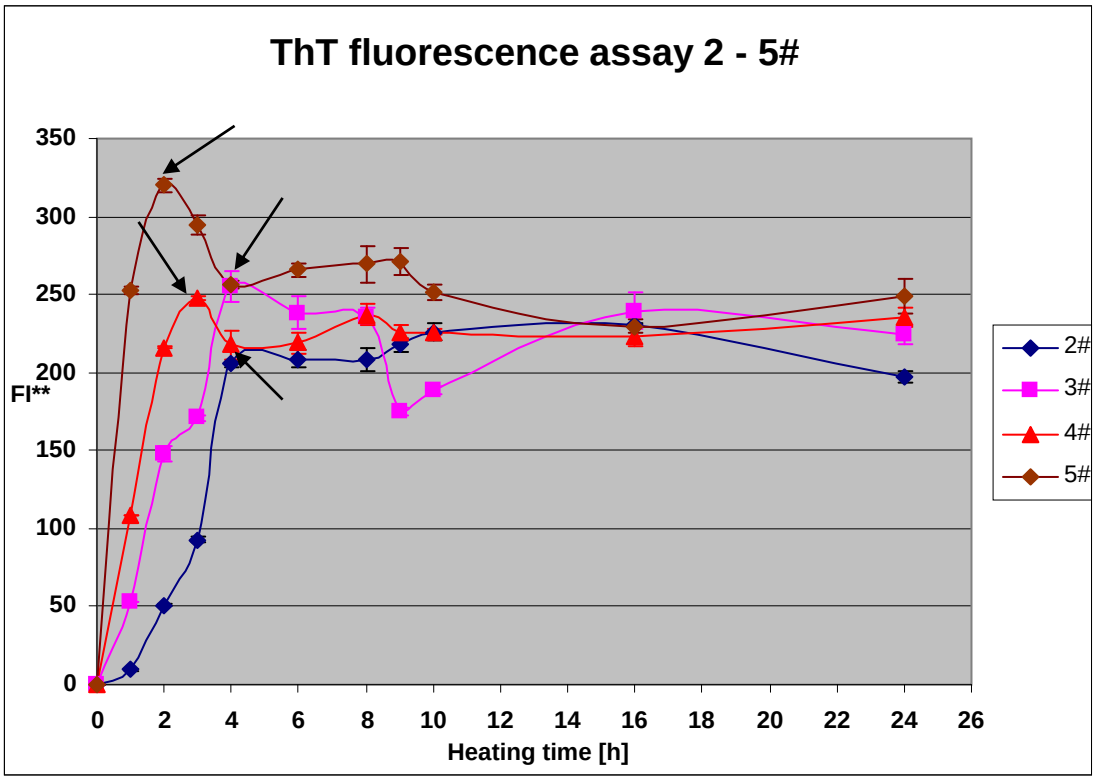

Block 2 Trial 6#, 7#, 8# and 9#

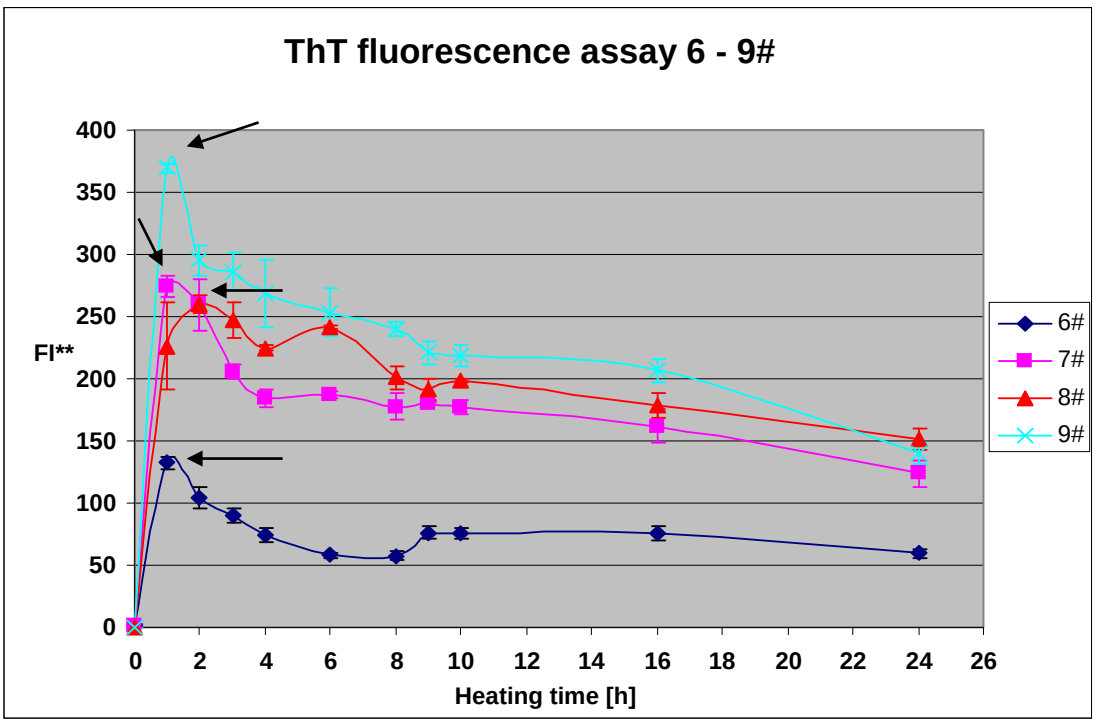

Block 3 Trial 1#, 19#, 20# and21#

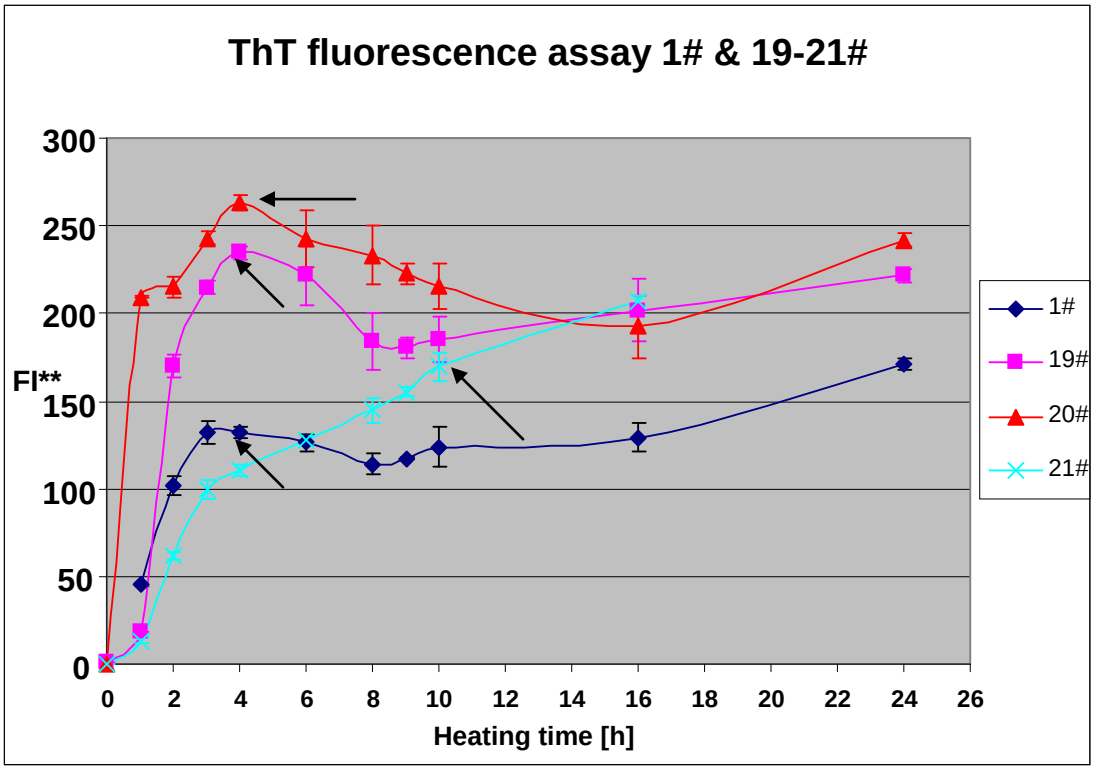

Block 4 Trial 10#, 11#, 12# and 13#

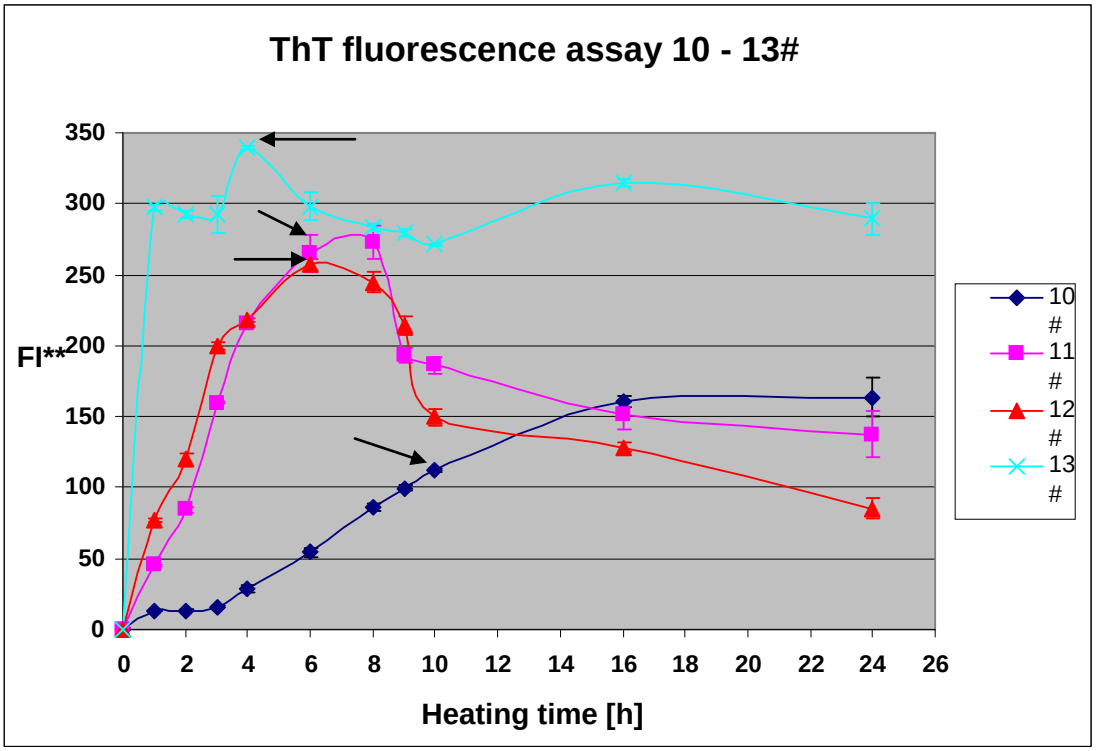

Block 5 Trial 18#, 22# and 25#

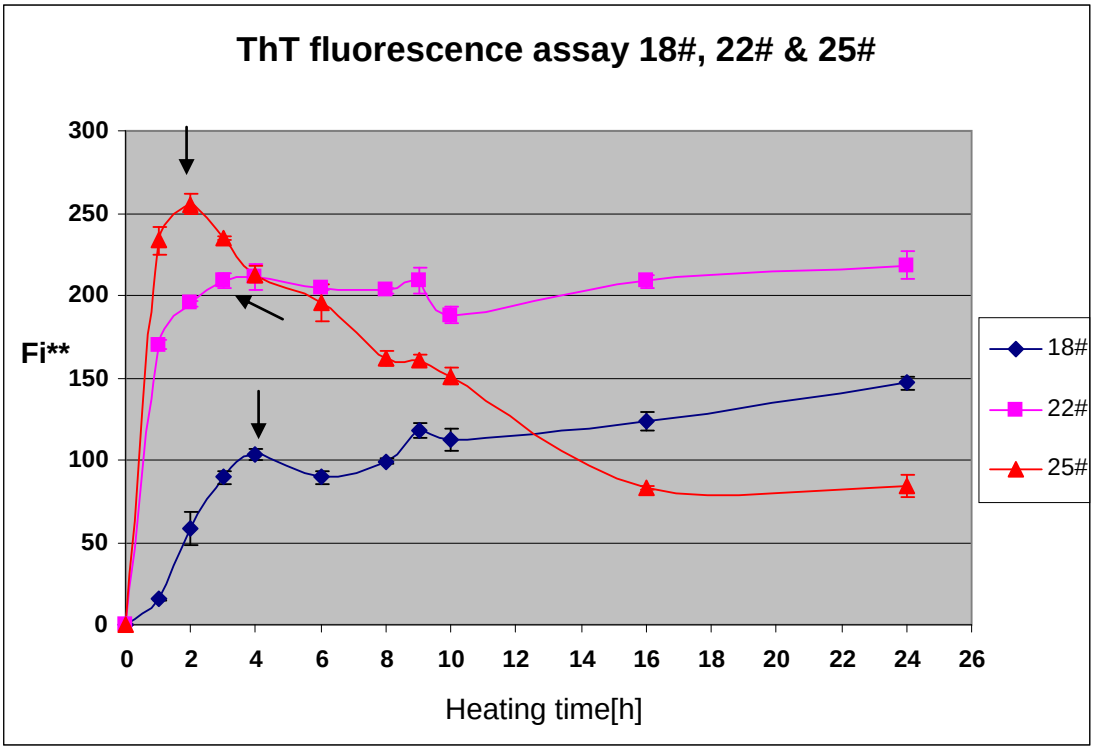

Block 7 Trial 14#, 15#, 16# and17#

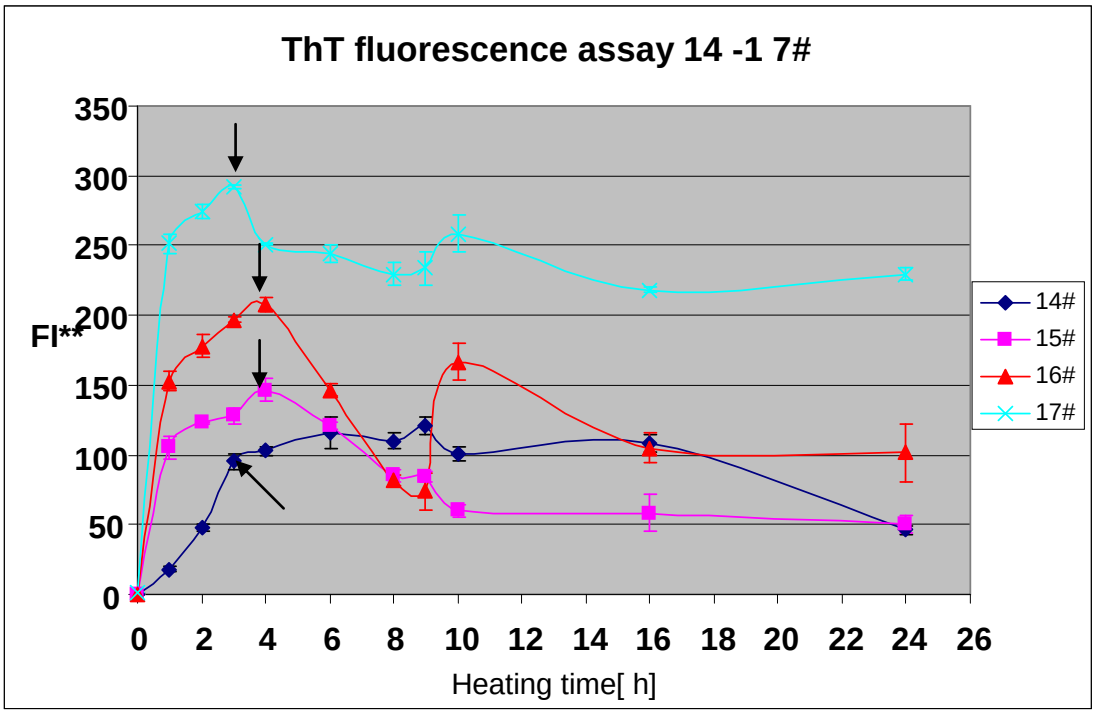

Block 6 Trial 23# & 24#, Block 8 26# & 27#

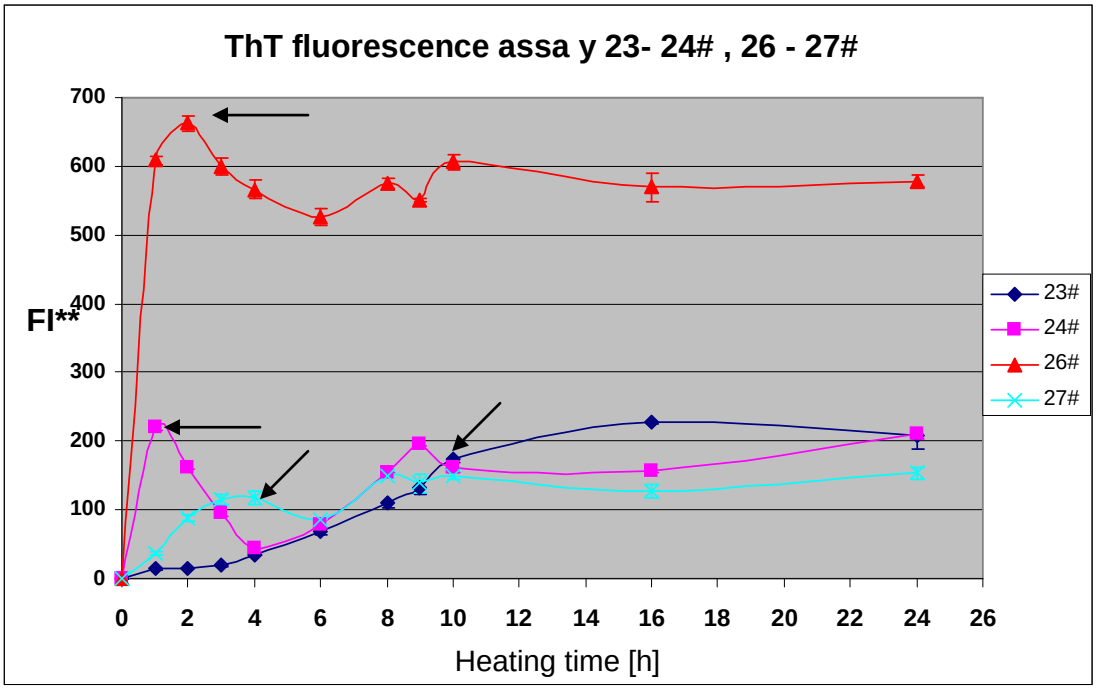

Appendix 6.3 Statistical analyses of the CCC experiment results (using Minitab 15.0 software)

- **One-way ANOVA: FI** (at peak time) versus formulation (in 1 block)**

```
Source       DF      SS     MS       F      P
Treatment    24  963189  40133  283.89  0.000
Error        56    7916    141
Total        80  971106

S = 11.89   R-Sq = 99.18%   R-Sq(adj) = 98.84%


                         Individual 95% CIs For Mean Based on
                         Pooled StDev
Level  N    Mean  StDev  -----+---------+---------+---------+----
 1     9  117.56  15.51    (*
 2     3  205.29   4.90          (*)
 3     3  254.69  20.86             (*)
 4     3  247.71   3.31             (*
 5     3  319.82   8.36                 (*)
 6     3  132.51   8.61     (*)
 7     3  274.38  14.47              (*)
 8     3  260.06  11.82             (*)
 9     3  369.42   6.43                      (*)
10     3  173.78   4.13        (*)
11     3  265.45  22.08              (*)
12     3  256.76   6.95             (*)
13     3  339.79   2.39                   (*)
14     3   95.52   9.62  (*)
15     3  146.56  14.16      (*)
16     3  207.45   8.47          (*)
17     3  291.73   2.35                *)
18     3  234.57   7.13            (*)
19     3  263.04   6.77              (*
20     3  169.93  13.99       (*)
21     3  211.56  13.89          (*)
22     3  173.39   6.21        (*
23     3  221.15   8.58           (*)
24     3  255.53  11.49             (*)
25     3  662.80  18.24                                       (*)
                         -----+---------+---------+---------+----
                            150       300       450       600

Pooled StDev = 11.89
```

- **Response Surface Regression of ThT fluorescence intensity ($\underline{FI^{**}_{peak}}$) at peak time versus block and the four factors.**

ThT fluorescence assays results of all trials (1#-27#) were included in the Response Surface Regression analysis.

Response Surface Regression: FI versus A-NaCl, $CaCl_2$, C-temp, D-pH**

The analysis was done using coded units.

Estimated Regression Coefficients for FI**

Term	Coef	SE Coef	T	P
Constant	117.563	23.16	5.077	0.000
A-NaCl	61.641	16.37	3.765	0.000
B-$CaCl_2$	68.983	16.37	4.213	0.000
C-temp	-15.846	16.37	-0.968	0.337
D-pH	43.973	16.37	2.686	0.009
A-NaCl*A-NaCl	108.615	34.73	3.127	0.003
B-$CaCl_2$*B-$CaCl_2$	50.554	34.73	1.455	0.150
C-temp*C-temp	57.084	34.73	1.643	0.105
D-pH*D-pH	318.978	34.73	9.183	0.000
A-NaCl*B-$CaCl_2$	3.701	40.11	0.092	0.927
A-NaCl*C-temp	22.586	40.11	0.563	0.575
A-NaCl*D-pH	-15.677	40.11	-0.391	0.697
B-$CaCl_2$*C-temp	53.704	40.11	1.339	0.185
B-$CaCl_2$*D-pH	21.073	40.11	0.525	0.601
C-temp*D-pH	-75.849	40.11	-1.891	0.063

S = 69.4676 PRESS = 490285
R-Sq = 67.20% R-Sq(pred) = 49.51% R-Sq(adj) = 60.25%

Analysis of Variance for FI**

Source	DF	Seq SS	Adj SS	Adj MS	F	P
Regression	14	652606	652606	46615	9.66	0.000
Linear	4	193375	193375	48344	10.02	0.000
Square	4	429678	429678	107420	22.26	0.000
Interaction	6	29553	29553	4925	1.02	0.420
Residual Error	66	318499	318499	4826		
Lack-of-Fit	10	310583	310583	31058	219.70	0.000
Pure Error	56	7916	7916	141		
Total	80	971106				

Unusual Observations for FI**

Obs	StdOrder	FI**	Fit	SE Fit	Residual	St Resid
25	25	263.940	392.567	30.632	-128.627	-2.06 R
26	26	666.871	480.514	30.632	186.357	2.99 R
52	52	242.440	392.567	30.632	-150.127	-2.41 R
53	53	678.653	480.514	30.632	198.139	3.18 R
79	79	260.219	392.567	30.632	-132.348	-2.12 R
80	80	642.867	480.514	30.632	162.354	2.60 R

R denotes an observation with a large standardized residual.

Estimated Regression Coefficients for FI** using data in uncoded units

Term	Coef

Constant	117.563
A-NaCl	30.8207
B-$CaCl_2$	34.4915
C-temp	-7.92305
D-pH	21.9867
A-NaCl*A-NaCl	27.1538
B-$CaCl_2$*B-$CaCl_2$	12.6385
C-temp*C-temp	14.2709
D-pH*D-pH	79.7445
A-NaCl*B-$CaCl_2$	0.925322
A-NaCL*C-temp	5.64638
A-NaCL*D-pH	-3.91928
B-$CaCl_2$*C-temp	13.4261
B-$CaCl_2$*D-pH	5.26826
C-temp*D-pH	-18.9623

- **Response Surface Regression of <u>peak time</u> versus block and the four factors.**

ThT fluorescence assays results of all trials (1#-27#) were included in the Response Surface Regression analysis.

Response Surface Regression: Time versus A-NaCl, β-lactoglobulin-$CaCL_2$, C-temp, D-pH

The analysis was done using coded units.

Estimated Regression Coefficients for peak time

Term	Coef	SE Coef	T	P
Constant	4.0000	0.8022	4.986	0.000
A-Nacl	-0.6667	0.5672	-1.175	0.263
B-$CaCl_2$	-0.6667	0.5672	-1.175	0.263
C-temp	-3.1667	0.5672	-5.583	0.000
D-pH	1.8333	0.5672	3.232	0.007
A-Nacl*A-Nacl	-0.1667	1.2033	-0.139	0.892
B-$CaCl_2$*B-$CaCl_2$	-0.1667	1.2033	-0.139	0.892
C-temp*C-temp	1.3333	1.2033	1.108	0.290
D-pH*D-pH	-2.1667	1.2033	-1.801	0.097
A-Nacl*B-$CaCl_2$	-0.5000	1.3894	-0.360	0.725
A-Nacl*C-temp	1.5000	1.3894	1.080	0.302
A-Nacl*D-pH	-1.0000	1.3894	-0.720	0.485
B-$CaCl_2$*C-temp	2.5000	1.3894	1.799	0.097
B-$CaCl_2$*D-pH	-1.0000	1.3894	-0.720	0.485
C-temp*D-pH	-1.0000	1.3894	-0.720	0.485

S = 1.38944 PRESS = 133.44
R-Sq = 82.61% R-Sq(pred) = 0.00% R-Sq(adj) = 62.31%

Analysis of Variance for peak time

Source	DF	Seq SS	Adj SS	Adj MS	F	P
Regression	14	110.019	110.0185	7.8585	4.07	0.010
Linear	4	85.667	85.6667	21.4167	11.09	0.001
Square	4	12.602	12.6019	3.1505	1.63	0.230
Interaction	6	11.750	11.7500	1.9583	1.01	0.460
Residual Error	12	23.167	23.1667	1.9306		
Lack-of-Fit	10	23.167	23.1667	2.3167	*	*
Pure Error	2	0.000	0.0000	0.0000		
Total	26	133.185				

Unusual Observations for peak time

Obs	StdOrder	peak time	Fit	SE Fit	Residual	St Resid
25	25	2.000	0.000	1.061	2.000	2.23 R

R denotes an observation with a large standardized residual.

Estimated Regression Coefficients for peak time using data in uncoded units

Term	Coef
Constant	4.00000
A-Nacl	-0.333333
B-$CaCl_2$	-0.333333
C-temp	-1.58333
D-pH	0.916667

A-Nacl*A-Nacl	-0.0416667
B-CaCl2*B-$CaCl_2$	-0.0416667
C-temp*C-temp	0.333333
D-pH*D-pH	-0.541667
A-Nacl*B-$CaCl_2$	-0.125000
A-Nacl*C-temp	0.375000
A-Nacl*D-pH	-0.250000
B-$CaCl_2$*C-temp	0.625000
B-$CaCl_2$*D-pH	-0.250000
C-temp*D-pH	-0.250000

Appendix 7.1 Comparison of the control trials

The control trials were the ThT fluorescence assays of β-lactoglobulin fibril formation under control conditions (pH 2.0, 80 °C and low ionic strength). The trials were from different trials and experiments that carried out in this study.

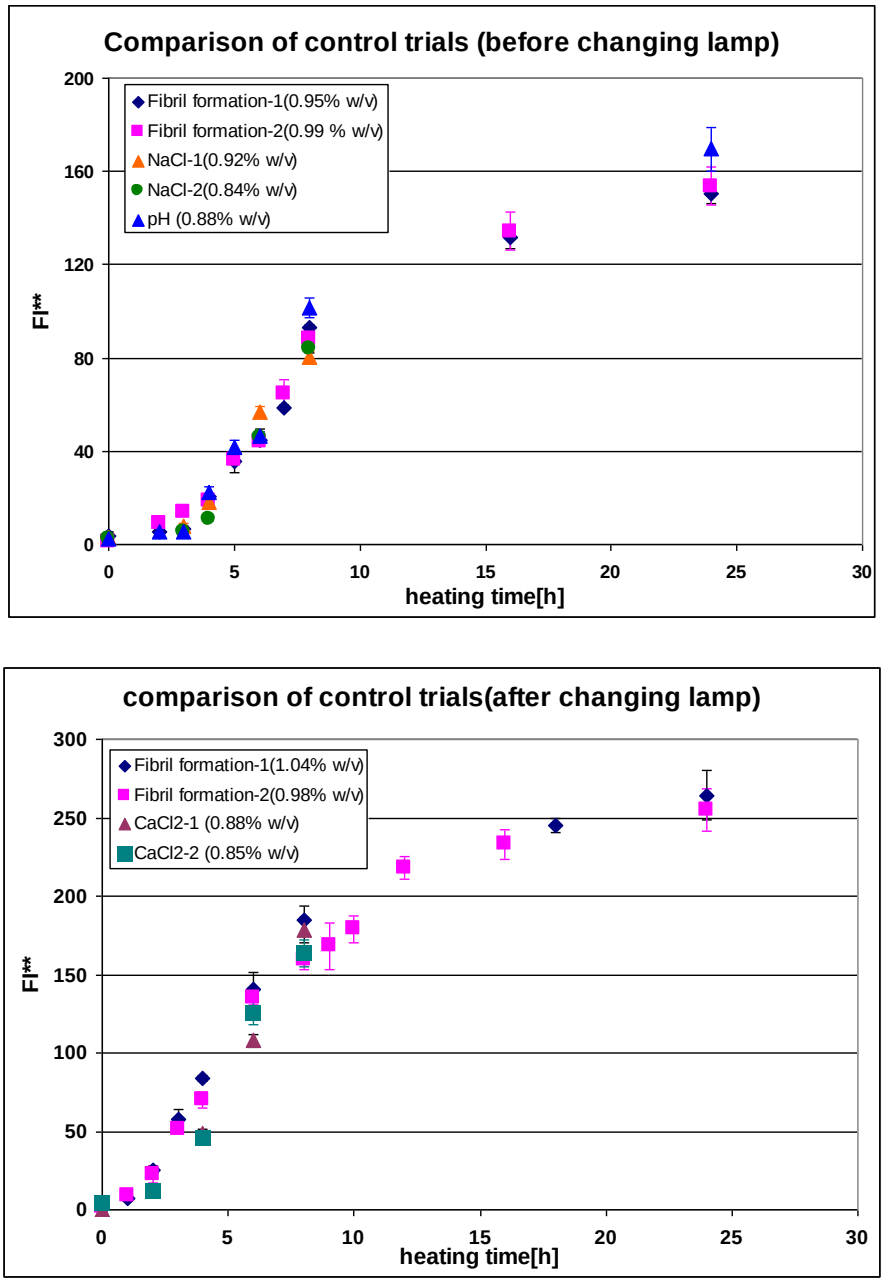

Figure 7.1.A Comparison of the control trials from different experiments. (before and after changing the lamp of the fluorescence meter, RF-1501 SHIMADZU).